uOttawa

L'Université canadienne
Canada's university

FACULTÉ DES ÉTUDES SUPÉRIEURES ET POSTOCTORALES

uOttawa

L'Université canadienne
Canada's university

FACULTY OF GRADUATE AND POSDOCTORAL STUDIES

Justin Caravaggio
AUTEUR DE LA THÈSE / AUTHOR OF THESIS

M.Sc. (Cellular and Molecular Medicine)
GRADE / DEGREE

Department of Cellular and Molecular Medicine
FACULTÉ, ÉCOLE, DÉPARTEMENT / FACULTY, SCHOOL, DEPARTMENT

Insulin Degrading Enzyme and its Role in Atherosclerosis

TITRE DE LA THÈSE / TITLE OF THESIS

Ross Milne
DIRECTEUR (DIRECTRICE) DE LA THÈSE / THESIS SUPERVISOR

CO-DIRECTEUR (CO-DIRECTRICE) DE LA THÈSE / THESIS CO-SUPERVISOR

Balawant Tuana

Yves Marcel

Gary W. Slater
Le Doyen de la Faculté des études supérieures et postdoctorales / Dean of the Faculty of Graduate and Postdoctoral Studies

Insulin Degrading Enzyme And Its Role In Atherosclerosis

Justin W. Caravaggio

Thesis submitted to:
Faculty of Graduate and Postdoctoral Studies in
partial fulfillment of the requirements for the
MSc. Degree in Cellular and Molecular Medicine

Department of Cellular and Molecular Medicine
Faculty of Medicine
University of Ottawa

Your file Votre référence
ISBN: 978-0-494-74150-4
Our file Notre référence
ISBN: 978-0-494-74150-4

Abstract

The type-A scavenger receptor (SR-A) plays a major role in the uptake of modified lipoproteins leading to foam cell formation and fatty streak development in artery walls. Our lab previously showed that a peptide known as insulin degrading enzyme (IDE) is able to bind the SR-A cytoplasmic domain *in vitro*. The present study provides evidence that male low density lipoprotein receptor-null (LDLr-/-) mice on a high fat diet, generate significantly more atherosclerotic lesion in aortic root and the aortic intimal surface when reconstituted with IDE-null (IDE-/-) bone marrow derived cells compared to those reconstituted with wild type bone marrow. Total serum cholesterol and the LDLr cholesterol fraction was also significantly increased in male LDLr-/- mice reconstituted with IDE-/- bone marrow. Macrophages procured from IDE-/- mice showed no difference in uptake of modified LDL compared to wild type cells but may be able to accumulate more cholestertyl ester than wild type cells. Our findings reveal that IDE expression likely exerts an anti-atherogenic effect via cholesterol metabolism, although further in vitro experiments are required to elucidate an exact mechanism.

Table of Contents

List of Tables

Page

List of Figures

Page

List of Abbreviations

Aβ	amyloid beta
ACAT	acyl-coenzyme A:cholesterol acyltransferase
acLDL	acetylated low density lipoprotein
AD	Alzheimer's disease
AGE	advanced glycation end (product)
AICD	amyloid precursor protein intracellular cytoplasmic domain
Apo	apolipoprotein
APP	amyloid precursor protein
BMDC	bone marrow derived cell
BMDM	bone marrow derived macrophage
BMT	bone marrow transplant
CE	cholesteryl ester
CETP	cholesteryl ester transfer protein
DM2	type 2 diabetes
DMEM	Dulbecco's modified Eagle's medium
EDTA	ethylenediaminetetraacetic acid
FPLC	fast protein liquid chromatography
GK	Goto-Kakizaki (rat)
HDL	high density lipoprotein
IDE	insulin degrading enzyme
IDL	intermediate density lipoprotein
LCAT	lecithin-cholesterol acyltransferase
LDL	low density lipoprotein
LDLr	low density lipoprotein receptor
LPL	lipoprotein lipase
nLDL	native low density lipoprotein
NO	nitric oxide
OCT	optimal cutting temperature (medium)
oxLDL	oxidized low density lipoprotein
PCR	polymerase chain reaction

PFA	paraformaldehyde
PDI	protein disulfide isomerase
ROS	reactive oxygen species
SR-A	type-A scavenger receptor
VLDL	very low density lipoprotein
VSMC	vascular smooth muscle cell

Acknowledgments

First and definitely foremost in my acknowledgments is the late Dr. Stewart Whitman. I would like to thank Stew for not only giving me the chance to partake in his research, but also for opening my eyes to a whole new universe. His endless dedication to the lab and its goals was an inspiration for me, and I'm very certain, many others as well. I can't thank Dr. Ross Milne enough for always having an open door and for sacrificing his time to be on my committee and provide excellent feedback. Mirela Hasu deserves many thanks and a big hug. Mirela was the workhorse of our lab, not only taking the time to assist with my experiments, but also as a teacher of methodologies. Special thanks to Mohamed Thabet for his patience, guidance and teachings. Thanks to Dr. Robin Maclaren, whose tutelage I felt helped me grow into a much more prepared and organized graduate student. A special thanks to Jessica Gage and Sarah Burchat for trying to keep my head screwed on straight and easing my transition into grad school, the entire way through. I would also like to acknowledge all the hard work done by the ACVS crew downstairs, who without, this study would not be possible. I'd like to thank all the peers that I had the privilege to meet and work beside during my time at the Heart Institute. It will be difficult to find another atmosphere so collaboration driven towards success. Whether it be at conferences or in the lab, I felt I formed many connections that are now and always will be important to me. Finally I would like to thank my parents, for without their guidance I would not be where I am now.

Chapter 1: Introduction

Atherosclerosis is a major cause of morbidity and mortality in both developed and underdeveloped countries around the world. Although there are many risk factors, a major step in the disease is the recruitment of macrophages to arterial vessel walls. Macrophages are able to endocytose modified forms of low density lipoprotein (LDL) present within the vessel wall, in an unregulated fashion, via the type A scavenger receptor (SR-A). The extensive literature on SR-A biology provides roles for this protein in both foam cell and lesion formation in well characterized atherosclerosis mouse models. To date, little is known about the signalling characteristics of SR-A. As such, it was a recent goal of our lab to identify any novel SR-A protein interactions. Affinity chromatography pull-down using the SR-A cytoplasm domain as bait, revealed the association of a protein known as insulin degrading enzyme (IDE). IDE has well documented roles in the pathologies leading to type 2 diabetes as well as Alzheimer's disease, which both have intrinsic links to atherosclerosis. The present study aims to determine if IDE knockout in bone marrow-derived cells (BMDC) promotes diet-induced atherosclerotic lesion development in low density lipoprotein receptor-null ($LDLr^{-/-}$) mice. Secondarily, the ability of $IDE^{-/-}$ bone marrow-derived macrophages (BMDM) to bind and take up cholesterol and become foam cells will be examined.

Chapter 2: Background

2.1 Atherosclerosis

Atherosclerosis is a disease characterized by the deposition of plaque within the interior layer of arterial walls. Said plaque is composed of a core of macrophage foam cells, T cells, and extracellular lipid droplets. The core is surrounded by smooth muscle cells and collagen-rich matrix. The accumulation of plaque can lead to narrowing of the arteries; also know as stenosis, thus restricting blood flow to major organs. Restricted blood flow to the heart, brain and peripheral organs results in insufficient oxygen supply and can therefore lead to heart attack, stroke and peripheral artery disease, respectively. Currently, there is no single defined cause of atherosclerosis, but there exists many risk factors that can increase the chances of its progression. Some factors can be controlled, such as a maintaining a healthy diet, choosing not to smoke, and avoiding a sedentary lifestyle. Other factors such as age, sex and familial genetics cannot be controlled. Due to its many risk factors and complicated manifestations, atherosclerosis is one of the deadliest killers in the world.

The cellular and molecular events contributing to the generation of atheromatous lesions have been heavily researched in an attempt to alleviate or reverse their pathological consequences. It is believed that when elevated blood plasma levels of low density lipoprotein (LDL or "bad cholesterol") are present, this can lead to the chronic presence of LDL in the arterial wall. Upon entering the arterial wall, these LDL particles can become trapped within the extracellular matrix of the tunica intima, and subsequently undergo modifications such as oxidation by free radicals, leading to a new species of lipoprotein termed oxidized or modified LDL (Kunitomo, 2007) The vascular endothelial cells view the modified LDL as foreign and thereby become activated, resulting in the induction of leukocyte recruitment, increased permeability and edema. Of the leukocytes recruited, arguably the most crucial in terms of atherogenesis is the monocyte-derived macrophage. Macrophages are scavenging white blood cells that subject the modified LDL to endocytosis, in an attempt to clear it from the tunica media. Macrophages are able to take up modified LDL via cell surface receptors known as scavenger receptors. The uptake of cholesterol via scavenger receptor-mediated endocytosis is unrestricted, and as a result, the

macrophage becomes engorged with cholesterol, giving these macrophages a foaming appearance morphologically, hence these cells are also referred to as foam cells. During early stages of lesion formation, foam cells are the main cellular component of atherosclerotic lesions. The unregulated accumulation of cholesterol by macrophages eventually leads to the death of the foam cell, which results in the deposition of the accumulated cholesterol within the vessel wall as a core of developing necrotic lipid and cellular debris.

Figure 1. Model of atherosclerosis

There are a number of cellular and molecular determinants involved in the formation of the fatty streak. Increased levels of circulating atherogenic lipoproteins such as LDL are able to cross the vascular endothelium and accumulate in the intima where they can become chemically modified via oxidation. These modified lipoproteins initiate the migration and adhesion of monocytes from the lumen. Transmigration of monocytes into the intima results in macrophage differentiation and upregulation of the type A-scavenger receptor (SR-A). Unregulated uptake of modified lipoproteins by SR-A continues until the macrophage becomes a lipid-laden foam cell. Foam cells actively secrete reactive oxygen species (ROS), matrix metalloproteinases (MMP) and proinflammatory cytokines, thereby exacerbating the growth of the fatty streak. The accumulation of foam cells forms a fatty streak which is the first grossly observed morphological change seen in atherosclerosis.

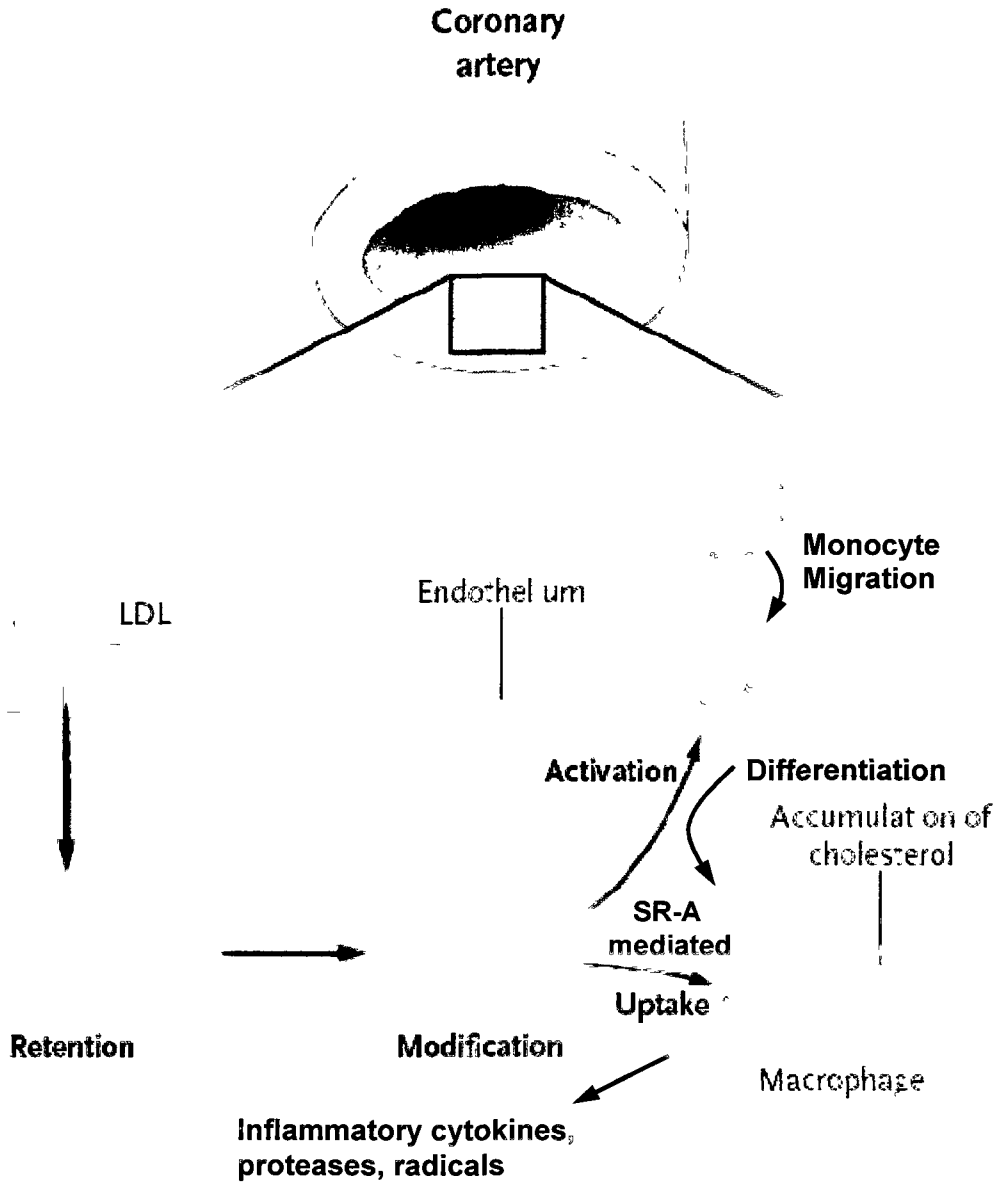

[Adapted with permission from the New England Journal of Medicine (Hansson, 2005)]

The type A scavenger receptor (SR-A) is one species of scavenger receptor identified as being responsible for the unregulated influx of lipoprotein-derived lipids into macrophages, and therefore a critical factor in foam cell formation. Along with this role, it has been shown that SR-A encompasses critical roles related to the inflammatory process in host defense, cellular activation, adhesion and signalling. These processes indicate a multifunctional role for SR-A in the progression of atherosclerosis, and therefore it must be considered an important target for therapeutic purposes and prevention. To review the putative role of SR-A in atherosclerosis, it is important to fully understand lipoprotein biology and how scavenger receptors impact this biology as well as the models that are used to study these fields

2.2 Lipoprotein structure and composition

The major lipids found in human plasma are cholesterol, cholesteryl esters, triglycerides and phospholipids. The regulation of lipid transport is of great importance, as lipids serve as sources of energy, as components of cell membranes, and as precursors for steroid hormones and bile acids. The major neutral lipids transported through the blood stream are triglycerides and cholesteryl esters, but they are insoluble in aqueous solutions and therefore must be protected from plasma by a coating of amphipathic molecules.

Such protection is provided by lipoproteins, which are macromolecular complexes capable of carrying various lipids and proteins in plasma. The lipoprotein core is comprised of hydrophobic triglyceride and cholesteryl ester molecules, which are enveloped by an amphipathic monolayer of phospholipids, free cholesterol, and proteins.

The proteins, called apoproteins (or apolipoproteins), are critical regulators of lipid transport and metabolism. All lipoproteins possess a continuum of particles differing gradually in density as well as lipid and apoprotein composition, so there are distinct subclasses that can be isolated by various physical methods. The distinct classes of lipoproteins have been defined by their physical-chemical characteristics (Ginsberg, 1998): chylomicrons, very low density lipoprotein (VLDL), intermediate density lipoprotein (IDL),

low density lipoprotein (LDL), and high density lipoprotein (HDL). The physical-chemical characteristics of the major lipoprotein classes are shown below.

Table 1: Physical and chemical characteristics of the major lipoprotein classes

Lipoprotein	Density (g/dL)	Molecular Weight (daltons)	Diameter (nm)	Lipid (%)		
				TG	CHOL	PL
Chylomicrons	0.95	400×10	75-1200	80-95	2-7	3-9
VLDL	0.95-1.006	$10\text{-}80\times10^6$	30-80	55-80	5-15	10-20
IDL	1.006-1.019	$5\text{-}10\times10^6$	25-35	20-50	20-40	15-25
LDL	1.019-1.063	2.3×10^6	18-25	5-15	40-50	20-25
HDL	1.063-1.21	$1.7\text{-}3.6\times10^5$	5-12	5-10	15-25	20-30

TG = triglycerides; CHOL = cholesterol; PL = phospholipids; VLDL = very low density lipoprotein; IDL = intermediate density lipoprotein; LDL = low density lipoprotein; HDL = high density lipoprotein.

(Adapted from Ginsberg, 1998)

2.3 Lipoprotein components

Cholesterol

Cholesterol is a lipid carried within the lipoprotein capsule which functions as a component of cell membranes and a precursor in steroid and hepatic bile acid synthesis. Cholesterol is the major core lipid of LDL and HDL, although VLDL and chylomicron remnants have the potential to carry significant quantities of cholesterol as well. Cholesterol can be obtained from dietary sources and be synthesized in many tissues, but in the plasma it is carried primarily as cholesteryl ester within lipoproteins. A small proportion of lipoprotein cholesterol is carried as free cholesterol in the surface monolayer of the lipoprotein particle. Free cholesterol on the lipoprotein surface can be esterified in plasma by the enzyme lecithin cholesterol acyl transferase (LCAT), which allows cholesterol to translocate from the surface into the core of the particle.

Triglycerides

Triglycerides are the major lipid in chylomicrons and VLDL that are synthesized in the small intestine, liver and adipose tissue, and can be stored in the liver and fat cells where they serve as energy substrates. Triglycerides are formed from a single molecule of glycerol which is esterified to three fatty acids. When the body requires fatty acids as an energy source, the hormone glucagon signals the breakdown of the triglycerides by lipases to release free fatty acids.

Phospholipids

The majority of lipoprotein surface area is composed of phospholipids that form monolayers which act as interfaces with both the polar plasma components and the non-polar lipids of the lipoprotein core. Lecithin (phosphatidylcholine) is the major phospholipid in plasma and is the source of linoleate for cholesteryl ester formation by the LCAT reaction.

Apoproteins

Found on the surface of lipoproteins, apolipoproteins provide structural stability and have critical roles in regulating lipoprotein metabolism. Some apolipoproteins act as cofactors for plasma lipid-modifying enzymes or as ligands for cell surface lipoprotein receptors.

The apoB proteins have a well studied association with heart disease. There are two isoforms present in the plasma: apoB100 which is a large hydrophobic protein synthesized almost exclusively in the liver, and apoB48 in the small intestine (Kane *et al.*, 1980). ApoB100 is the major apolipoprotein of VLDL, IDL, and LDL, comprising approximately 30%, 60%, and 95% of the protein in these respective lipoproteins (Ginsberg, 1998). ApoB100 contains an LDL receptor-binding domain that is involved in the uptake of plasma LDL and possibly some VLDL and IDL by tissues. ApoB100 is necessary for the initial assembly and secretion of VLDL by the liver, and individuals who do not synthesize normal apoB100 do not secrete VLDL (Yao and McLeod., 2004). High levels of apoB100 can lead to competition for the LDL receptor (LDLr), resulting in longer LDL residence time in the plasma. Therefore, in the plasma, apoB has a crucial role in the catabolism of LDL via interaction with the LDL receptor.

The apoB48 isoform, whose sequence is identical to the amino-terminal 2152 amino acids of apoB100, is derived from the apoB100 transcript through an mRNA-editing mechanism. Found on chylomicrons, apoB48 is necessary for intestinal assembly and secretion of these lipoproteins (Gotto, Pownall and Havel, 1986). ApoB48 seems to have no role other than to direct the initial assembly and secretion of chylomicrons, as it has no binding site for the LDL receptor. Interestingly, apoB48 is only secreted from intestinal enterocytes in humans whereas in mice and rats, it is also secreted from hepatocytes

ApoE is synthesized primarily in the liver and is found on all lipoproteins except LDL (Mahley, 1988). ApoE facilitates the binding of triglyceride-rich lipoprotein remnants to liver and peripheral receptors such as LDLr and the low density lipoprotein receptor-related protein (LRP) that determines their clearance (Weisgraber *et al.*, 1982). ApoE has

three isoforms, differing in DNA sequence, amino acid composition and receptor-binding affinity. The normal variant, apoE-3, is associated with normal VLDL and LDL metabolism. Apo E-2 cannot bind to the LDL receptor and its presence, particularly in the homozygous state, can be associated with the accumulation of cholesteryl ester-enriched VLDL. Apo E-4 binds normally to the LDL receptor but is associated with higher levels of LDL cholesterol (Kaprio *et al.*, 1991; Xhignesse *et al.*, 1991), thought to be due to more efficient absorption of dietary cholesterol, resulting in downregulation of the LDL receptor. There are other apolipoproteins with various critical functions in lipid metabolism, but for the purposes of this review, I will restrict my discussion to apoB and apoE.

2.4 Endogenous lipid transport

The liver is responsible for the assembly and secretion of apoB-containing lipoproteins, mainly VLDL. VLDL assembly takes place in the endoplasmic reticulum, with maturation occurring in the Golgi apparatus of hepatocytes prior to secretion (Dixon and Ginsberg, 1993).

The major role of apoB100 is the transport of lipids out of the liver. Therefore, the secretion and degradation of apoB is dependent on the availability of triglycerides, cholesteryl esters and phospholipids. In fact, several studies indicate that triglyceride availability is the major factor in the post-translational regulation of apoB secretion (Dixon and Ginsberg, 1993). Moreover, in the absence of adequate triglyceride levels, apoB undergoes post translational degradation (Wang *et al.*, 1993). Large triglyceride-rich VLDL are secreted when excess triglycerides are synthesized, such as in obesity, in persons consuming a diet high in simple carbohydrates, and in untreated diabetes mellitus (Howard, 1987). Large, triglyceride-rich VLDL seem to be characteristic of the type of apoB lipoprotein that is assembled and secreted by individuals with familial hypertriglyceridemia (Kissebah *et al.*, 1981).

The availability of lipids can also determine the rate of particle secretion. This is well illustrated by the link between rates of fatty acid flux and the secretion of apoB-containing lipoproteins. Numerous states, in which fatty acid flux is increased such as obesity and

diabetes mellitus, are associated with increased rates of VLDL apoB secretion. In fact, the link between insulin resistance and increased plasma VLDL seems to be related to increased plasma free fatty acid levels (Reaven, 1998).

Another parameter of VLDL secretion is insulin availability. Evidence has been presented that hyperinsulinemia can increase VLDL synthesis and secretion. There are strong correlations between levels of plasma insulin, measurements of insulin action, levels of plasma VLDL, and rates of VLDL secretion into plasma in normal and diabetic subjects. However, a causal relationship between insulin secretion and VLDL production has yet to be proven. Higher rates of free fatty acid flux to the liver are commonly associated with insulin resistance-hyperinsulinemia, and this may be the basis for increased production of VLDL (Yki-Jarvinen and Taskinen, 1988).

2.5 Exogenous (dietary) lipid transport

Chylomicrons transport dietary fats, cholesterol, and fat-soluble nutrients. The chylomicron surface is composed of phospholipids, apoB48, and apoA-I, A-II, and A-IV. The assembly and secretion of apoB48-containing lipoproteins, based on studies of primary cultures of intestinal cells seem to parallel those processes in the liver for apoB100-containing lipoproteins, in that the availability of core lipids, triglyceride, and cholesteryl ester drives the secretion of chylomicrons. Upon entry into plasma, chylomicrons become mature by acquiring apoC-I, apoC-II, apoC-III, and apoE from the surface of HDL. At this time, transfer of free and esterified cholesterol and of phospholipids from HDL also occurs. With the newly acquired apo C-II protein the chylomicron interacts with lipoprotein lipase (LPL), and core triglyceride hydrolysis is facilitated, releasing glycerol and fatty acids from the core for subsequent absorption in peripheral tissue (primarily muscle and adipose tissue).

Triglyceride hydrolysis mediated by LPL is accompanied by a decrease in core volume and surface area of the chylomicrons and by transfer of phospholipid, free cholesterol and apoC-II back to HDL. The remaining chylomicron remnant particles are cholesteryl ester and apoE-enriched, and therefore remain in circulation until they interact with chylomicron remnant receptors on hepatocytes (LDLr and LRP) to be removed from

the circulation. Subsequent endocytosis and lysosomal hydrolysis results in the release of glycerol and fatty acids into the cell (Gotto *et al.*, 1986)

The mouse model used in the current study is the LDLr knockout, so as to have higher amounts of atherogenic, apoB-100 containing lipoproteins in the plasma. As such, the final section of this lipoprotein review will focus on LDL metabolism.

LDL is generated primarily by the catabolism of VLDL and IDL within plasma; but also to some extent by hepatic secretion (Arad *et al.*, 1990) Regardless of the origin of LDL formation, their core lipid composition can be significantly affected by the triglyceride-rich apo B lipoproteins via the action of cholesteryl ester transfer protein (CETP) (Tall, 1990). Due to CETP activity, high levels of triglyceride-rich lipoproteins can drive the exchange of LDL cholesteryl ester for chylomicron or VLDL triglyceride. This newly triglyceride-enriched LDL can then interact with LPL, or hepatic lipase, generating smaller, denser LDL that are relatively lipid-depleted. These smaller LDL may be more atherogenic than normal sized LDL, as they do not interact as well with the LDL receptor and may be more likely to undergo oxidative modification (Austin *et al.*, 1994).

Clearance of plasma LDL is mainly determined by the availability/activity of LDL receptors (Brown and Goldstein, 1984). The LDL receptor is a glycoprotein present on the cell surfaces of nearly all tissues in the body. LDL-associated apo B-100 or lipoproteins containing apo E interact with the LDL receptor, where they are subsequently internalized and delivered to lysosomes. Within the lysosome, cholesteryl ester is converted to free cholesterol and apoproteins are degraded to amino acids. Free cholesterol is delivered to the cytoplasm where it inhibits sterol regulatory element binding protein (SREBP) mediated transcriptional regulation of target genes involved in cholesterol synthesis. When cellular cholesterol rises the translocation of SREBP to the golgi is inhibited, as are subsequent signalling steps which ultimately involve the binding of transcription factors to sterol response elements in the promoter area of target genes including hydroxymethylglutaryl-coenzyme A (HMG-CoA) reductase, the rate-limiting enzyme in cholesterol biosynthesis and the LDLr itself (Brown and Goldstein, 1997). Cellular cholesterol homeostasis is

maintained in this fashion. Therefore, lack of LDL receptors results in unregulated cellular cholesterol metabolism as well as significantly increased plasma LDL cholesterol levels.

Figure 2. The receptor-mediated endocytosis of LDL

A) Nascent LDL receptors are synthesized and packaged into vesicles in the Golgi complex. LDL dissociates from its receptors in the acidic environment of the endosome.

B) The vesicles are transported to and fuse with the plasma membrane.

C) LDL receptors on the plasma membrane are clustered within clathrin-coated pits.

D) LDL particles bind with LDL receptors via interactions of the ligand-binding domain and apoB100.

E) Internalization of the LDLr complex through endocytosis of the coated pit. Subsequent fusion with lysosomes decreases the pH of the vesicle causing the dissociation of LDL from the receptor.

F) LDL receptors are transported back to the plasma membrane for re-use

G) LDL particles are degraded into free cholesterol and amino acids.

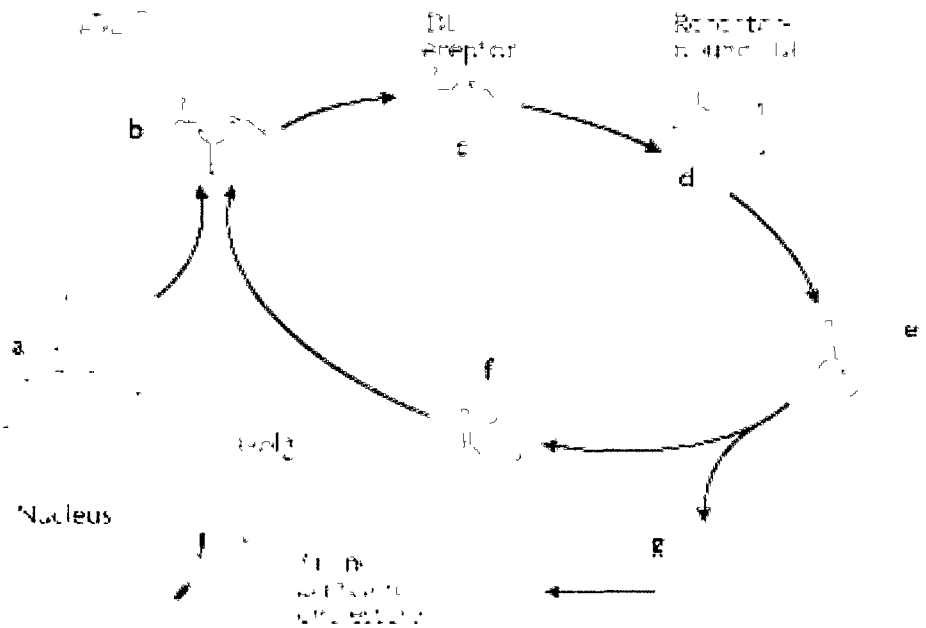

[Adapted with permission from the Nature Publishing Group, (Kishor *et al.*, 2008)]

LDL receptor-mediated endocytosis is not the only method of LDL uptake into a cell, as some pathways utilize non-receptor pathways. These may include fluid phase endocytosis, some of which may be facilitated by binding of lipoproteins to cell surface proteoglycans. It is also likely that some portion of clearance is via other specific receptors, such as LRP and scavenger receptors. Thus, increases in non-LDL receptor-mediated uptake could occur in situations in which LDL oxidation is increased. Much attention has been placed on elucidating the physiology of lipid metabolism in health and disease. In the last couple of decades, researchers have turned to mouse models in order to accurately study these phenomena.

2.6 Mouse models

For many years, the mouse has been a desirable model in which to study various pathologies. The mice are easy to breed, have a relatively short generation time and are highly available, expressing many phenotypes through transgenic approaches. Also, because of their small size, researchers are able to cost-effectively house many mice, thereby increasing the statistical significance of their studies. The major caveat of the murine model within atherosclerosis studies lies in the fact that the model is naturally resistant to atherosclerosis. Because of this phenomenon, mice must become dyslipidemic before atherosclerosis can be initiated. In order to do so, genetic manipulation of gene-encoded proteins involved in lipoprotein metabolism must be induced.

Researchers have developed two genetically modified models that greatly increase the susceptibility of the mouse to atherosclerosis. These are the apoE-null ($apoE^{-/-}$) and LDLr-null ($LDLr^{-/-}$) mouse models. Before going into details of each model, it should be understood that both the $apoE^{-/-}$ and $LDLr^{-/-}$ null mice have many beneficial attributes in common with each other. These mice are produced in large numbers at the Jackson Laboratory, so they are readily available when desired. Both knockouts will yield decent litter sizes, with $apoE^{-/-}$ litters of 6-8 and LDLr litters of 4-6, on average (Whitman, 2004). And finally, the lesions produced in both models have been well documented, so it allows

the researcher to expect a specific stage of lesion within a given time frame. By this token, the models allow for an increased efficiency in time management.

The apoE$^{-/-}$ mouse was first developed by Jorge Piedrahita *et al.* The rationale for developing this model is based on the finding that apoE is the most potent ligand for LDL receptor-mediated removal of lipoprotein remnants from circulation. ApoE-enriched lipoprotein particles, such as VLDL and IDL, are cleared by the LDL receptor (Winder *et al.*, 1980). Also, smaller chylomicron remnants (also enriched in apoE) can be cleared by either the LDL receptor or the chylomicron remnant receptor (Hui *et al.*, 1981; Mahley *et al.*, 1981). ApoE is thus responsible for the cellular uptake of these lipoprotein particles, so by creating a murine model devoid of the apoE protein, Piedrahita had generated an animal much more athero-susceptible than the C57BL6 mouse.

As is suspected, the ability of apoE-deficient mice to clear plasma lipoproteins is greatly impaired, thus yielding a dyslipidemic mouse. For instance, another group led by Andrew Plump created apoE-deficient mice by homologous recombination in ES cells. When fed a low fat, low cholesterol chow diet these apoE$^{-/-}$ mice had plasma cholesterol levels of 494 mg/dl compared to 60 mg/dl in WT animals, and when challenged with a high fat western-type diet, apoE$^{-/-}$ mice had plasma cholesterol levels of 1821 mg/dl compared with 132 mg/dl in wild type mice fed the same diet (Plump *et al.*, 1992). Lipoprotein profiling deduced that the massive increase in cholesterol levels was due to an increase in VLDL-sized particles. Wild type mice have their VLDL levels ranging at about 10-20 mg/dL while in comparison, apoE-null mice have more than 300 mg/dL of their cholesterol in the VLDL density (Plump *et al.*, 1993). ApoE-deficient mice had developed atherosclerotic lesions in the aorta and coronary and pulmonary arteries by 10 weeks of age. A third group, led by Janine H. van Ree, researched the effects of apoE knockout on hyperlipidemia and obtained results consistent with the previous two groups (van Ree *et al.*, 1994), thus solidifying the role of apoE in lipoprotein metabolism.

Another advantage of apoE deficiency is the well documented phenotypical change over the course of time. Characterization of lesion formation was a goal in the very first

apoE-deficient mouse study. In a chow-fed, 3-month-old mouse, fatty streak formation was observed in the proximal aorta. On the same diet, foam cell lesions were observed by light microscopy at 10 weeks of age. Intermediate lesions containing foam cells and smooth muscle cells were seen at 15 weeks, and fibrous plaques appeared at 20 weeks of age (Piedrahita *et al.*, 1992). On a human-like western-type diet, lesion formation is greatly accelerated and lesion size is increased. In 10-week old animals fed this diet for only 5 weeks, developing lesions are 3-4 times the size of those observed in mice fed the regular chow diet (Piedrahita *et al.*, 1992).

In another study by Nakashima *et al.*, gross and histological observations of lesion progression in the apoE$^{-/-}$ mouse were established. On both regular chow and western diets, apoE-null mice were predisposed to lesion development in the aortic root, the lesser curvature of the aortic arch, the branches of the brachiocephalic, right common carotid, pulmonary, superior mesenteric and both renal arteries, as well as the aortic bifurcation. In older animals, lesions were detected in the descending thoracic, lower abdominal, proximal coronary, common iliac, and femoral arteries. Lesions in these groups were primarily detected at 10 weeks of age in the group fed the chow diet, and 8 weeks of age in the group that was fed the Western diet (Nakashima *et al.*, 1994).

Subsequent histological observations made by the same group confirmed that only apoE-null mice developed lesions, and not the control group. The earliest observation using electron microscopy revealed monocytic adhesion to the endothelium throughout the arterial tree at 6 weeks of age. Along with this recruitment of monocytes, the erratic presence of foam cells had accumulated within the subendothelium. Mice fed the chow diet had the same histological results after 8 weeks, but the number of cells recruited was much less than that of the western diet-fed models (Nakashima *et al.*, 1994). Foam cell lesions were observed in the western diet-fed mice after 8 weeks of age and in the mouse fed chow diet after 10 weeks. At 20 weeks of age, mice fed the western diet had developed intermediate lesions that consisted of foam cells and proliferated smooth muscle cells. After 30 weeks, mice on the chow diet still had lesions consisting of only foam cells (Nakashima *et al.*,

1994), insinuating that the chronic high fat diet has an appreciable effect on factors effecting the stimulation of smooth muscle cell proliferation.

Another murine model of atherosclerosis was developed in 1993 by a research team led by Shun Ishibashi. The group knocked out the LDLr gene via homologous recombination and observed evidence of hypercholesterolemia due to a seven-to-nine-fold increase in IDL and LDL with no change to HDL fractions (Ishibashi *et al.*, 1993). In $LDLr^{-/-}$ mice injected with radio labelled VLDL and LDL, the half-lives of the lipoproteins were prolonged by 30-fold and 2.5-fold, respectively. Clearance of radiolabelled HDL remained the same. When fed a diet with 0.2% cholesterol and 10% Coconut oil, LDLr null mice responded with a vast increase in IDL and LDL particles, in contrast to wild type mice, in which lipoproteins did not change (Ishibashi *et al.*, 1993). Finally, to show that these dyslipidemic results were due to the LDLr deficiency, Ishibashi restored the expression of the LDLr via injection of adenovirus encoding for the protein of the gene. Within 4 days after injection, the IDL/LDL levels were normalized.

Humans and rabbits deficient in LDLr will develop severe hypercholesterolemia and pronounced atherosclerosis (Brown and Goldstein, 1990; Buja *et al.*, 1983), but mice will only develop a slight hypercholesterolemia when fed a regular diet (Ishibashi *et al.*, 1993). However, LDLr-null mice are very susceptible to lesion formation when exposed to a dietary modification. For instance, the primary atherogenic diet developed in the laboratory of Dr. Beverly Paigen contained 15% saturated fat, 1.25% cholesterol and 0.5% cholic acid, which led to large atherosclerotic lesions throughout the aorta (Ishibashi *et al.*, 1994). Advantageously, more recent studies have shown that the same results can be obtained with diets excluding cholic acid, which is an unnatural constituent that can lead to hepatotoxicity over long periods of time (Plump and Breslow, 1995). In this way, dyslipidemia can be induced with a diet that is much more indicative of a human western diet.

Tangirala and colleagues studied the extent of lesion formation between genders in LDLr-deficient and apoE-deficient mice. The study analyzed data from 16 LDLr-deficient and 15 apoE-deficient mice that had been exposed to the same diets and experimental

conditions. It was found that male LDLr-deficient mice showed significantly more atherosclerosis than females (29.2 +/- 3.1% of the aortic surface vs. 14.8 +/- 3.2%; $P < 0.005$), whereas the average plasma cholesterol levels of males and females were similar. ApoE-deficient mice also showed a trend towards more lesions in males than in females (27.4 +/- 6.3% of the aortic surface vs. 17.1 +/- 1.6%; $P < 0.005$). It is interesting that the extent of aortic atherosclerosis observed in males of both strains was similar, but the average plasma cholesterol levels were much higher in $apoE^{-/-}$ mice than in $LDLr^{-/-}$ mice (1916 +/- 187mg/dL in $apoE^{-/-}$ males vs. 895 +/-116 mg/dL in LDLr males) (Tangirala *et al.*, 1995). The fact that apoE-null and LDLr-null mice have such a similar occurrence of atherosclerosis, coupled with such a skewed total cholesterol analysis suggest that perhaps LDL-associated cholesterol is more atherogenic than VLDL-associated cholesterol.

Researchers now have options as to how they wish to study atherosclerosis, but it is crucial that protocols utilizing these mouse models are standardized in terms of dietary composition and duration of administration. In this way, true and consistent results can be obtained from murine models that are applicable to the human pathology. The model of atherosclerosis for this study will be the $LDLr^{-/-}$ mouse, fed a high fat diet for 8 weeks. Due to its ability to generate consistent lesions the $LDLr^{-/-}$ mouse is an excellent model to study SR-A biology.

2.7 Scavenger receptors and SR-A

This aptly named group of receptors has been found to bind and 'scavenge' a large array of modified self and non-self ligands, and are thus considered as pattern recognition receptors implicated in both innate and adaptive immunity. Such a wide variety of ligand binding among scavenger receptors led to their categorization into individual classes. Krieger *et al.* (1997) introduced a classification system, which characterizes eight different subclasses (Class A, B, C, D, E, F, G and H), based upon structural differences. The first scavenger receptor to be cloned was type A (SR-A) and was done so using bovine mRNA (Kodama *et al.*, 1990). SR-A has been shown to possess three splice variants, respectively

SR-AI, SR-AII and SR-AIII (Matsumoto *et al.*, 1990). SR-A III was not discovered until recently, but was found to be non-active and sequestered to the endoplasmic reticulum (Gough *et al.*, 1998).

2.7.1 SR-A substrates

It was in 1979 that Goldstein and colleagues discovered scavenger receptors, while trying to decipher how cholesterol was transferred from LDL to atherosclerotic plaques (Goldstein *et al.*, 1979). This protein found on macrophages was revealed to mediate the uptake and degradation of acetylated LDL, thereby causing an increase of intracellular cholesterol deposition. SR-A is able to preferentially bind more extensively oxLDL, recognizing the modified apolipoprotein B (apoB) protein component of this particle (Lougheed *et al.*, 1996; Zhang *et al.*, 1993). By this logic, the scavenger type receptor was originally defined as having affinity for modified LDL, be it oxidized or acetylated.

In addition, SR-A also bind apoptotic cells, β-amyloid (Aβ) peptide, anionic phospholipids, and advanced glycation end-products (Murphy *et al.*, 2005), confirming roles in type II diabetes, Alzheimer's disease and apoptotic cell clearance. These receptors have also been implicated in both innate and adaptive immune responses through their recognition of pathogens and pathogen-associated molecules. For instance, a group showed that mice lacking SR-A expression were more susceptible to infection *in vivo* by the Gram-positive pathogen *Listeria monocytogenes* and the viral pathogen HSV-1 (Suzuki *et al.*, 1997). Furthermore, the demonstration that the SR-A receptor can recognize the lipid A moiety of lipopolysaccharide (Hampton *et al.*, 1991) and that SR-A-null mice are protected from endotoxic shock in an LPS challenge model strengthens the idea of SR-A as an integral pattern recognition receptor of the innate immune system (Hawthorn *et al.*, 1997). Recent studies suggest that among lipopolysaccharides, the bacterial ligands recognized by SR-A include peptidoglycan and lipoteichoic acid as well as various other bacterial surface proteins (Pluddemann, Mukhopadhyay, and Gordon, 2006), thus adding to the already broad array of SR-A ligands.

2.7.2 SR-A structure

In 1990, molecular cloning of bovine SR-A led to the discovery that the type A scavenger receptor is a transmembrane glycoprotein, consisting of six domains (Kodama *et al.*, 1990). In humans, the gene coding for the six domains spans 80 kb and contains 11 exons (Emi *et al.*, 1993). Of the six domains, the collagen domain has been shown to be the binding site for modified lipoproteins. A lycine motif exists within this domain, which forms a positively charged groove for ligands of polyanionic nature to fit nicely (Doi *et al.*, 1993). The domains of SR-A were characterized by Kodama and group to consist of a cytoplasmic tail, a transmembrane domain, a spacer region, an alpha helical coiled-coil domain, a collagenous domain and a C-terminal cysteine rich domain (Kodama *et al.*, 1990).

Figure 3. Schematic representation of SR-A (type I and II) structure

The types I and II share 5 identical domains. The 110 amino acid C-terminal cysteine-rich domain of the type I receptor is replaced with a 6-amino acid C-terminus in the type II receptor. These receptors are usually co-expressed and they display the same ligand binding affinities.

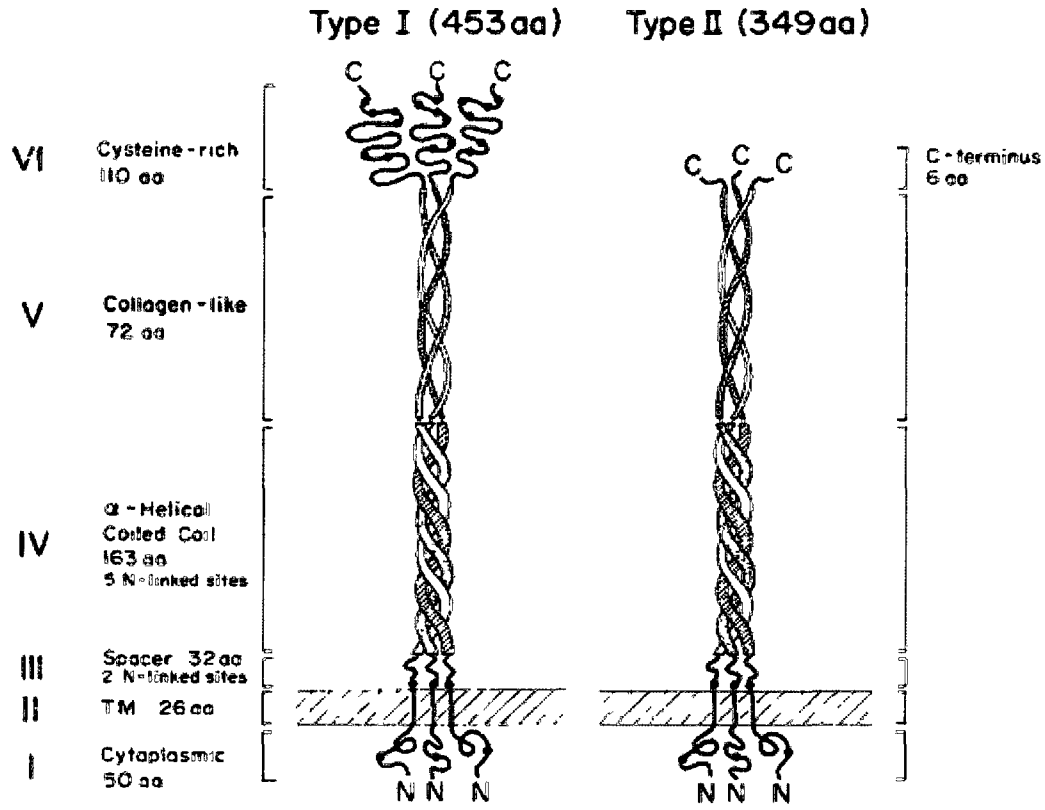

[Adapted with permission from John Wiley and Sons, (Bowdish and Gordon, 2009)]

Domains of the utmost importance to this study include the cytoplasmic and the collagen-like domains. Of the three isoforms, SR-AI and SR-AII share identical domains with exception to SR-AI having an additional C-terminal cysteine-rich domain (Kodama *et al.*,1990). The function in the C-terminal cysteine-rich domain of SR-AI and differences in expression and physiological function of the SR-A1 and SR-AII are not known (Kodama *et al.*, 1990). The third isoform SR-AIII has a truncated collagenous region and has no established role (Gough *et al.*, 1998) and therefore, no bearing in this study. For the remainder of this review, SR-A will depict SR-A types I and II unless otherwise stated.

Upon ligand binding, SR-A mediates ligand internalization and via signalling pathways, concomitantly induces transcription of cytokines respective to the specific ligand (Pluddemann, Neyen, and Gordon, 2007). Studies by Freeman *et al.* (1991) have elucidated that acetylated LDL and oxidized LDL will compete with their own binding sites, but not for each others, suggesting they bind different sites in the collagen domain. Extended knowledge of these SR-A domains and their functions is crucial to understand not only the role of SR-A in normal ligand uptake, but also pathophysiological processes. Much controversy was spent over whether or not SR-A mediated adhesion was controlled by the same factors controlling receptor endocytosis. In 2003, Kosswig and group determined that these two phenomena required two distinct domains (Kosswig et al., 2003).

2.7.3 SR-A expression

SR-A is expressed by macrophages, foam cells, smooth muscle cells (Bickel and Freeman, 1992) and endothelial cells (Daugherty *et al.*, 1997), which are all able to take up modified LDL. AP-1 sites found within the SR-A promoter area have been shown to induce transcription of SR-A within monocyte colonies upon stimulation with macrophage colony stimulating factor (Moulton *et al.*, 1994). Elevated expression of SR-A within atherosclerotic lesions was also controlled by these AP-1 elements, thus conferring that the AP-1 site may be a potential target in SR-A studies. SR-A expression has been found to be quite low on isolated monocytes, but greatly upregulated upon macrophage differentiation, as well as on dendritic cell surfaces (Becker *et al.*, 2006), thus further confirming SR-A's

role in innate immunity. SR-A types I and II have both been shown to be present in atherosclerotic lesion-forming areas. Some reports have accounted for expression of SR-A on smooth muscle cells surrounding lesion areas. Other studies did not find SR-A expression on smooth muscle cells (Mietus-Snyder *et al.*, 1997) but still witnessed expression on macrophage foam cells within the lesions (Lumoa *et al.*, 1994).

2.7.4 SR-A roles in atherosclerosis

There are a number of ways that SR-A function can contribute to atherosclerosis. One of the dominant key steps to the progression of atherogenesis is the differentiation of monocytes into macrophages, and their subsequent adherence to other cells such as endothelial cells, smooth muscle cells and/or other macrophages. Strong in vitro data suggests that SR-A expression is imperative for this adherence. SR-A is also responsible for the uptake of apoptotic cellular debris within lesion areas thereby directly affecting macrophage retention in the arterial wall. Also, the arterial basement membrane proteins can undergo non-enzymatic glycation during aging and at an accelerated rate in diabetic patients. As time passes, these glycosylated proteins form advanced glycation end products (AGE). Studies have shown these AGE products to be taken up via SR-A signalling pathways (Araki *et al.*, 1997). Another group showed that macrophages were able to attach themselves to surfaces containing glucose modified basement membrane collagen IV, through SR-A interaction (El *et al.*, 1994). In vitro experiments by Fukuhara-Takaki *et al.*, (2004) showed that human monocyte-derived macrophages displayed increased SR-A expression under high glucose conditions, along with an increase in endocytic uptake of modified LDLs. Moreover, uptake of modified LDLs was also increased in macrophages obtained from diabetic mice, and a study by Guest *et al.*, used flow cytometry to show that macrophages from diabetic mice have an 80% increase in SR-A expression compared to cells from WT mice (Guest *et al.*, 2007). These results are significant because they highlight the role of SR-A in atherogenesis, but it also provide a potential explanation to the trend seen with accelerated atherogenesis in diabetic patients. Subsequently, further *in vitro* studies have shown ligation of SR-A with AGE products results in cytokine release that leads to a prolonged inflammatory response (Palkama, 1991); thereby strengthening the

atherogenic cycle. The cytokines released act upon endothelial cells, smooth muscle cells and other macrophages, thus causing a snowball effect. Binding of LDL or AGE products results in the activation of macrophages, although, different ligands within a lesion will illicit a different cytokine to be produced and this is why SR-A can be found to have both anti and pro-atherosclerotic properties. Of most relevance to the current study was a recent publication by (Wang *et al.*, 2009), wherein they show a novel peptide association with the cytoplamic domain of SR-A resulting in a decreased acLDL binding and uptake.

The results of SR-A regulation in various models have been mixed. In the $apoE^{-/-}$ mouse model of atherosclerosis, SR-A deficiency led to a 58% decrease in lesion development in the aortic root (Suzuki *et al.*, 1997), while another $apoE^{-/-}$ mouse study has shown that overexpression of SR-A failed to affect lesion progression (Van *et al.*, 2000). In the $LDLr^{-/-}$ mouse model of atherosclerosis, the results of SR-A regulation have also shown varying results. One study demonstrated that an $SR\text{-}A^{-/-}/LDLr^{-/-}$ mouse model showed a 20% decrease in atherosclerosis (Sakaguchi *et al.*, 1998), while another group showed that overexpression of SR-A in an $LDLr^{-/-}$ model resulted in a 27% decrease in the disease (de Winther *et al.*, 1999). The significance here is that SR-A does exhibit a role in lesion formation, albeit pro or anti -atherosclerotic.

A large collaborative effort studied aortic root atherosclerosis in $apoE^{-/-}$ $CD36^{-/-}$ $SR\text{-}A^{-/-}$ mice, as assessed by morphometry, electron microscopy, and immunohistochemistry. The results showed no decrease in lesion area or *in vivo* foam cell formation when compared to $apoE^{-/-}$ mice. Interestingly, $apoE^{-/-}$ $CD36^{-/-}$ $SR\text{-}A^{-/-}$ lesions showed reduced expression of inflammatory genes and morphological analysis revealed an approximate 30% decrease in macrophage apoptosis and a striking approximate 50% decrease in plaque necrosis in aortic root lesions of these mice (Manning-Tobin *et al.*, 2009). This study suggests that the *in vivo* function of scavenger receptors may hold more prominent roles in lesion complexion and plaque stability. Whether SR-A plays a role in all stages lesion progression or just some niches has yet to be fully elucidated, but the current literature is promising and thus warrants further investigation into this proteins role in atherosclerosis.

Previous studies conducted by our lab have shown that binding of SR-A to modified LDL not only functions in the uptake of modified LDL, but SR-A also participates as a signal transducer via activation of a secondary messenger signalling peptide associated with the cytoplasmic domain. (Whitman Lab, unpublished data). Subsequent efforts to determine the identity of an adapter protein bound to the cytoplasmic domain were conducted. Using a 58 amino acid polypeptide representing the cytoplasmic domain of SR-A fused to glutathione S-transferase (GST) to affinity purify proteins that associate with the SR-A cytoplasmic tail, a distinct protein band was discovered after exposure to mouse macrophage lysate. Sequencing of the band and subsequent confirmation with commercial antibody has identified the protein as insulin degrading enzyme (IDE).

Figure 4. A) Schematic of affinity chromatography pull-down

We used a strategy of affinity chromatography in conjunction with primary protein sequencing by matrix-assisted laser desorption / ionization mass spectroscopy to identify novel proteins that associate with the SR-A cytoplasmic tail. Cytosol from J774 mouse macrophages was incubated with either a purified *E.coli*-expressed recombinant fusion protein composed of the cytoplasmic tail of SR-A, a thrombin-cleavage site and glutathione-S-transferase (GST) (SRA-cytoplasmic tail-GST) or with recombinant GST. After incubation, the mixtures were subjected to affinity chromatography on a glutathione-sepharose column and cytosolic proteins that bound to the SRA-cytoplasmic tail-GST or to GST were eluted following thrombin digestion. Eluted proteins were subjected to SDS polyacrylamide gel electrophoresis and bands representing proteins that had associated with the SRA cytoplasmic tail-GST but not with GST alone were cut out and identified by matrix-assisted laser desorption / ionization mass spectroscopy. The specificity of the interactions was subsequently confirmed by western blotting.

A)

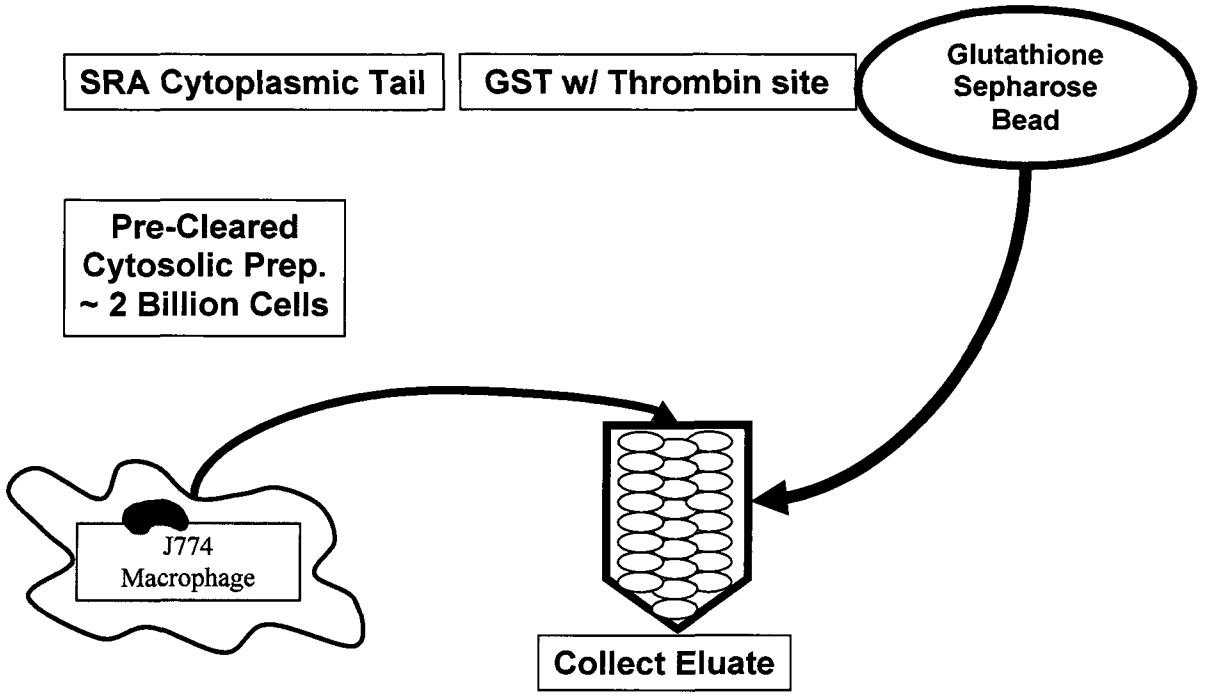
SRA Cytoplasmic Tail
GST w/ Thrombin site
Glutathione Sepharose Bead
Pre-Cleared Cytosolic Prep. ~ 2 Billion Cells
J774 Macrophage
Collect Eluate

Figure 4. B) Affinity chromatography elution and use of primary antibody

Silver stained SDS-PAGE of fractions from the affinity column. A novel protein of ~110 kDa was found to associate with the GST-SRA tag, but not with GST alone (red outline). By mass spectroscopy, the protein was identified as insulin degrading enzyme. A second protein with of larger molecular weight (indicated by the arrow) also specifically bound to the GST-SRA was identified as E3 ubiquitin ligase. (B). Subsequent analysis of the thrombin elution with a commercially available antibody confirmed the identity of the ~110 kDa protein band as insulin degrading enzyme (C).

B)

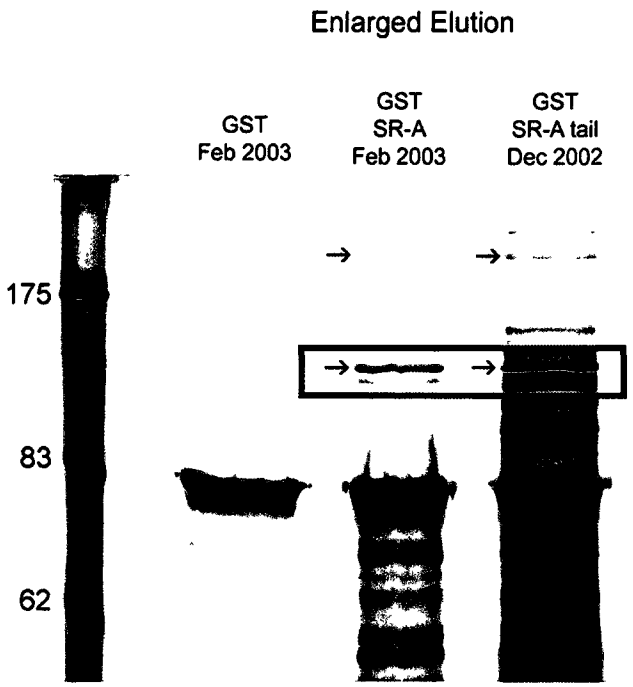
Enlarged Elution
GST
Feb 2003
GST
SR-A
Feb 2003
GST
SR-A tail
Dec 2002
175
83
62

C)

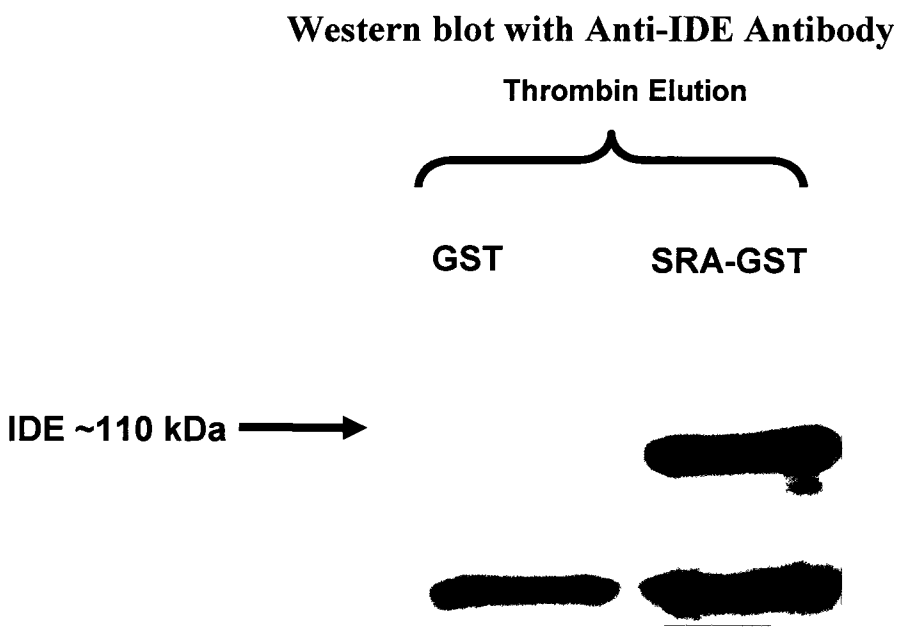
Western blot with Anti-IDE Antibody
Thrombin Elution
GST
SRA-GST
IDE ~110 kDa

2.8 Insulin Degrading Enzyme

IDE is a110-kDa, ubiquitously expressed zinc-metalloendopeptidase that has shown to be located in cytosol, peroxisomes, and on the cell surface (Duckworth, Bennett, and Hamel, 1998). It has been established (Song *et al.*, 2005) that IDE exists as a mixture of monomers, dimers, and tetramers. The gene encoding IDE is located within a region of chromosome 10 where interestingly, recent reports have identified a locus associated with Late Onset Alzheimer's Disease (LOAD) (Bertram *et al.*, 2000).

2.8.1 IDE structure

Structures of human IDE in complex with amyloid-Beta (Aß), insulin B chain, amylin, and glucagons were shown in a study (Shen *et al.*, 2006). These structures reveal that IDE has 56-kDa amino and carboxy terminal domains, IDE-N and IDE-C, which are joined by a 26-amino acid loop. The amino- and carboxy-terminal domains of IDE form an enclosed cage just large enough to encapsulate insulin. Interaction between IDE-N and IDE-C keep the degradation chamber of IDE inaccessible to substrates. Repositioning of the IDE domains enables substrate access to the catalytic cavity (Shen *et al.*, 2006). The amino and carboxy terminal domains are like two bowl-shaped halves joined by a hinge at one end and held closed by a latch of hydrogen bonds on the other end. When the bowls join together, they enclose a chamber with a base that measures 35 x 34 x 30 angstroms and a height of 36 angstroms, which is just large enough to contain relatively small peptides (Malcolm *et al.*, 2006).

Biochemical and structural assays carried out by Shen *et al* (2006) have confirmed that there are at least four factors contributing to the substrate recognition of IDE. The first factor involves favorable binding of the substrate N terminus and cleavage sites to the ß-strands within IDE. Substrate-bound IDE structures reveal that IDE substrates need to undergo a conformational switch to form ß-strands with two discrete regions of IDE for its degradation (Li *et al.*, 2006). The second factor requires solid anchoring of the cleavage site in the catalytic cleft. For the most optimal binding conditions, substrates must not have a

significant positive charge at their C-terminus, in order to avoid charge repulsion. Hormones such as atrial natriuretic peptide, glucagon and insulin growth factor II lack positive charges at their C-terminals and therefore, are good IDE substrates. The last factor is size, since the catalytic chamber is only large enough to fit relatively small peptides (~50 amino acids) (Malcolm *et al.*, 2006). This molecular foundation for substrate recognition and allosteric regulation of IDE could aid in designing IDE-based therapies. As discussed later IDE may have implications in the regulation of cerebral Aß deposition, blood sugar concentrations and possibly atherogenesis.

Figure 5. Insulin degrading enzyme action and regulation

a) The crystal structures of IDE reported by Shen *et al.* reveal a latch mechanism (shown in green) that holds the enzyme in a closed state, delaying entry of the substrate or exit of the cleavage products.

b) Mutations (shown in red) are able to disrupt the latch promote the open conformation of the enzyme. Mutants such as these accept substrates and release products more readily than naturally occurring IDE, thereby increasing their activity.

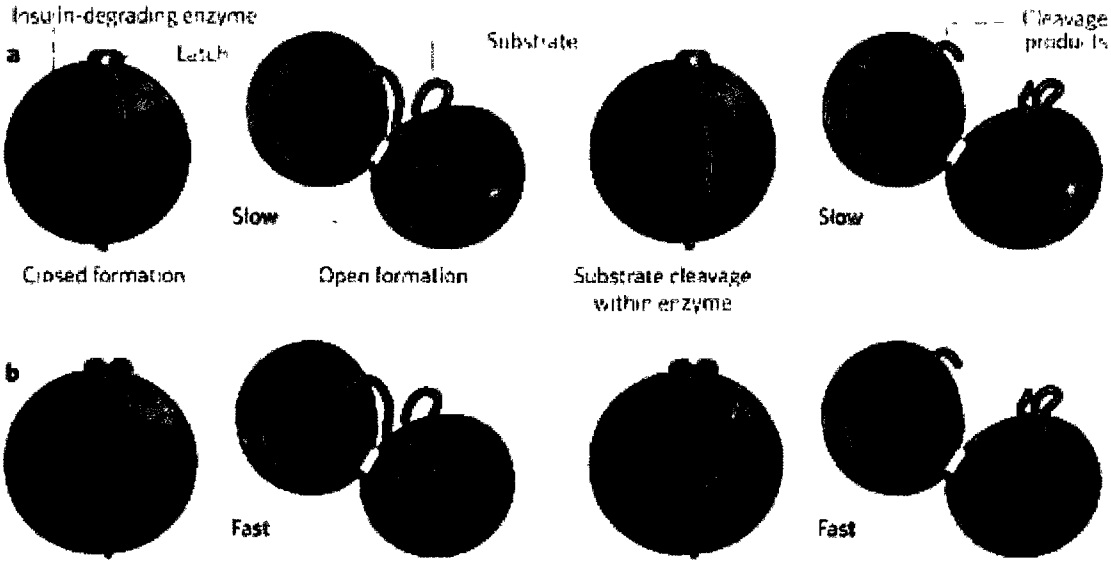

[Adapted with permission from Nature Publishing Group, (Leissring and Selkoe, 2006)]

2.8.2 IDE expression

Immunohistochemical staining was performed on a human, multi-organ tissue microarray, including pancreas, lung, kidney, central/peripheral nervous system, liver, breast, placenta, myocardium, striated muscle, bone marrow, thymus, and spleen. IDE protein was expressed in all the tissues assessed as well as trophoblast cells and granulocytes (Weirich *et al.*, 2008). Although IDE is ubiquitously expressed, its highest expression is in the liver, testes, muscle and brain (Kuo, Montag, and Rosner, 1993). Its expression has been shown to be regulated during cellular differentiation and growth, with IDE mRNA levels increasing in the brain and testes when development progresses (Baumeister *et al.*, 1993). Taking this further, Runyan *et al.* (1979) showed that IDE expression is affected by aging, with IDE activity significantly reduced in both the muscles and liver of old animals, compared to that of young animals.

Although most IDE is intracellular, a fraction of the enzyme was shown to be labeled by a membrane-impermeable agent, thus indicating that IDE is present on the extracellular surface of some cells (Seta and Roth, 1999). In terms of insulin signalling, this may indicate that IDE could participate in insulin degradation extracellularly, especially considering that receptor-bound insulin has been shown to bind IDE (Yonezawa *et al.*, 1988).

The exact mechanism by which IDE locates itself outside the cells has yet to be fully elucidated, however it appears to be expressed on the surface of some cells as well as in extracellular compartments. Qiu (2006) identified intact IDE in human CSF, further implicating that IDE can be secreted and does exist in extracellular fluid under physiological conditions.

2.8.3 IDE activity and regulation

Zn^{2+} is the metal bound to IDE. The active site of IDE consists of the sequence His-Glu-aaaa- His (HEXXH), where the two histidines facilitate the binding of the zinc atom, while the glutamate plays an essential role in catalysis (Authier *et al.*, 1996; Becker and

Roth, 1995). In terms of cellular insulin degradation, the effects of modifiers (*e.g.*, Ca^{++}) and inhibitors [*e.g.*, bacitracin and *N*-ethylmaleimide (NEM)] are consistent with the properties of IDE (Ryan *et al.*, 1985). Intracellular insulin degradation is initiated in endosomes, which contain IDE (Pell *et al.*, 1986), and it has been shown that cellular and endosomal degradation both respond to modifiers of IDE activity. IDE is sensitive to chelators, although inactivation requires extensive treatment with EDTA. Metal-deprived enzyme or enzyme that has been mutated to remove the Zn^{++} binding site retains substrate binding activity but is without proteolytic activity (Gehm *et al.*, 1993).

Other divalent cations may play a role in the activity of IDE, as chelator-inactivated enzyme can be reactivated by Zn^{++}, Mn^{++}, Co^{++}, and Ca^{++}. For instance the Zn^{++} reactivation curve shows a pattern with low concentrations activating the enzyme and higher concentrations inhibiting. However, other divalent cations that reactivate the enzyme show little inhibition at higher concentrations and can increase activity above that of the starting material. In particular, Ca^{++} may play a role in the activity of the enzyme in cells as Ca^{++}-depleted muscle has decreased insulin degradation and reduced IDE activity, which is restored with Ca^{++} addition (Ryan *et al.*, 1985).

IDE also exhibits allosteric properties, such as being activated by peptide associations. Interestingly, it was shown that some peptides activated IDE toward Aβ peptide cleavage but not toward insulin cleavage (Song *et al.*, 2003). An approximately 2.5-fold increase in the rate of Aß peptide hydrolysis is produced by peptide dynorphin B-9, but with insulin as substrate, dynorphin B-9 is inhibitory (Song *et al.*, 2003). Thus, it is apparent various substrates of IDE are suggested to affect catalytic activity and cause local conformational changes that affect the allosteric properties of the enzyme. This finding implicates that if IDE were to be used as a therapeutic target, it may be possible to control its specificity and rate of activity, in order to optimize the treatment.

2.8.4 IDE substrates

IDE's substrates share little to no homology within their primary amino acid sequence, but have similar secondary structure and amyloidogenic character (Bennett, Duckworth and Hamel, 2000). Therefore, it has been suggested that IDE likely plays a role in catabolic regulation, such as the prevention of amyloid deposit formation by cleaving the component peptides. Most notably, IDE has been shown to hydrolyze Aß and insulin, which are peptides associated with Alzheimer disease (AD) and diabetes, respectively (Im *et al.*, 2007). Cleavage of Aß by IDE resulted in the decrease of neurotoxic effects of the peptide and prevented the deposition of Aß onto a synthetic amyloid deposit (Mukherjee *et al.*, 2000). It has been shown in cell cytosol fractions that IDE also degrades the Aß precursor protein (APP) intracellular domain (AICD) (Edbauer *et al.*, 2002) which can otherwise reach the nucleus (Kimberly *et al.*, 2001), and participate in transcriptional regulation (Cao and Sudhof, 2001).

To establish whether IDE hypofunction decreased Aβ and insulin degradation *in vivo* and as a result, chronically increased their levels, Farris and group utilized mice with homozygous deletions of the IDE gene (Farris *et al.*, 2003). IDE deficiency resulted in a >50% decrease in Aβ degradation in both brain membrane and primary neuronal cultures, with a similar deficit in insulin degradation in liver. The $IDE^{-/-}$ mice showed increased cerebral accumulation of endogenous Aβ, a hallmark of AD, and demonstrated hyperinsulinemia and glucose intolerance, which are hallmarks of DM2 (Farris *et al.*, 2003).

Also, it has been shown that ubiquitin forms a complex with, and inhibits the activity of IDE within the cells (Saric *et al.*, 2003), thus suggesting another regulatory mechanism of IDE's activity within the cell. These results back up the theory that IDE is widely functional throughout different tissue types and therefore may posses multiple effects on biochemical processes. More will be reviewed on IDE`s roles in DM2 and AD further on.

2.8.5 IDE and its role in insulin degradation and type 2 diabetes

The first step of insulin degradation is the same as in insulin action; binding to the receptor. This finding has led to the paradigm that degradation of receptor bound insulin is able to terminate insulin action. As described, the initial step of insulin processing is receptor binding. Internalized, receptor-bound insulin can either return intact or partially degraded insulin back to the circulation or deliver the hormone to an intracellular site (Hamel *et al.*, 1987). These pathways include degradation of insulin in endosomes just before acidification (Surmacz *et al.*, 1988; Backer *et al.*, 1990) or delivery of intact insulin and degradation products to other subcellular sites. In fact, Hamel further showed that the degradation products of isolated rat liver endosomes were identical to the products extracted from intact cells. (Hamel *et al.*, 1988) There is good evidence that IDE plays a large role in endosomal insulin degradation. Western-blot analysis of endosomal protein with anti-IDE antibody has shown IDE to be present in endosomes, and the degradation products are consistent with limited cleavage of insulin by this enzyme (Hamel, Mahoney, and Duckworth, 1991). Further, overexpression of IDE in cultured cells has been found to increase the rate of insulin degradation (Kuo *et al.*, 1994), while the injection of IDE specific antibodies into the cells inhibited the process of insulin degradation (Shii *et al.*, 1986). Not all insulin is degraded, as a substantial portion can be returned to circulation intact or partially degraded (Levy and Olefsky, 1987). In fact, the amount of endosomal insulin degraded does not exceed 50% and the remainder is delivered to other subcellular compartments such as cytosol, nucleus and lysosomes (Harada *et al.*, 1995; Authier *et al.*, 1996; Hari *et al.*, 1987).

It has not been fully established as to how insulin reaches other cellular compartments, but there is good evidence that IDE may play various roles. Internalized insulin has been shown to cross-link to cytosolic IDE (Hari *et al.*, 1987), and another group showed that pharmacological inhibition of cytosolic IDE activity increased insulin translocation to the nucleus (Harada *et al.*, 1994). Harada also showed that inhibited IDE activity due to high cytosolic insulin levels also resulted in more nuclear insulin (Harada *et*

al., 1993), suggesting that IDE not only degrades receptor bound insulin, but cytosolic IDE may chaperone insulin to other subcellular sites, including the nucleus. Therefore, modulation of IDE activity may significantly affect insulin accumulation and signalling.

IDE is able to complex with, and regulate certain cytosolic organelles, specifically proteasomes, androgen and glucocorticoid receptors. IDE activates proteasome and steroid receptors by increasing proteasome proteolytic activity and increasing steroid receptor binding to DNA (Kupfer *et al.*, 1993). Since inhibition of protein degradation, fatty acid oxidation, and steroid action are biological effects of insulin (Smith *et al.*, 1997), these findings raise the possibility that a direct cytosolic interaction of internalized insulin with IDE could be involved in these cellular effects, thus modulating protein and fat metabolism (Duckworth *et al.*, 1997). Therefore, most evidence supports a role for IDE as the primary degradative mechanism, although other systems (PDI, lysosomes, and other enzymes) undoubtedly contribute to insulin metabolism. Additionally, more recent studies support a multifunctional role for IDE, as an intracellular binding and regulatory protein.

Leissring and colleagues used an $IDE^{-/-}$ mouse model to study the effects of IDE deficiency and its contribution to a diabetic phenotype. Indeed, IDE-null mice showed a 2.8 fold increase in their fasting serum insulin levels. Fasting glucose levels remained unchanged, although IDE-null mice showed marked hyperglycemia at 1 hour and 2 hours post glucose load, compared to WT controls. Additionally, liver membrane and cytosolic fractions from $IDE^{-/-}$ mice showed a near 50% decrease in the degradation of insulin compared to controls. Therefore, Leissring shows that IDE deficiency is sufficient to cause chronic hyperinsulinemia and postprandial hyperglycemia, which are two hallmark features of DM2.

2.8.6 IDE in Alzheimer's disease

Several epidemiology studies have shown that type 2 diabetes increased the risk of Alzheimer's disease (AD) in both cross-sectional and prospective populations. Further,

elevated peripheral insulin, a common indicator of type 2 diabetes, has been identified as a possible independent risk factor of AD. In studies following large populations prospectively, type 2 diabetes subjects as compared to the non-diabetic control group have double the risk of AD (Arvanitakis *et al.*, 2004). Moreover, the rate of onset of AD is higher among patients who have suffered from type 2 diabetes for more than 5 years compared to those with a disease duration of less than 5 years (Leibson *et al.*, 1997). Furthermore, several studies have shown that serum insulin concentrations were higher among AD patients as compared to a control group (Carantoni *et al.*, 2000).

The link between diabetes and AD is shown in the GK rat, which is an animal model of type 2 diabetes. IDE gene mutations cause a naturally occurring, partial loss of IDE function, and this is sufficient to cause diabetes in these animals, which phenotypically express hyperinsulinemia and glucose intolerance (Farris *et al.*, 2004). This model was used by Farris and colleagues to show that naturally occurring IDE missense mutations in a well-characterized rat model of type 2 diabetes resulted in decreased catalytic efficiency and a significant 15 to 30% deficit in the degradation of both insulin and Aβ. Since Aβ is secreted extracellularly, and is deposited outside the neurons in the AD brain, another group took an approach to screen for any secreted protease(s) in neuronal and non-neuronal cell culture media for their ability to degrade Aβ. Among all secreted proteases from the cells, only IDE degraded Aβ (Qiu et al., 1998). The group also showed that under physiological conditions IDE is secreted at high levels from the microglial cells, and degrades Aβ extracellularly. The mechanisms of IDE secretion are still poorly understood. However, another group showed that extracellular IDE levels decrease and Aβ levels increased when the generation of multivesicular bodies was interfered with, thereby suggesting IDE excretion via exosomes (Bulloj *et al.*, 2010). These results further reinforce the importance of functional IDE in the catabolism of extracellular Aβ, but more importantly show that IDE is able to be secreted from another form of resident macrophage.

It is hypothesized that IDE plays a major role in the association of hyperinsulinemia and type 2 diabetes with AD. Qiu *et al.* (1998) presents evidence that AD may be caused by decreased Aβ clearance by IDE, or by IDE deficiency itself. Aß-degrading activity of IDE

was shown to be lower in AD brains than controls (Perez *et al.*, 2000), while the amount of hippocampal IDE protein was also found to be reduced in AD brains as compared to controls (Cook *et al.*, 2003). A murine IDE knockout model showed elevated Aβ levels in the brain (Farris, 2003), while enhanced IDE activity in an IDE/APP (amyloid precursor protein) double transgenic murine model showed decreased Aβ levels and thereby reduced AD pathology (Leissring *et al.*, 2003). Therefore, IDE activity is a crucial determinant in Aβ deposition and Alzheimer's disease.

2.9 Alzheimer's disease and type 2 diabetes links to atherosclerosis

The pathogenesis that is primarily responsible for vascular dementia appears to involve chronic hypoperfusion (Aliev *et al.*, 2008), which is a direct manifestation of atherosclerosis. Various animal model studies have revealed that the formation of Aβ and other derivatives of APP are key factors in cellular changes in the AD brain, including the generation of free radicals (Selkoe, 2001), oxidative damage (Mattson, 2004), and inflammation (Tanzi and Bertram, 2005). Recent molecular, cellular, and gene expression studies have revealed that Aβ enters mitochondria, induces the generation of free radicals, and leads to oxidative damage in post-mortem brain neurons from AD patients and in brain neurons from cell models and transgenic mouse models of AD (Cardoso *et al.*, 2001; Lustbader *et al.*, 2004). Further, immunohistochemical analyses have identified Aß peptide in advanced human coronary artery atherosclerotic lesions (Koldamova *et al.*, 2005). Studies have also shown a positive link between cellular cholesterol metabolism and Aß deposition in the brain and vasculature (Koldamova *et al.*, 2005; Hirsch-Reinshagen *et al.*, 2005). Furthermore, cholesterol oxidation products generated during atherosclerosis have been reported to accelerate Aß fibril formation, thereby providing a potential mechanism for the accumulation of this peptide in atherosclerotic lesions (Zhang et *al.*, 2004). The deposition of Aß within the coronary arteries suggests that IDE function and/or expression may be altered, just as is seen in AD brains. The relationship between cholesterol metabolism and Aß deposition in the brain and vasculature further supports the paradigm that vascular dementia can be attributed to atherosclerosis of the brain vasculature. These

results strengthen the converging factors central to Alzheimer's and atherosclerosis and place IDE at their crossroads.

In fact, both AD and DM2 seem to share a common etiology, in that they both exhibit amyloid aggregation within neurons and B-cell islets respectively. A cohort study revealed that AD patients more commonly had type II diabetes, impaired fasting glucose and islet amyloid than non-AD controls (Janson *et al.*, 2004). Evidence is growing to link precursors of amyloid deposition in the brain and pancreas with the pathogenesis of Alzheimer disease and type II diabetes. Therefore it is of great interest to note the selective affinity of IDE for peptides of amyloidogenic nature (de Tullio *et al.*, 2008)

Diabetic patients have an increased risk for cardiovascular complications with respect to the general population. Macrovascular complications such as atherosclerosis and coronary artery disease are usually preceded by endothelial dysfunction, a condition characterized by impaired vasorelaxation which results from reduced bioavailability of the endothelial mediator nitric oxide (NO) (Nacci, 2009). NO is among endothelial mediators released by endothelial cells in response to insulin stimulation. Therefore, metabolic abnormalities associated with diabetes, such as insulin resistance, dyslipidemia, compensatory hyperinsulinemia and hyperglycemia may all contribute to impair NO bioavailability, via accelerated NO degradation by ROS (Potenza, 2009) and abnormal vasodilatation in diabetic patients. Besides vasodilatation, NO inhibits platelet activation, prevents leukocyte adhesion, and inhibits VSMC migration and proliferation (Nacci, 2009), which are all factors that occur within atherogenesis.

Macrophage-related oxidative stress plays an important role in the inflammatory process in atherosclerosis. Recently, dextromethorphan (DXM), a common cough-suppressing ingredient, was found to inhibit the activation of microglia, the resident macrophage in the nervous system. Microglia pretreated with DXM was shown to significantly suppress the production of tumour necrosis factor-alpha, monocyte chemoattractant protein-1, interleukin-6, interleukin-10, and superoxide in macrophage cell culture after stimulation (Liu, 2009), which would result in a reduction of monocyte recruitment, extravasation as well as oxidative stress.

Inflammation and oxidative stress are central in the pathogenesis of atherosclerosis. Monocyte-derived superoxide contributes to the oxidative stress in the vessel wall inflammation, which is required for LDL cholesterol oxidation (Cathcart *et al.*, 1989). Superoxide also stimulates monocytes to secrete a variety of pro-inflammatory factors such as tumour necrosis factor-alpha, monocyte chemoattractant protein-1, interleukin-6, and interleukin-10, all of which are important regulators or modulators of the inflammatory reaction in the vessel wall (Ohara *et al.*, 1993). Moreover, the scavenger receptors, which are thought to be culprits involved in various aspects of pro-atherosclerotic events, have been shown to have roles in Alzheimer's disease (Husemann *et al.*, 2002) and type 2 diabetes (Horiuchi *et al.*, 2003) (via interaction with Aß and AGE products, respectively).

Chapter 3: Rationale and Objectives

The effects of modifying SR-A expression *in vivo* has yielded both anti- and pro-atherogenic results, but almost all studies regarding a change in SR-A expression have shown a change in lesion development. Due to this trend, there is a strong consensus in the atherosclerosis community that SR-A function encompasses a major role in the disease process. This justifies the requirement for a clearer mechanistic knowledge of this protein's function and regulation. When taking into consideration that both IDE and SR-A have been shown to share pathological links to Alzheimer disease and type 2 diabetes, as well as our lab's finding that IDE binds the cytoplasmic domain of the SR-A protein, it seems logical that IDE may contribute to SR-A's role in these pathologies, as well as atherosclerosis. The purpose of this study is to determine if IDE expression/knockout by cells of the hematopoietic system have any role in the pathology of atherosclerosis. To show this, our lab will lethally irradiate in the $LDLr^{-/-}$ and $IDE^{-/-}/LDLr^{-/-}$mice and use subsequent bone marrow transplantation in order to generate unique chimera mouse models of atherosclerosis to determine if reconstitution with marrow from IDE competent versus IDE deficient mice will yield less atherosclerotic lesion formation. Along with this, *ex vivo* assays will determine if IDE expression by bone marrow-derived cells plays a role in foam cell formation and if this is dependant on SR-A function. A better understanding of the role of IDE in macrophage SR-A function may prove to be an important step in the direction of developing a therapeutic treatment for atherosclerosis.

Objectives and Hypothesis

Hypothesis:

IDE expression in bone marrow-derived cells has a significant effect of decreasing atherosclerotic lesion burden, and foam cell formation.

Aims:

1. Determine the contribution of IDE to lesion formation in 4 *in vivo* models of atherosclerosis susceptible mice:
    A) Determine the contribution of IDE knockout solely in bone marrow-derived cells to lesion formation by performing a bone marrow transplant from WT and IDE $^{-/-}$ mice into LDLr$^{-/-}$ mice. (WT = control)
    B) Determine the contribution of IDE expression solely in bone marrow-derived cells to lesion formation by performing a bone marrow transplant from WT and IDE$^{-/-}$ mice into IDE $^{-/-}$LDLr$^{-/-}$ mice. (IDE$^{-/-}$ = control)

2. Demonstrate a role for IDE in foam cell formation *in vitro* by determining if in the absence of IDE the progression of foam cell formation is altered in bone marrow-derived macrophages, using:
    A) Oil red O staining of lipid uptake
    B) AcLDL binding assay
    C) AcLDL uptake assay
    D) Cholesteryl ester accumulation assay

Chapter 4: Experimental Procedures

4.1 Animal care

$IDE^{-/-}$ and $LDLr^{-/-}$ mice, backcrossed >20 times into a C57BL/6 background, were obtained from Dr. Suzanne Guenette (Harvard Medical School) and the Jackson Laboratory (Bar Harbor), respectively. $IDE^{-/-}$ mice where crossed with C57BL/6 mice to generate F1 $IDE^{+/-}$ mice, which were subsequently bred together to generate F2 $IDE^{+/+}$ and $IDE^{-/-}$ littermates to serve as the BM-donors. In similar fashion, F1 $IDE^{+/-}$x $LDLr^{-/-}$ mice were bred together to generate F2 $IDE^{-/-}$x $LDLr^{-/-}$ and $IDE^{+/+}$x $LDLr^{-/-}$ littermates to serve as the second set of bone marrow-recipients. Polymerase chain reaction was carried out on DNA from mouse tail samples to screen for IDE and LDLr gene expression. This investigation conforms to the *Guide for the Care and Use of Laboratory Animals* published by the US National Institutes of Health (NIH Publication No. 85-23, revised 1996).

4.2 Bone marrow transplant study

To study the effect of hematopoietic cell IDE expression and knockout in atherosclerosis formation, we conducted a bone marrow transplant (BMT) study. $LDLr^{-/-}$ and $IDE^{-/-}LDLr^{-/-}$ mice were used as recipients and both $IDE^{+/+}$ and $IDE^{-/-}$ were the genotypes of the donor mice, so as to test the effect of hematopoietic cell IDE protein expression and knockout, respectively. Before going on study, mouse genotypes were confirmed via PCR and agarose gel electrophoresis.

4.3 Bone marrow transplant procedure

The technique of bone marrow transplantation was carried out using essentially the same procedures described by both Boisvert *et al.* and by Linton *et al.*, with a few minor modifications as noted below. Eight-week old, donor mice (genotype noted in table above) were maintained on antibiotic-containing water for 1 week before irradiation. Animals were

irradiated with a total of 900 Rads from a cesium source delivered in two equal doses 3 hours apart. Donor bone marrow cells (1×10^7) were injected into a tail vein of irradiated recipient mice (Figure 6). Four weeks after transplantation, the mice were placed on regular drinking water. Six weeks after transplantation, the mice were placed on a diet enriched in saturated fat (21% of wt/wt) and cholesterol (0.15%; Harlan Teklad diet #88137) and maintained for an additional 8 weeks. Successful reconstitution of bone marrow was confirmed by PCR genotyping of the recipient mouse femoral BM cells.

Figure 6. Experimental outline of the bone marrow transplant study

A) A schematic representation of the *in vivo* mouse study.

Briefly, at 7 weeks of age, recipient and donor mice were put on antibiotic-containing water in sterile conditions. At 8 weeks, recipient mice were lethally irradiated and received bone marrow from sacrificed donor mice. There was a recovery period of 6 weeks in sterile conditions, followed by 8 weeks of a high fat diet. At 22 weeks of age, recipient mice were sacrificed and tissues were collected. Approximately 15 recipient mice were required per group, with 1 donor providing enough bone marrow for 3 recipients.

B) Schematic representation of bone marrow transplant chimeras.

The purpose of the first BMT study (X) was to determine the effect of IDE knockout solely in bone marrow-derived cells (BMDC), using IDE-null BMDC reconstitution into $LDLr^{-/-}$ recipients as the experimental group and WT BMDC reconstituted into $LDLr^{-/-}$ recipients as the control. Study (Y) employs the reverse BMT, where the effect of IDE expression solely in BMDC is established. $IDE^{-/-}/LDLr^{-/-}$ recipients are reconstituted with either WT BMDCs (experimental groups) or $IDE^{-/-}$ BMDCs (control group)

A)

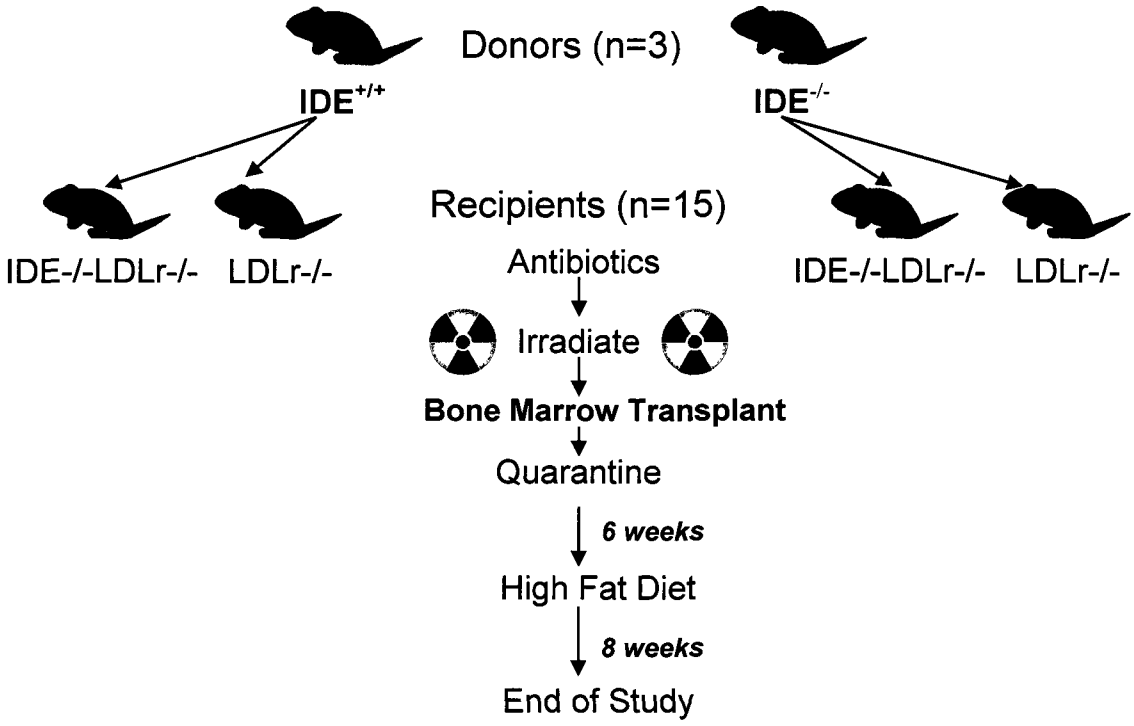
Donors (n=3)
IDE+/+
IDE-/-
Recipients (n=15)
IDE-/-LDLr-/-
LDLr-/-
IDE-/-LDLr-/-
LDLr-/-
Antibiotics
Irradiate
Bone Marrow Transplant
Quarantine
6 weeks
High Fat Diet
8 weeks
End of Study

B)

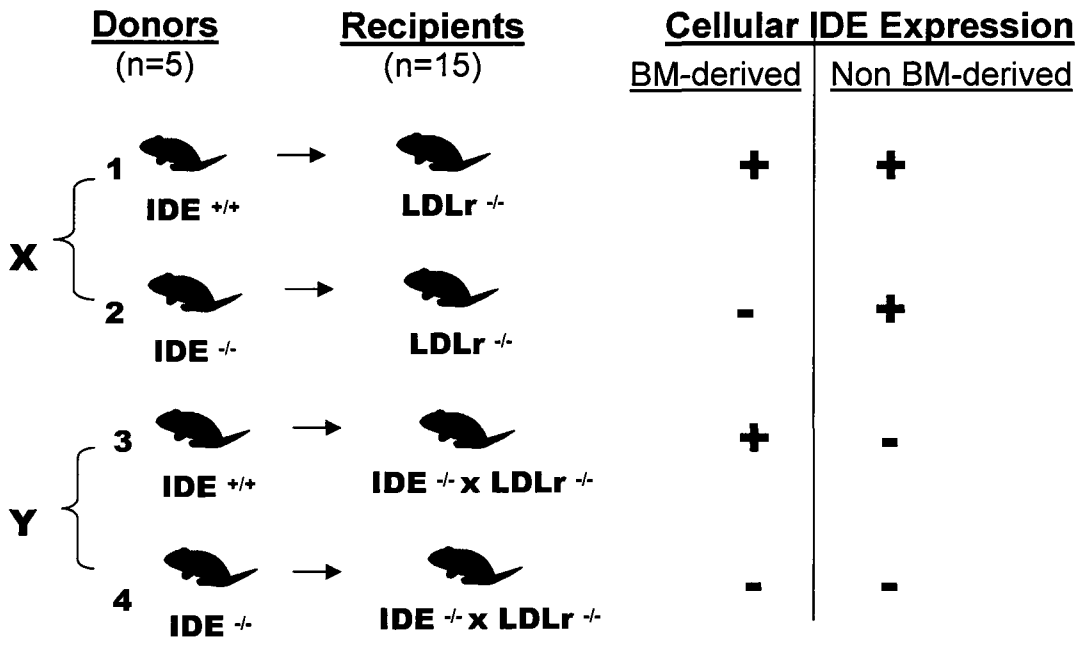
Donors
(n=5)
Recipients
(n=15)
Cellular IDE Expression
BM-derived
Non BM-derived
X
1
IDE +/+
LDLr -/-
+
+
2
IDE -/-
LDLr -/-
-
+
Y
3
IDE +/+
IDE -/- x LDLr -/-
+
-
4
IDE -/-
IDE -/- x LDLr -/-
-
-

4.4 Tissue collection

At the end of the study, all mice were euthanized by intraperitoneal injection of pentobarbital and 3-4 mL of blood plasma was collected immediately from a left ventricle puncture with a 5 mL syringe. All mice were subsequently perfused with phosphate-buffered saline, by means of a puncture to the left ventricle and perfusate being drained from a severed right atrium. The spleen was removed and dissected, with half being frozen at -80°C for subsequent RNA analysis, and the other half being placed in a plastic mold and embedded with optimum cutting temperature (OCT) medium and snap frozen on a metal plate cooled in liquid nitrogen. The hearts were separated from the aorta at the base and also embedded in OCT and stored at -20°C. Aortas were dissected from the proximal ascending aorta to the bifurcation of the iliac artery, with the use of a dissecting scope and then stored in 4% PFA until further preparation.

4.5 Histological staining of aortic root with Sudan IV

Hearts embedded in OCT were stored at -20°C until time of analysis. Sectioning of heart tissue was carried out with the use of a Leica Cryostat, cutting serially at 10 microns per slice and adding 9 sections to each slide, for a total of 10 slides and 90 sections per mouse. Lesion size in the ascending aorta was determined from four Sudan IV stained serial sections, cut 10 μm thick, and collected at 100 μm intervals. Sections were started at the region where the aortic sinus becomes the ascending aorta. Sections were digitally photographed with the Photometrics Coolsnap *cf* camera and the lesion area was determined using Image Pro software. The mean lesion area derived from the four serial sections was taken as the average lesion size for each animal.

Figure 7. Aortic root lesion analysis methodology

A diagram of the mouse heart showing the region of the ascending aorta where serial sections were collected for lesion measurement. To measure atherosclerotic lesion size within the ascending aorta, the mean lesion area was calculated from 4 transverse Sudan IV-stained sections, collected at 100 um apart and beginning at the appearance of the coronary ostia. Lesion areas were measured using Image Pro software.

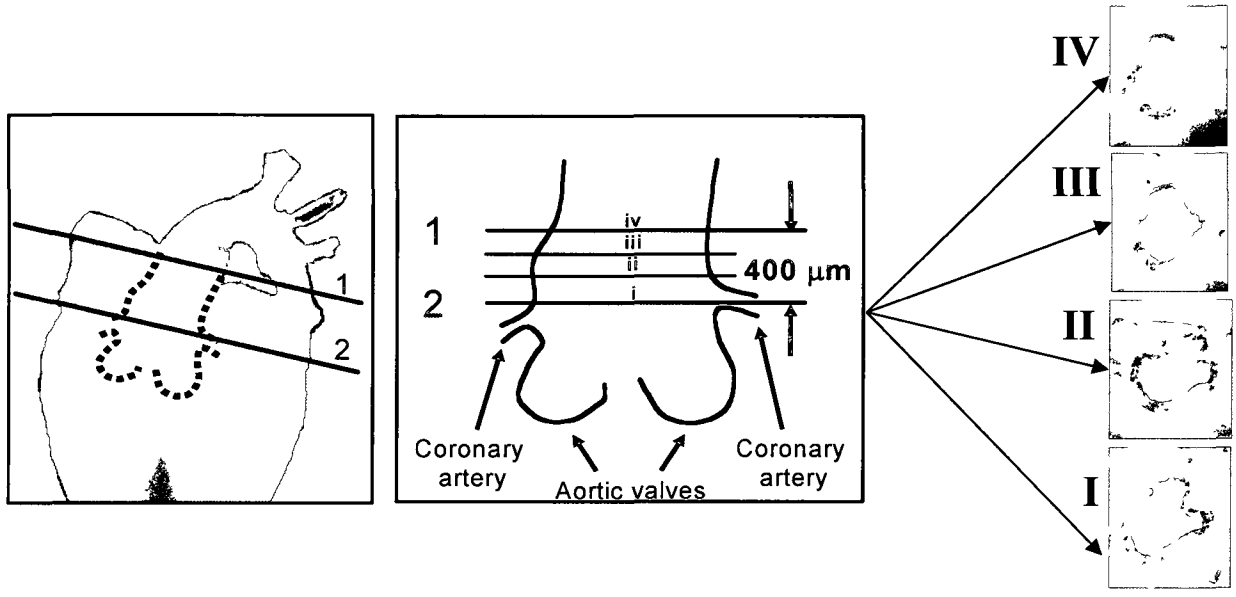
1
2
1
2
iv
iii
ii
i
400 μm
Coronary artery
Aortic valves
Coronary artery
IV
III
II
I

4.6 *En face* aorta lesion analysis

The entire mouse aorta was dissected from the proximal ascending aorta to the bifurcation of the iliac artery, with use of a dissecting microscope. Adventitial fat was removed and the aorta was opened longitudinally. The intimal surface was exposed by a longitudinal cut through the inner curvature of the aortic arch and down the anterior portion of the remaining aorta. Another cut was made through the greater curvature of the aortic arch to the subclavian branch. Now fully opened, the aortas are pinned flat onto dissecting wax, and photographed at a fixed magnification (Figure 10. A). Digital photographs were taken with a Photometrics Coolsnap *cf* camera and printed to subsequently have the surface areas of the arch and lesions traced (Figure 10.B). The total aortic areas and lesion areas were subsequently calculated using Image Pro Software. Final results are to be reported as a % of the total aortic area that contained lesions.

4.7 Lipid and lipoprotein analysis

Blood samples were kept on ice until being centrifuged at 10000 rpm for 2 minutes for plasma separation. Blood plasma was placed at 4°C for fast protein liquid chromatography (FPLC) lipoprotein analysis and at -20°C for total plasma cholesterol analysis until time of analysis. Subsequently total cholesterol levels were determined on all plasma samples using an enzymatic assay kit (Wako Cholesterol E, CHOD-DAOS Method, Catalog # 439-17501). Plasma samples from 5 mice of each experimental group were subjected to FPLC and total cholesterol concentration of individual fractions were determined via enzymatic assay (Genzyme, Cholesterol assay. Catalog # 234-60).

Figure 8. *En face* aorta lesion analysis methodology

Briefly, this technique involved the removal of the entire length of the aorta. Aortas were fixed in 4% PFA until time of analysis. The intimal surface was exposed by a longitudinal cut through the inner curvature of the aortic arch and down the anterior portion of the remaining aorta. Another cut was made through the greater curvature of the aortic arch to the subclavian branch. The tissue was then pinned to a dark surface, as shown (Figure A). The aortas were then digitally photographed, printed and scanned. Subseqent tracing of the superior 3mm of the aorta as well as all the individual lesions was done. (Figure B) Using ImagePro software to calculate the total aortic surface area as well as lesion areas, atherosclerosis was defined by % lesion area

A)

B)

4.8 Qualitative oil red O staining of WT and IDE-null BMDCs

Procured BMDCs from WT and IDE-null mice were plated in L929 conditioned media and incubated for 7 days at 37°C, to allow for differentiation into macrophages. Eight-well slides were treated with 100 μg/mL of native LDL (nLDL) and 100 μg/mL of acLDL after a 2-hour serum free starvation period. The nLDL was obtained by density gradient ultracentrifugation of plasma from a male familial hypercholesterolemic donor (Havel *et al.*, 1955) and acLDL was obtained by repetitive additions of acetic anhydride, as described by Goldstein and colleagues (1979). At time points 2h, 6h, 24h and 48h, medium was aspirated and cells were washed 3 times with 1X PBS, then were fixed with 4% paraformaldehyde for 20 minutes. After another 3 washes, cells were stained with oil red O (ORO) for 20 minutes, followed by another washing step and then 30 seconds of hematoxylin staining. Images of ORO uptake were taken at 2, 6, 24 and 48 hours.

4.9 Bone marrow extraction

WT and IDE null mice, at 2-3 months of age were sacrificed. Bone marrow was flushed from their tibias and femurs with L929 conditioned media. Cells from mice within the same group were pooled and the total number determined with the Beckman Coulter Vi-Cell counter. Cells were plated in 12-well and 24-well plates for various assays, as described below.

4.10 Tritiated cholesterol uptake assay

Bone marrow is obtained from the femurs and tibias of either wild type or IDE-null mice. Bone marrow-derived cells (BMDC) were plated at a density of 1×10^6 cells per well in DMEM supplemented with 15% L929 conditioned media, 10% fetal bovine serum and 1% penstrep. Cells were then incubated for 7 days at 37°C, 5% CO_2. After one week the medium was aspirated and the adherent cells were washed 2 times with warm DMEM. Bone marrow-derived macrophages (BMDMs) were subsequently treated with 50 μg/mL of

either native LDL or acetylated LDL for 2, 6, 24 or 48 hours. Tritiated cholesterol was incorporated into native and acLDL before addition to the cells. After 24 hours exposure, the medium was aspirated and the cells were washed 2 times with 1X PBS. 0.5mL of 0.5 N NaOH was added to each well overnight to lyse the cells. 200 μL of lysate was taken from each well, and mixed with ~2mL of ecolite scintillation cocktail. Using a scintillation counter, counts per minute were determined from each well. The Lowry Protein assay was utilized to determine the amount of cellular protein per well, so the final results are expressed as the CPM/μg protein.

4.11 Statistical analysis

Data analysis was performed using SigmaStat 2.03 software (SPSS Inc. Chicago, IL). For each parameter, the mean and standard error of the mean was calculated. Analysis between groups was evaluated by an unpaired Students T-test. Power calculation from previous studies use sample sizes large enough to attain a power of 0.8 for a 20% change in lesion size. Values ≤ 0.05 will be considered statistically significant. These numbers suggest that a sample size of 15 mice per group will be sufficient to provide statistically significant results with 95% confidence.

Chapter 5: Results

5.1 Aortic Root Lesion Analysis

There is nothing presently in the literature to indicate that dysregulation of IDE will affect atherosclerosis in mice. However, the observation by Whitman that IDE binds the cytoplasmic domain of SR-A provides a rationale for further investigation, especially considering SR-A knockdown decreased lesion development in both $LDLr^{-/-}$ and $apoE^{-/-}$ mice (Sakaguchi *et al.*, 1998; Suzuki *et al.*, 1997).

The goal of the present study was to assess the effect of IDE knockdown in BMDC on atherosclerosis, in an $LDLr^{-/-}$ recipient. Briefly, 8 week old $LDLr^{-/-}$ mice underwent lethal irradiation and were reconstituted with wild type or $IDE^{-/-}$ bone marrow-derived cells and subsequently put on a high fat diet for 8 weeks. At 22 weeks of age, the chimeric mice were sacrificed. Tissues were collected from control and experimental mice and atherosclerotic lesion development within the ascending aorta was measured. To do so, the mean lesion area was derived from four serial Sudan IV-stained sections that were cut 10um thick and collected 100um apart (Figure 7.).

Male $LDLr^{-/-}$ mice that were reconstituted with $IDE^{-/-}$ bone marrow had more than a 2-fold increase in aortic root atherosclerosis, compared to recipients that received WT bone marrow ($P < 0.05$, Figure 9.A). Interestingly, there was no difference in aortic root atherosclerosis between the two female groups (Figure 9.B), and both female chimeric groups had the same amount of atherosclerosis as the male $LDLr^{-/-}$ mouse reconstituted with $IDE^{-/-}$ bone marrow, suggesting an atheroprotective role for IDE in males.

Figure 9. Lesion area in the aortic root of LDLr $^{-/-}$ mice which have been reconstituted with WT or IDE$^{-/-}$ BMDC

Lesion area throughout the aortic root of LDLr$^{-/-}$ mice reconstituted with IDE$^{+/+}$ BMDC (■) or IDE$^{-/-}$ BMDC (▲). Following an 8-week high fat diet, male (A) and female (B) LDLr$^{-/-}$ mice hearts were harvested from mice whose bone marrow was repopulated with WT or IDE$^{-/-}$ marrow. Analysis was focused on the average total lesion area calculated from 4 transverse sections, 100 um apart (beginning at the appearance of the coronary ostia). Values are expressed as means +/- the SEM.

A)

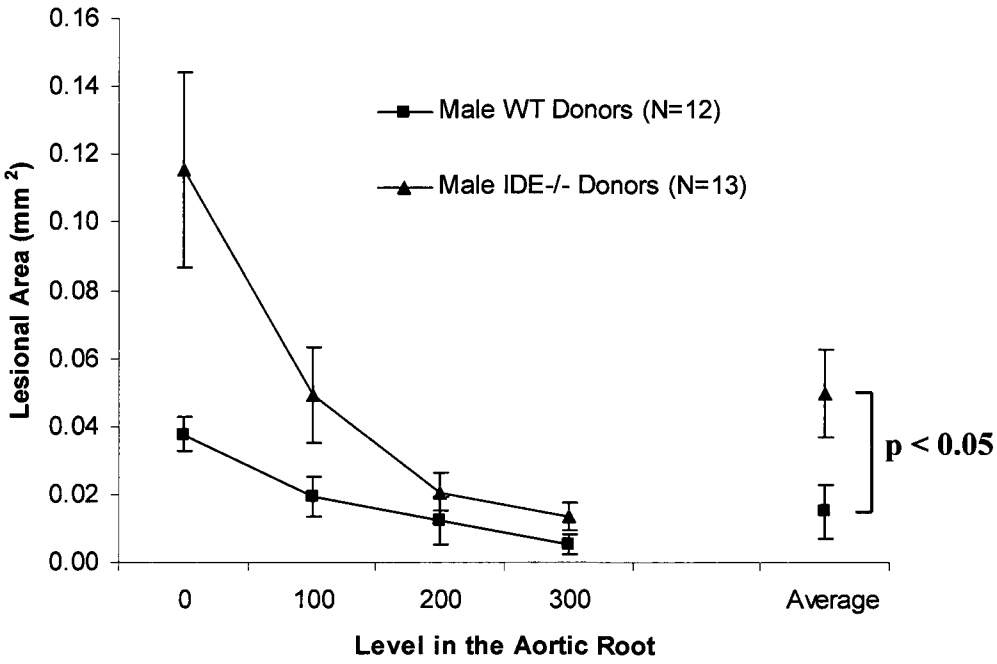
0.16
0.14
0.12
0.10
0.08
0.06
0.04
0.02
0.00
Lesional Area (mm 2)
Male WT Donors (N=12)
Male IDE-/- Donors (N=13)
p < 0.05
0
100
200
300
Average
Level in the Aortic Root

B)

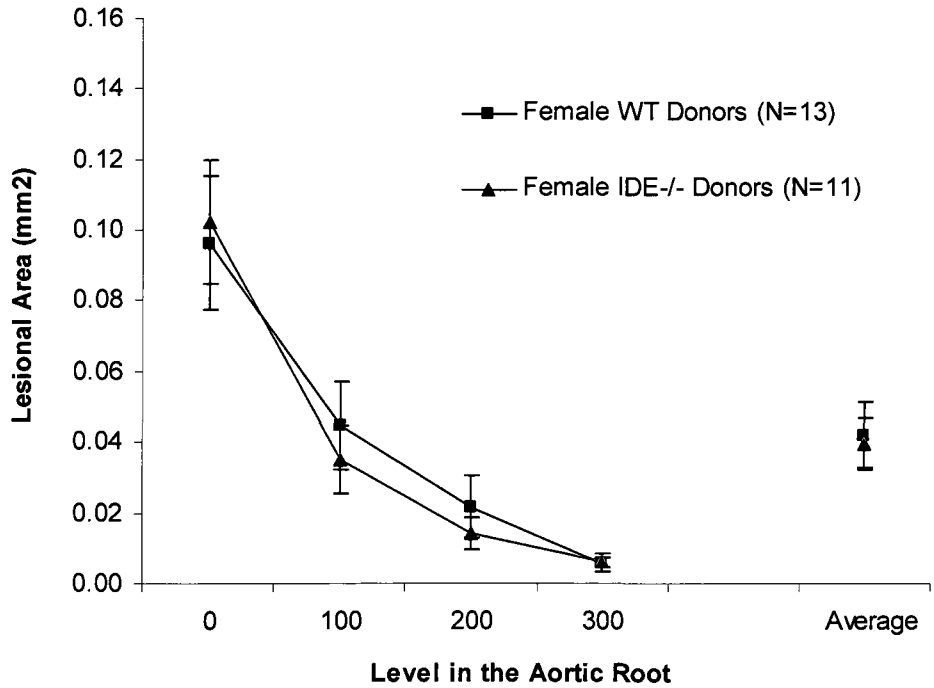
0.16
0.14
0.12
0.10
0.08
0.06
0.04
0.02
0.00
Lesional Area (mm2)
Female WT Donors (N=13)
Female IDE-/- Donors (N=11)
0
100
200
300
Average
Level in the Aortic Root

Subsequently, another goal of ours was to see the effect of IDE expression in bone marrow-derived cells on atherosclerosis, in $IDE^{-/-}/LDLr^{-/-}$ recipients. As hypothesized, we saw a greater than 2-fold reduction in aortic root atherosclerosis in male $IDE^{-/-}/LDLr^{-/-}$ recipients that received WT bone marrow, compared to those receiving $IDE^{-/-}$ bone marrow (Figure 10.A). Female chimeras showed no difference between groups (Figure 10.B) and once again had very similar sized lesions compared to the male recipients receiving $IDE^{-/-}$ bone marrow, indicating atheroprotection in males only when IDE is expressed.

Figure 10. Lesion area in the aortic root of male $IDE^{-/-}/LDLr^{-/-}$ mice which have been reconstituted with WT or $IDE^{-/-}$ BMDC

Lesion area throughout the aortic root of $IDE^{-/-}/LDLr^{-/-}$ mice reconstituted with $IDE^{+/+}$ BMDC (■) or $IDE^{-/-}$ BMDC (▲). Following an 8-week high fat diet, male (A) and female (B) $IDE^{-/-}/LDLr^{-/-}$ mice hearts were harvested from mice whose bone marrow was repopulated with WT or $IDE^{-/-}$ marrow. Analysis was focused on the average total lesion area calculated from 4 transverse sections, 100 um apart (beginning at the appearance of the coronary ostia). Values are expressed as means +/- the SEM.

A)

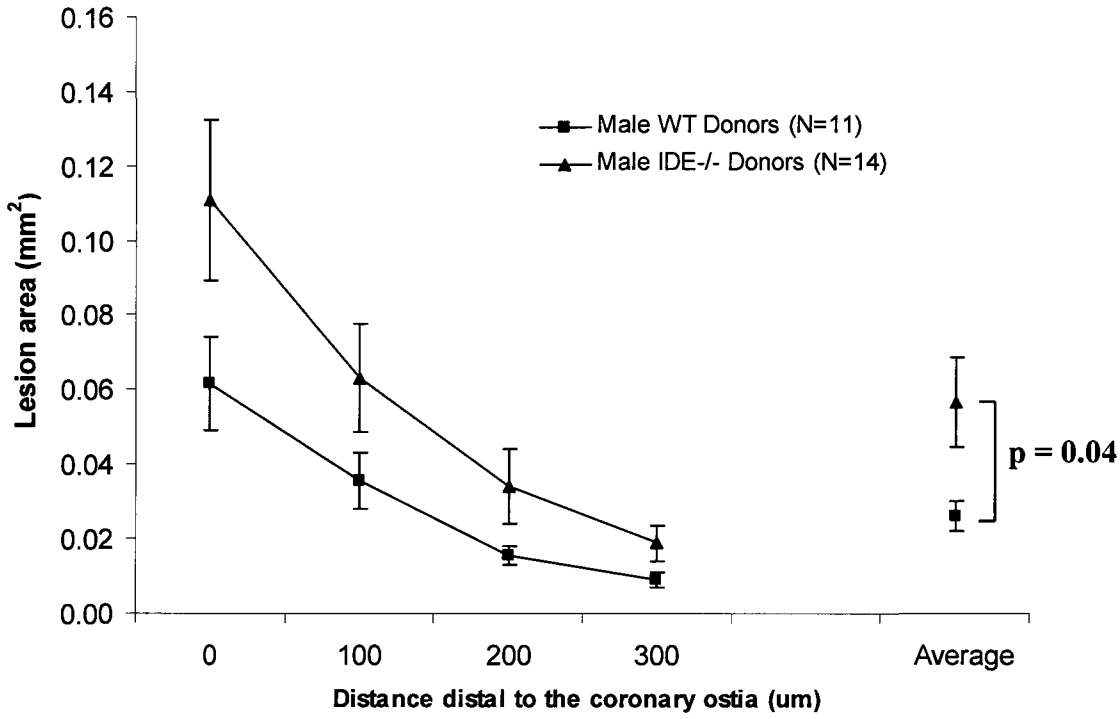
0.16
0.14
0.12
0.10
0.08
0.06
0.04
0.02
0.00
Lesion area (mm2)
Male WT Donors (N=11)
Male IDE-/- Donors (N=14)
p = 0.04
0
100
200
300
Average
Distance distal to the coronary ostia (um)

B)

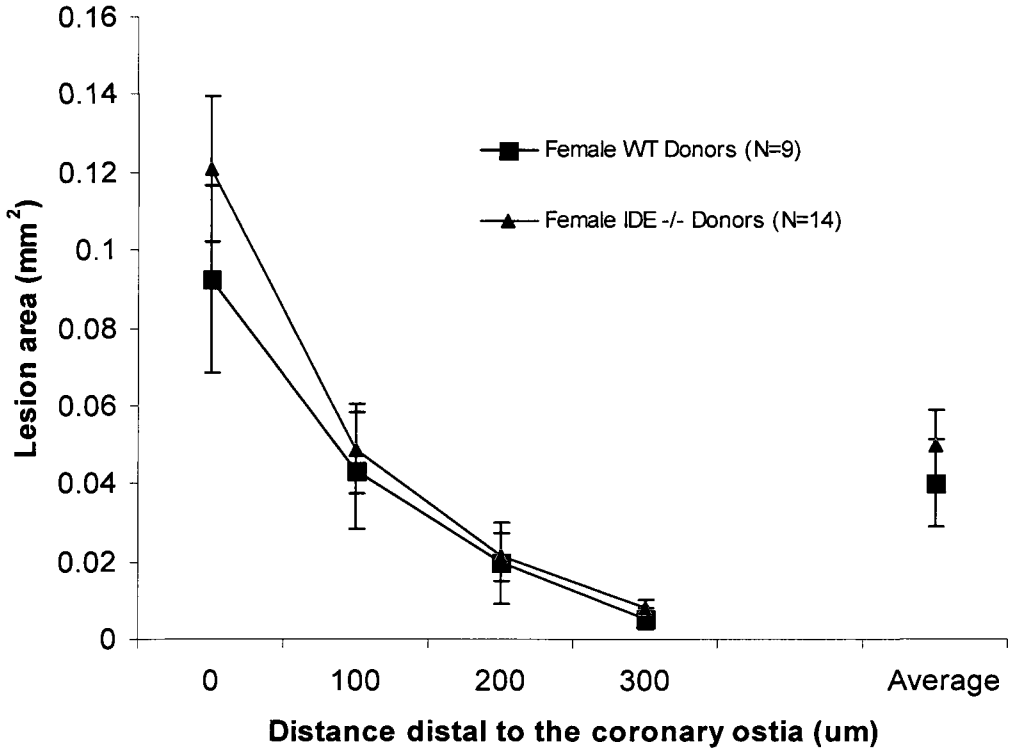
0.16
0.14
0.12
0.1
0.08
0.06
0.04
0.02
0
Lesion area (mm2)
Female WT Donors (N=9)
Female IDE -/- Donors (N=14)
0
100
200
300
Average
Distance distal to the coronary ostia (um)

5.2 *En Face* aortic lesion analysis

Historically, most atherosclerosis quantification in mice has been performed on lesions within the aortic root, as this was the only consistent lesion-prone area in which atherosclerosis was consistently present in all models. Such a method would not provide sufficient quantification of lesion in strains generating extensive atherosclerosis within the major portions of the aorta. More recently, genetically manipulated mice have permitted consistent atherosclerotic lesion development in other vascular areas. This has led to the use of *en face* analysis of lesions on the intimal surface of the aorta, as described by (Palinksi *et al.*, 1994).

The aim of this study was to measure atherosclerosis lesion development in a vascular bed other than the aortic root, under the same conditions used for aortic root analysis. As such, the very same mice used for aortic root analysis had their aortas removed, cleaned, cut longitudinally, pinned (Figure 8.A) and analyzed using image pro software. Lesion analysis was presented as % lesion area of the total surface area of the superior 3 mm of aorta (Figure 8.B).

Results from *en face* analysis revealed a greater than 5.5-fold increase in lesion size in male $LDLr^{-/-}$ mice receiving $IDE^{-/-}$ bone marrow compared to controls receiving WT bone marrow ($p < 0.001$, Figure 11.A). As was the case for the aortic root, analysis of female chimeric aortas revealed no differences in lesion size between groups (Figure 11.B).

The reverse bone marrow transplant yielded results as expected, although the difference in lesion area in the aortas of $IDE^{-/-}/LDLr^{-/-}$ male recipients of $IDE^{-/-}$ bone marrow compared to those receiving WT bone marrow (Figure 12.A) was less than that seen with the $LDLr^{-/-}$ male recipients (Figure 11.A). Lesions from $IDE^{-/-}/LDLr^{-/-}$ recipients reconstituted with IDE-null bone marrow were 1.5 fold larger than recipients receiving WT bone marrow ($P=0.043$, Figure 12.A). No significant differences were seen in the female arm of the study (Figure 12.B).

Figure 11. The % lesion area in the luminal surface of the aortic arch of LDLr $^{-/-}$ mice which have been reconstituted with WT or IDE$^{-/-}$ BMDC

Bar graphs represent % lesion area throughout the luminal surface of the aortic arch of LDLr$^{-/-}$ mice reconstituted with IDE$^{+/+}$ BMDC (black bar) or IDE$^{-/-}$ BMDC (red bar). Following an 8-week high fat diet, male (A) and female (B) LDLr$^{-/-}$ mice aortas were harvested from mice that were reconstituted with IDE$^{+/+}$ or IDE$^{-/-}$ marrow. Aortas were cleaned of adventitial fat, cut longitudinally and pinned for subsequent analysis with Image Pro software. Analysis was focused on the average total lesion area calculated from the most proximal 3 mm of the aortic arch. Values are expressed as means +/- the SEM.

A)

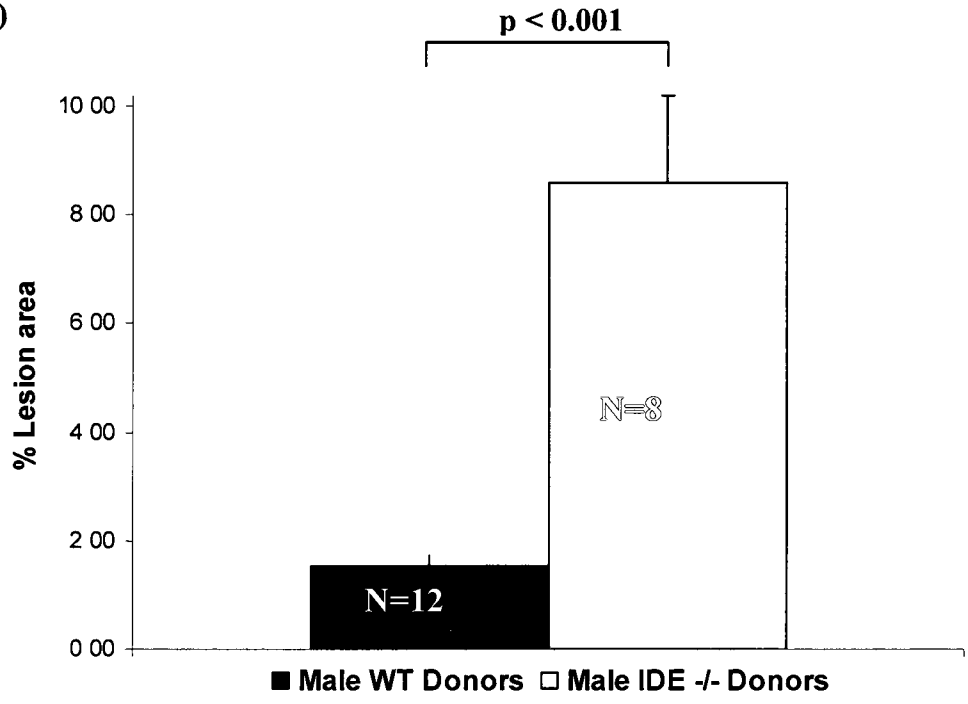
p < 0.001
10 00
8 00
6 00
4 00
2 00
0 00
% Lesion area
N=8
N=12
■ Male WT Donors □ Male IDE -/- Donors

B)

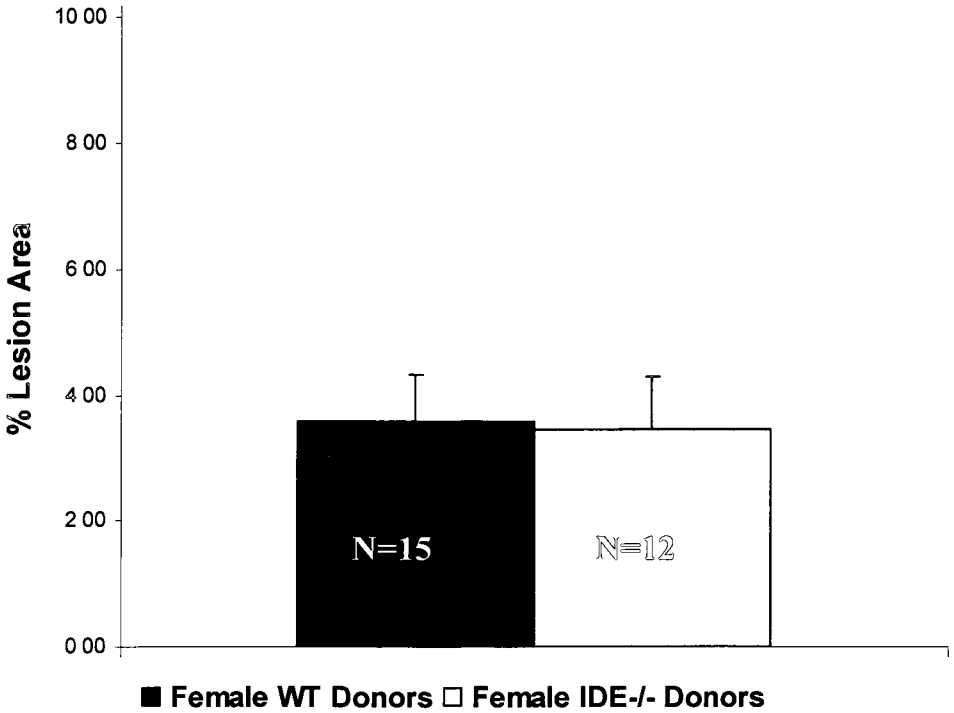
10 00
8 00
6 00
4 00
2 00
0 00
% Lesion Area
N=15
N=12
■ Female WT Donors □ Female IDE-/- Donors

Figure 12. The % lesion area in the luminal surface of the aortic arch of $IDE^{-/-}/LDLr^{-/-}$ mice which have been reconstituted with WT or $IDE^{-/-}$ BMDCs

Bar graphs represent % lesion area throughout the luminal surface of the aortic arch of $IDE^{-/-}/LDLr^{-/-}$ mice reconstituted with $IDE^{+/+}$ BMDC (black bar) or $IDE^{-/-}$ BMDC (red bar). Following an 8 week high fat diet, male (A) and female (B) $IDE^{-/-}/LDLr^{-/-}$ mice aortas were harvested from mice that were reconstituted with $IDE^{+/+}$ or $IDE^{-/-}$ marrow. Aortas were cleaned of any adventitial fat, cut longitudinally and pinned for subsequent analysis with Image Pro software. Analysis was focused on the average total lesion area calculated from the most proximal 3 mm of the aortic arch. Values are expressed as means +/- the SEM.

A)

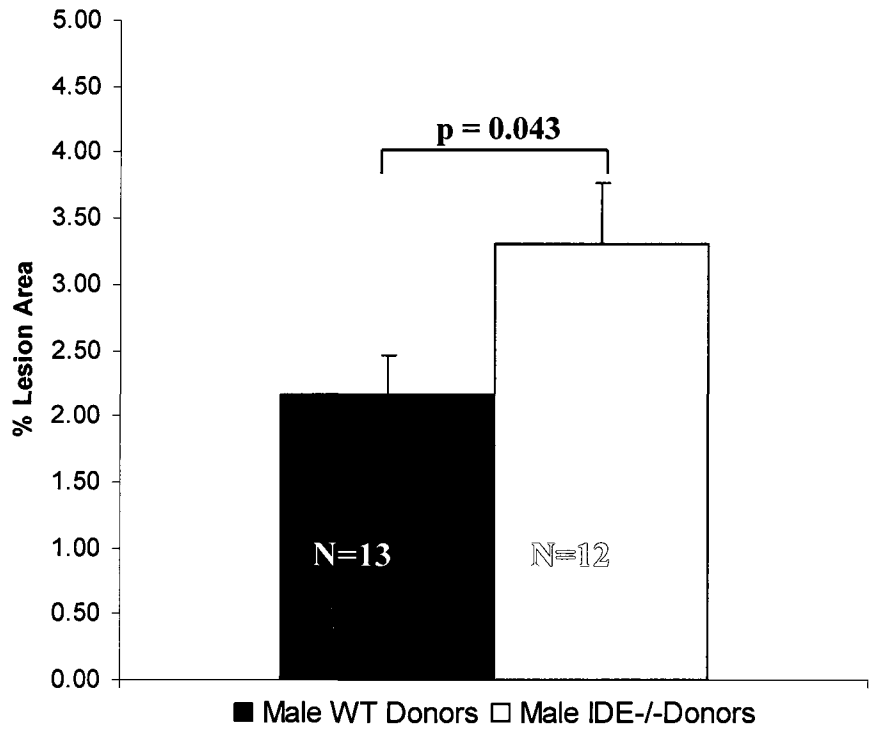
5.00
4.50
4.00
3.50
3.00
2.50
2.00
1.50
1.00
0.50
0.00
% Lesion Area
p = 0.043
N=13
N=12
Male WT Donors
Male IDE-/-Donors

B)

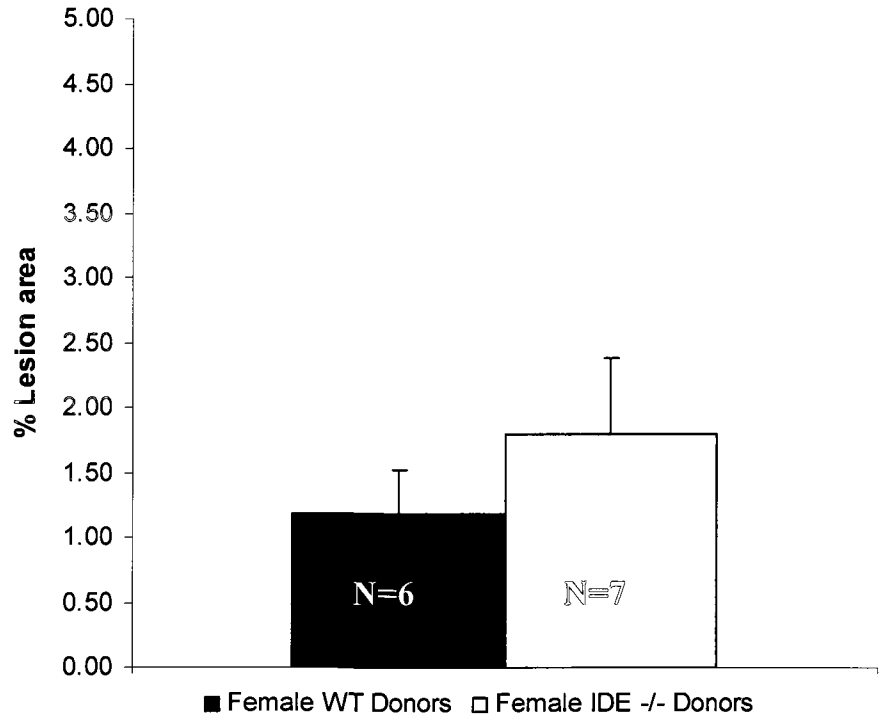
5.00
4.50
4.00
3.50
3.00
2.50
2.00
1.50
1.00
0.50
0.00
% Lesion area
N=6
N=7
Female WT Donors
Female IDE -/- Donors

5.3 Total serum cholesterol and serum lipoprotein profile

Our goal was to establish if the increased atherosclerosis in male recipients of $IDE^{-/-}$ BMDC was accompanied by and possibly due to increased total serum cholesterol. An enzymatic cholesterol assay was used on the serum of each mouse to determine the average cholesterol level per group. When IDE-deficient bone marrow was used to reconstitute $LDLr^{-/-}$ recipients, cholesterol levels were increased 44% ($P < 0.05$, figure 13.A) as compared to $LDLr^{-/-}$ recipients reconstituted with wild-type bone marrow. No significant difference was seen in female total cholesterol, which by coinciding with no change in female lesion size in two vascular beds, would be consistent with a cholesterol-mediated process (Figure 13.A).

The results of the total serum cholesterol assay for the reverse bone marrow transplant chimeras show modest, non-significant increases of 16% and 23 %, in serum cholesterol in both males and females that received $IDE^{-/-}$ BMDC, respectively (Figure 13.B). When compared to $LDLr^{-/-}$ male mice reconstituted with $IDE^{-/-}$ bone marrow, $IDE^{-/-}/LDLr^{-/-}$ mice reconstituted with $IDE^{-/-}$ bone marrow show both a smaller increase in plasma cholesterol and smaller increase in lesion size.

More important than the increase in total serum cholesterol is the fractional distribution between lipoprotein classes. As such, Superose 6 fast protein liquid chromatography was used to separate the serum (from 5 mice per group, chosen arbitrarily) VLDL/chylomicron, LDL and HDL fractions. Cholesterol concentrations of the FPLC fractions were determined and the mean values are presented graphically in Figures 14 and 15.

Male $LDLr^{-/-}$ recipients of $IDE^{-/-}$ bone marrow had a modest increase in LDL fraction (#, $P=0.03$, Figure 14.A), compared to recipients of WT bone marrow, which may account for the increase in total serum cholesterol as well as increased lesion size within this group. Female $LDLr^{-/-}$ mice showed no significant differences, aside from a modest increase in

their LDL fraction (*, P=0.01, #, P=0.03, Figure 14.B). Analysis of $IDE^{-/-}$ recipients (Figure 15) revealed increases in the atherogenic lipoprotein fractions in male recipients that received IDE-null bone marrow compared to controls (**, P<0.001; *, P=0.001; #, P=0.003; ‡, P=0.012, Figure 15.A). Female $IDE^{-/-}/LDLr^{-/-}$ recipients reconstituted with IDE-null bone marrow saw no significant differences other than a spike in VLDL cholesterol (†, P=0.015, Figure 15.B).

Figure 13. Determination of total serum cholesterol concentration

Bar graphs represent the average total serum cholesterol concentrations of LDLr-/- recipients (A) and IDE-/-LDLr-/- recipients (B) reconstituted with $IDE^{+/+}$ BMDC (black bar) or $IDE^{-/-}$ BMDC (red bar). Following an 8-week high fat diet, blood plasma was harvested from recipient mice that were reconstituted with $IDE^{+/+}$ or $IDE^{-/-}$ marrow. Total cholesterol levels were determined on all plasma samples using an enzymatic assay kit. Values are expressed as means +/- the SEM.

A)

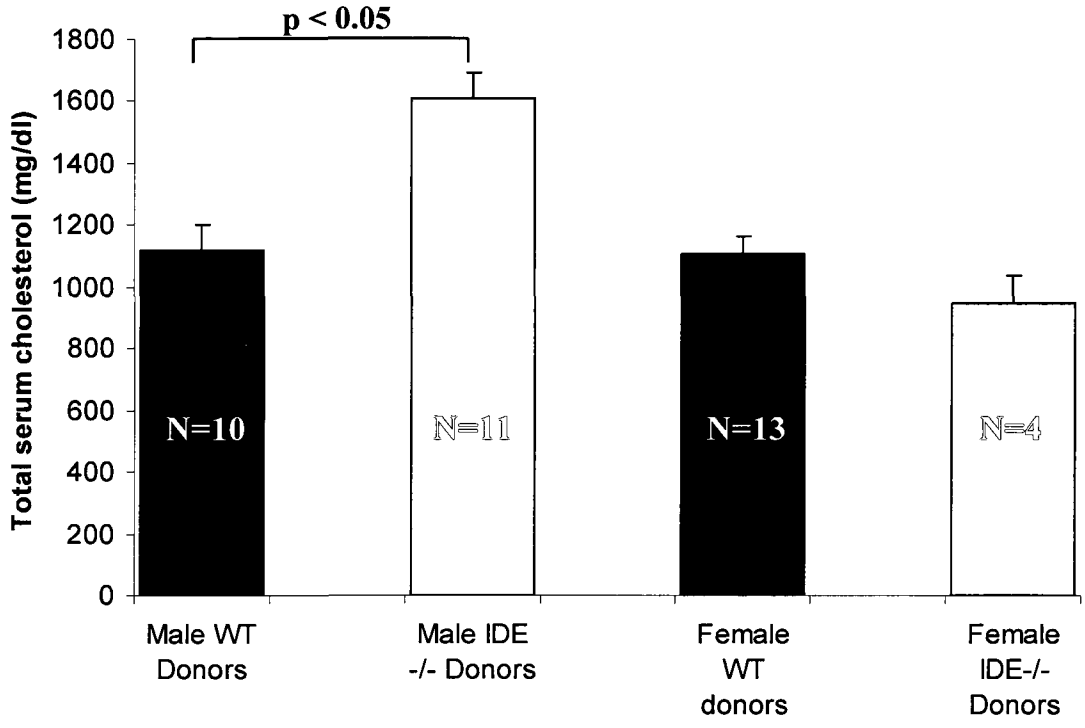
p < 0.05
Total serum cholesterol (mg/dl)
1800
1600
1400
1200
1000
800
600
400
200
0
N=10
N=11
N=13
N=4
Male WT Donors
Male IDE -/- Donors
Female WT donors
Female IDE-/- Donors

B)

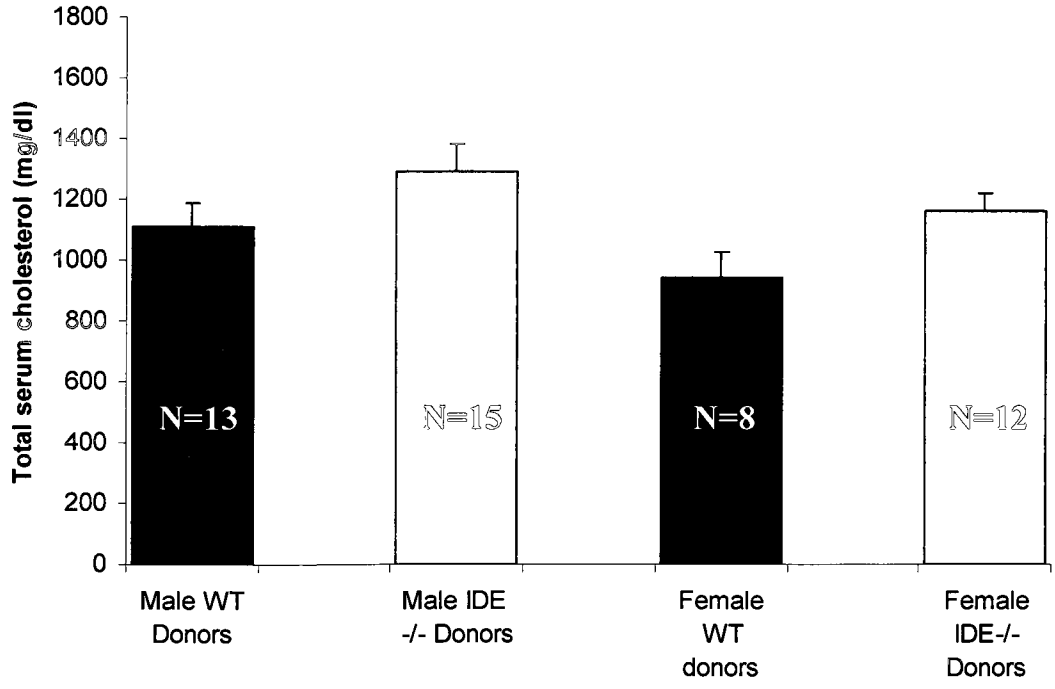
Total serum cholesterol (mg/dl)
1800
1600
1400
1200
1000
800
600
400
200
0
N=13
N=15
N=8
N=12
Male WT Donors
Male IDE -/- Donors
Female WT donors
Female IDE-/- Donors

Figure 14. Determination of cholesterol distribution in FPLC serum fractions of LDLr$^{-/-}$ mice reconstituted with WT or IDE$^{-/-}$ BMDC

Following an 8-week high fat diet, blood plasma was harvested from LDLr$^{-/-}$ recipient mice that were reconstituted with IDE$^{+/+}$ or IDE$^{-/-}$ marrow. Plasma samples from male (A) and female (B) LDLr$^{-/-}$ mice that were reconstituted with WT BMDC (■) or IDE$^{-/-}$ BMDC (▲) were subjected to FPLC and resolved by size exclusion chromatography. Total cholesterol concentration of individual fractions was determined via enzymatic assay. N=5 mice per group. Values are expressed as means +/- the SEM (*, P=0.01, #, P=0.03).

A)

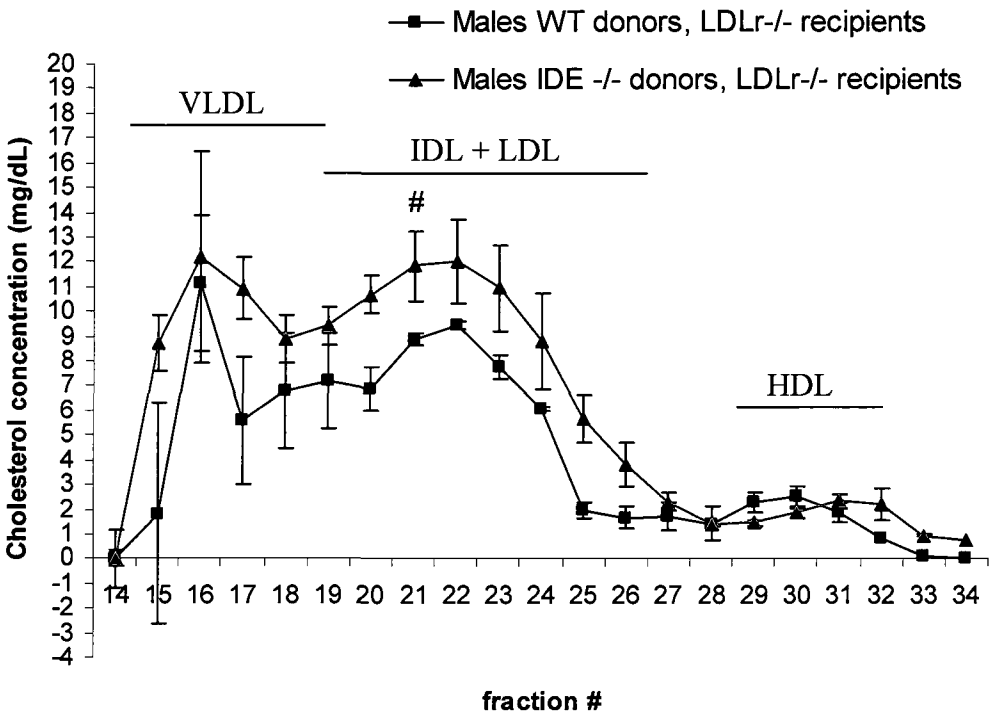
Males WT donors, LDLr-/- recipients
Males IDE -/- donors, LDLr-/- recipients
VLDL
IDL + LDL
HDL
#
Cholesterol concentration (mg/dL)
fraction #

B)

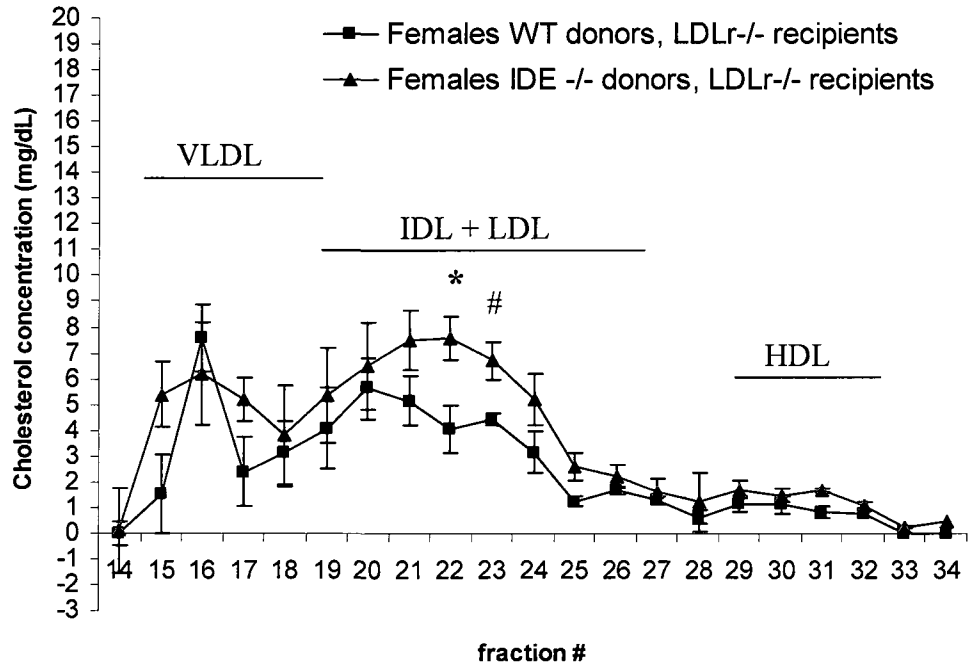
Females WT donors, LDLr-/- recipients
Females IDE -/- donors, LDLr-/- recipients
VLDL
IDL + LDL
HDL
*
#
Cholesterol concentration (mg/dL)
fraction #

Figure 15. Determination of cholesterol distribution in FPLC serum fractions of $IDE^{-/-}LDLr^{-/-}$ mice reconstituted with WT or $IDE^{-/-}$ BMDC

Following an 8-week high fat diet, blood plasma was harvested from $IDE^{-/-}LDLr^{-/-}$ recipient mice that were reconstituted with $IDE^{+/+}$ or $IDE^{-/-}$ marrow. Plasma samples from male (A) and female (B) $LDLr^{-/-}$ mice that were reconstituted with WT BMDC (■) or $IDE^{-/-}$ BMDC (▲) were subjected to FPLC and resolved by size exclusion chromatography. Total cholesterol concentration of individual fractions was determined via enzymatic assay. N=5 mice per group. Values are expressed as means +/- the SEM (**, $P<0.001$; *, $P=0.001$; #, $P=0.003$; ‡, $P=0.012$; †, $P=0.015$).

A)

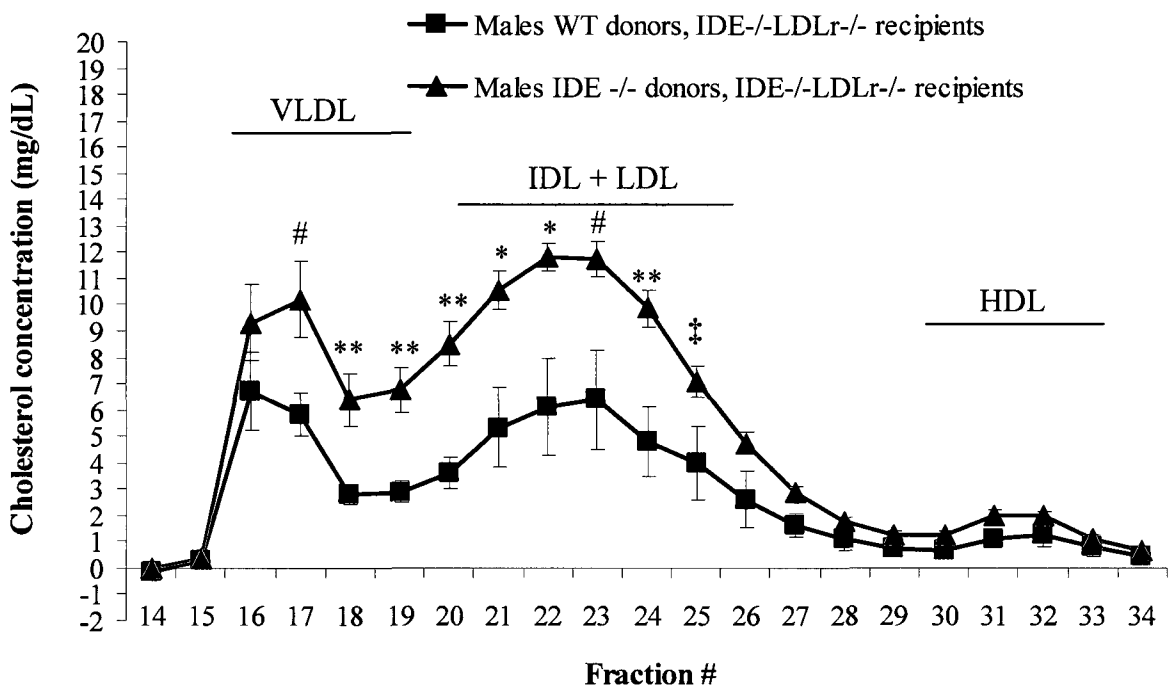
Males WT donors, IDE-/-LDLr-/- recipients
Males IDE -/- donors, IDE-/-LDLr-/- recipients
VLDL
IDL + LDL
HDL
Cholesterol concentration (mg/dL)
Fraction #

B)

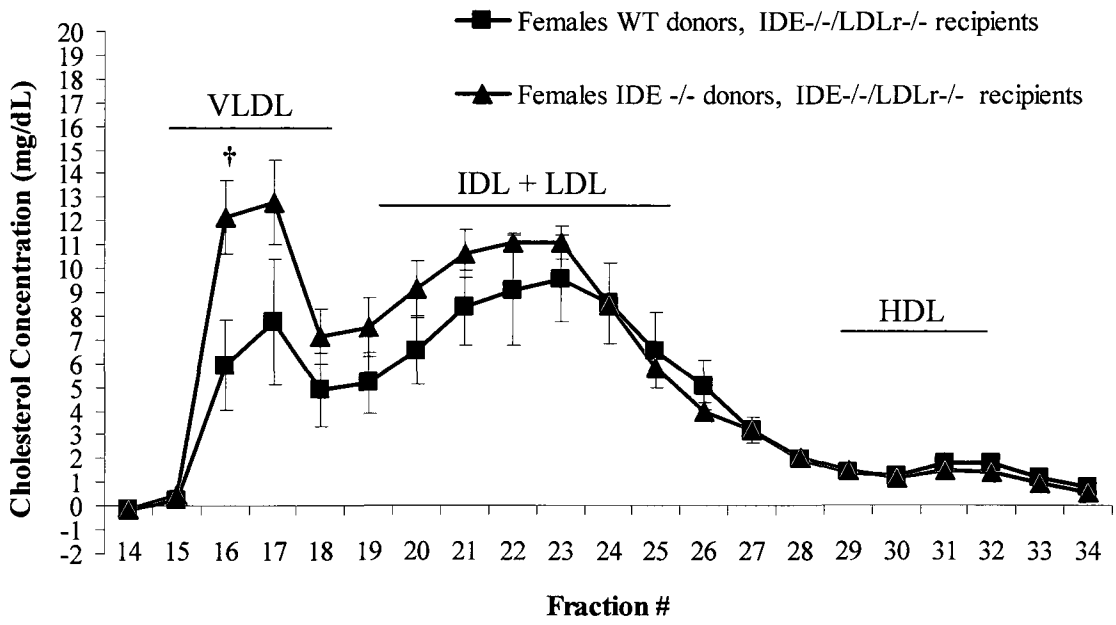
Females WT donors, IDE-/-/LDLr-/- recipients
Females IDE -/- donors, IDE-/-/LDLr-/- recipients
VLDL
IDL + LDL
HDL
Cholesterol Concentration (mg/dL)
Fraction #

5.4 Oil red O uptake assay

We turned to *ex vivo* methods to investigate how IDE deficiency could mechanistically lead to larger lesions. We proposed that since IDE associated with the cytoplasmic domain of SR-A, absence of IDE may promote lipid uptake and foam cell formation.

The first study conducted was an oil red O stain of IDE-null macrophages to assess the effect of IDE deficiency in lipid uptake. This involved the procurement of BMDCs from aged-matched WT and IDE-null mice, and their subsequent differentiation into macrophages. Macrophages were then incubated with either 100 μg/ml of native or acetylated LDL for 6 hours and then washed prior to staining. The cells were stained with Oil red O to show cholesteryl ester lipid droplets, while hematoxylin was used to visualize the nucleus. The purpose of this simple assay was two-fold: to determine if IDE-null cells can become foam cells and also to determine if they take up significantly different amounts of lipid than wild type cells.

Shown at 60X magnification with a light microscope, IDE-null BMDM treated with acLDL showed just as much oil red O binding compared to the control macrophages (Figure 16. D). This method was a qualitative approach to determine if foam cell formation took place with IDE deficiency and provided a rationale to approach the same problem quantitatively.

Figure 16. Foam cell formation in IDE$^{-/-}$ macrophages

Bone marrow derived macrophages were procured from either WT or IDE-null mice and cultured in the presence of 100 μg/mL native LDL or 100 μg/mL acetylated LDL. Cells were subsequently stained with haemotoxylin to identify the nucleus and Oil red O to visualize cytoplasmic cholesteryl ester droplets. Both WT (A) and IDE-null (B) BMDM show very little, if any cholesteryl ester droplets. However, treatment of macrophages with acetylated LDL was sufficient to cause foam cell formation in both WT(C) and IDE null (D) macrophages. Images are shown at 60x magnification.

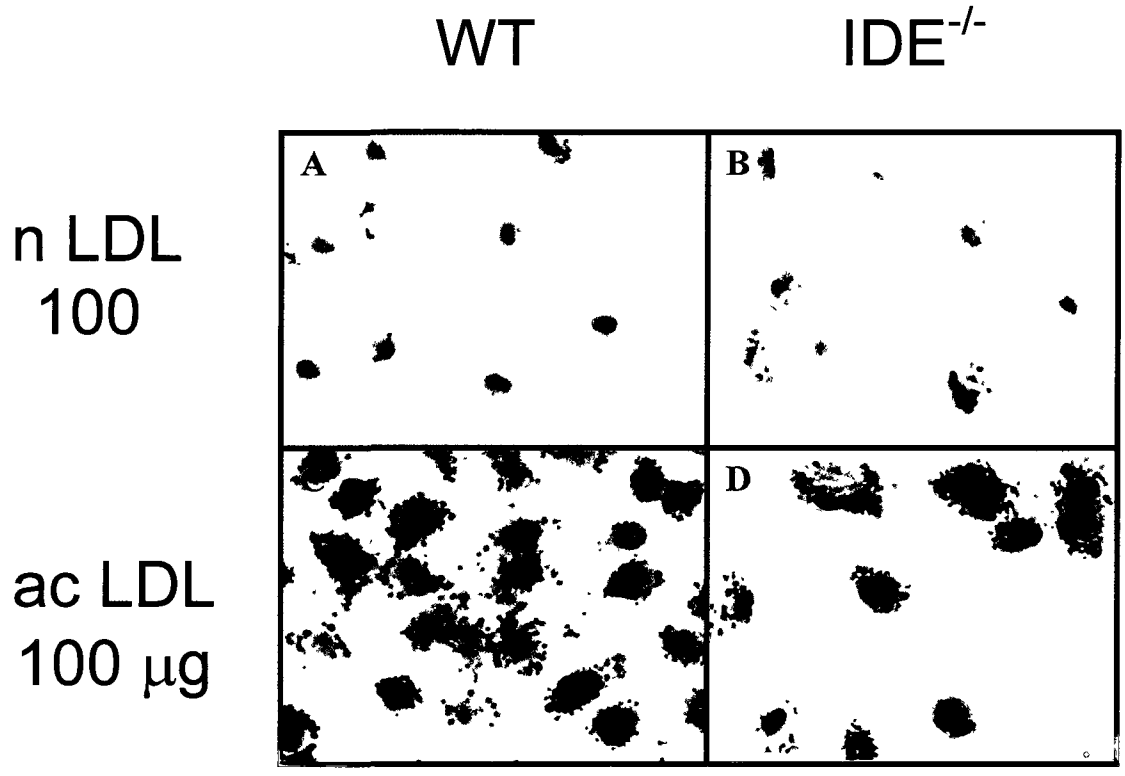
WT
IDE-/-
n LDL
100
ac LDL
100 µg
A
B
D

5.5 AcLDL binding assay

As our lab had previously shown that IDE can associate with the cytoplasmic domain of SR-A, it was of great interest to determine if knockout of IDE had any affects on SR-A-mediated binding of acLDL to the cell surface. To do this we employed a cell surface binding assay, using radioactively labeled cholesterol, which is a well established method to quantitatively measure cholesterol metabolism in cells. Briefly, wild-type and IDE-null bone marrow-derived macrophages were exposed to ^{3}H-cholesterol –acLDL for 1 hour at 4°C, to allow cell surface binding of the acLDL but not its endocytosis. Subsequent cell lysis and quantification of radiolabelled bound acLDL was carried out with a scintillation counter. Although this experiment was only done once in triplicate, the results show a marked decrease in acLDL binding to the cell surface of IDE-null bone marrow derived macrophages from both males and females, compared to WT BMDM (Figure 17).

Figure 17. Characterization of acLDL binding to the cell surface of BMDM from WT and IDE$^{-/-}$ mice

BMDM were procured from WT and IDE-null mice and subsequently washed 3 times with ice cold media and precooled at 4°C for 15 minutes to block endocytosis. Cells were then incubated with ^{3}H-cholesterol-acLDL (50μg/mL) with gentle rocking for 1 hour at 4°C, after which they were washed 3 more times with ice-cold PBS. Cells were lysed and bound radiolabelled acLDL was measured by liquid scintillation counting.

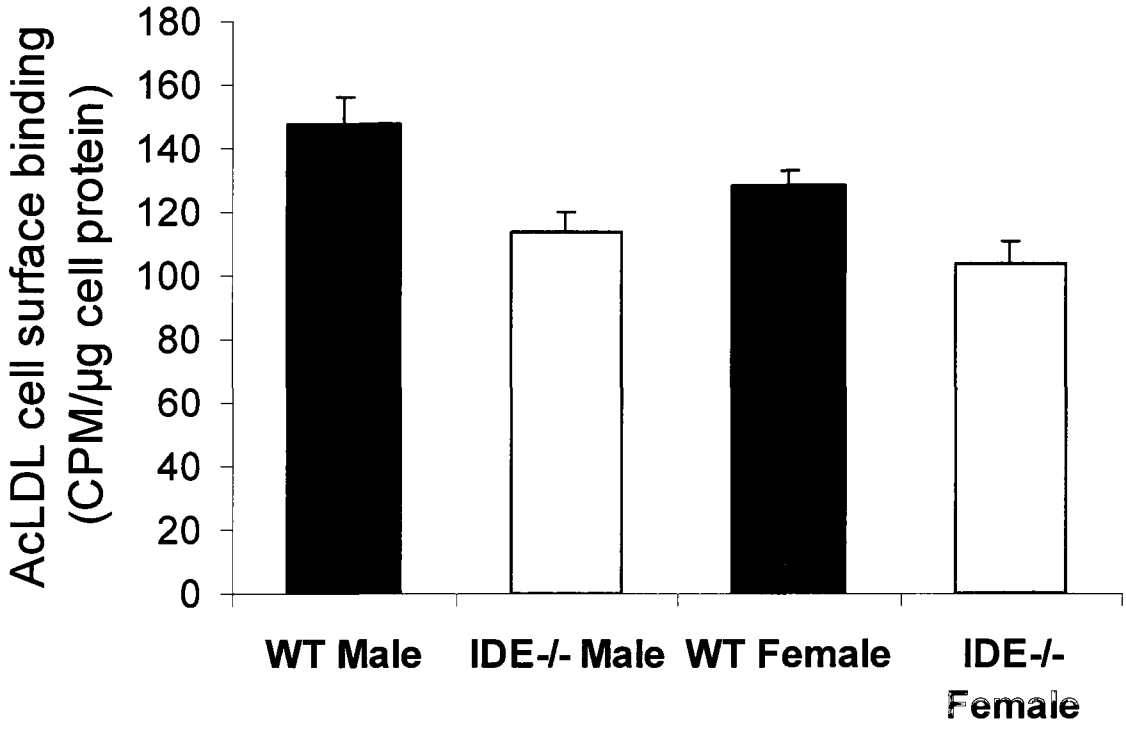
AcLDL cell surface binding
(CPM/µg cell protein)
180
160
140
120
100
80
60
40
20
0
WT Male
IDE-/- Male
WT Female
IDE-/-
Female

5.6 Tritiated-cholesterol uptake assay

Next, we set out to determine if larger lesions in recipients receiving IDE-null bone marrow could result from increased modified LDL cholesterol uptake. Briefly, tritium-labeled cholesterol was incorporated into native and acetylated LDL before being incubated with WT and $IDE^{-/-}$ BMDM for 2, 6, 12 and 24 hours. At the end of each time point the radioactive lipoprotein was washed away and cells were lysed, to subsequently have their radioactivity counted by a scintillation counter.

Analysis of BMDM from male mice revealed no significant differences in either native or acetylated LDL uptake at all time points (Figure 18). As expected, native LDL uptake quickly reached a plateau, while acetylated LDL uptake rose significantly at each successive time point.

5.7 Tritiated-oleate cholesteryl ester accumulation assay

Another similar assay that is based on the same fundamental methodology involves the treatment of cells with tritium-labeled oleic acid, as a means to measure foam cell formation. In brief, the macrophages were pretreated with tritiated oleate before the addition of either native or acetylated LDL for 6 hours and 24 hours. Cells were washed, lysed and the lipid fractions were separated via thin layer chromatography. Radioactivity within the cholesteryl ester fraction was measured and was a direct indication of the amount of cholesteryl ester accumulation

Analysis of male IDE-null BMDM revealed a 62% increase of radioactivity in the cholesteryl ester fraction, compared to WT control cells (Figure 19). The increase of radioactivity in this lipid fraction translates into an increase in CE accumulation. This experiment was only done once in triplicate and will have to be repeated, but it still shows a trend towards increased foam cell formation in IDE-null macrophages compared to controls.

Figure 18. Cholesterol uptake in WT and IDE$^{-/-}$ BMDM treated with either native or acetylated LDL for various time points

BMDM were procured and subsequently incubated with ^{3}H-cholesterol-AcLDL (50μg/mL) or ^{3}H-cholesterol-LDL (50μg/mL) for 2, 6, 24 and 48 hours in 1% FBS media. Cells were then washed 2X with ice-cold PBS, and following cell lysis endocytosed ^{3}H-cholesterol was measured by liquid scintillation counting. Counts per minute determined for each condition was normalized to cellular protein from each well, determined via Lowry Assay.

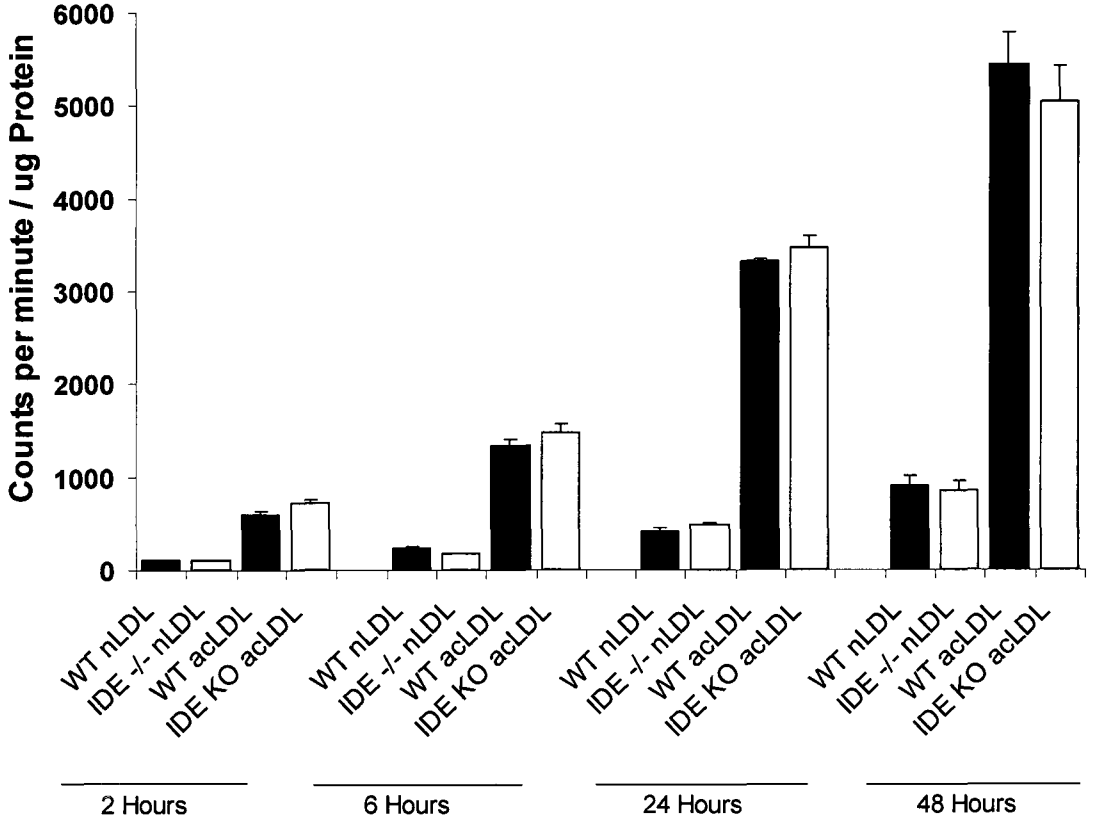
Counts per minute / ug Protein
6000
5000
4000
3000
2000
1000
0
WT nLDL
IDE -/- nLDL
WT acLDL
IDE KO acLDL
2 Hours
6 Hours
24 Hours
48 Hours

Figure 19. Cholesteryl ester formation in WT and IDE$^{-/-}$ BMDM treated with either native or acetylated LDL for various time points

BMDM were incubated with ^{3}H-oleate before being treated with 50μg/mL of either nLDL or acLDL for 6 hours. Cells were then washed 2X with ice-cold PBS, lysed with NaOH and subsequent separation of the lipid components was achieved via thin layer chromatography. Radioactivity within the cholesteryl ester fraction was determined by a scintillation counter.

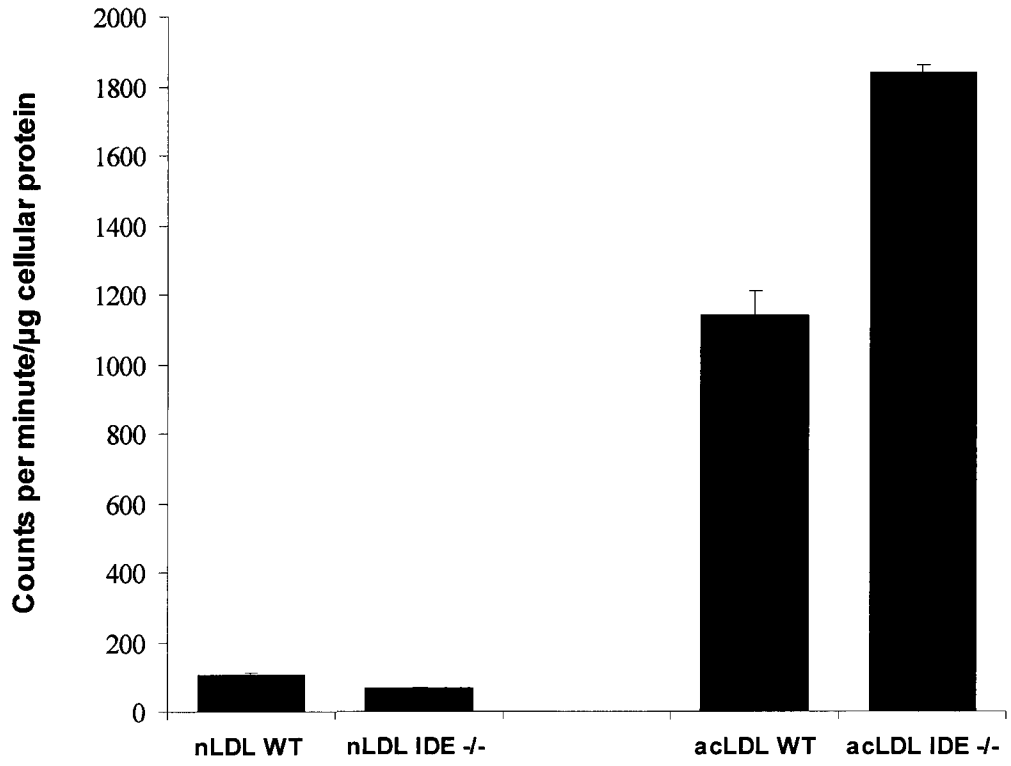
Counts per minute/µg cellular protein
2000
1800
1600
1400
1200
1000
800
600
400
200
0
nLDL WT
nLDL IDE -/-
acLDL WT
acLDL IDE -/-

Chapter 6: Discussion

The rationale for this study came from the observation that IDE associates with the cytoplasmic domain of SR-A. IDE deficiency is largely implicated in pathophysiologies associated with DM2 and AD. The genetic and pathological links between macrophage SR-A and IDE provide an excellent basis for the assumption that the IDE protein has an effect in the pathology of atherosclerosis. The principal hypothesis that I tested in this project was that IDE expression does exhibit an anti-atherogenic affect. In fact, when male LDLr knockout mice were reconstituted with $IDE^{-/-}$ BMDC, we saw a significant increase in atherosclerotic lesion size in both the aortic root and aortic arch of these mice, as well as an increase in total serum cholesterol and atherogenic lipoprotein fractions. The same atheroprotective role of IDE was shown in the reverse bone marrow transplant model, where $IDE^{-/-}/LDLr^{-/-}$ mice showed smaller lesions when reconstituted with wild-type BMDC. Mechanistically, an approach was taken to quantify the amount of cholesterol uptake into BMDM procured from either IDE-null or WT mice. Oil red O staining confirmed that IDE-null macrophages are able to become foam cells when stimulated with acetylated LDL. However, quantitative analysis showed no differences with 2, 6, 24, and 48 hours of lipoprotein treatment, suggesting that IDE may contribute to atherosclerosis in a manner other than lipid uptake.

6.1 Total serum cholesterol and atherosclerosis

The increase in atherosclerosis of male recipient mice reconstituted with $IDE^{-/-}$ BMDC may have been a result of increased macrophage cholesterol uptake and esterification due to their higher plasma cholesterol levels. The higher cholesterol levels in male mice reconstituted with $IDE^{-/-}$ bone marrow was unanticipated, but presumably results from increased production of apoB-containing lipoproteins in either the liver or intestine or impaired clearance of apoB-containing lipoproteins. As BMDC do not synthesize apoB, any effect of IDE on lipoprotein production would have to be indirect. As will be discussed in more detail below, IDE deficiency could potentially alter lipoprotein metabolism by increasing circulating insulin levels and by inducing insulin resistance. In contrast to

lipoprotein production, IDE deficiency in the bone marrow donor cells could directly influence plasma cholesterol levels if BMDC did contribute substantially to lipoprotein clearance. For example, if the absence of IDE compromised LDLr expression in BMDC, which, however, appears unlikely as Fazio and colleagues (1997) showed that BMDC LDLr-mediated lipoprotein clearance has no effect on cholesterol levels. It is clear that more work is required to elucidate how the IDE status of bone marrow derived cells is able to alter cholesterol levels. To determine the effect of IDE on lipoprotein production, male $LDLr^{-/-}$ mice that had been reconstituted with either wild type or $IDE^{-/-}$ bone marrow could be injected with ^{35}S amino acids and Triton 1339 which blocks lipolysis and, at subsequent time points, newly synthesized apoB48 and apoB100 could be quantified in plasma samples by sodium dodecylsulfate polyacrylamide gel electrophoresis (Voyiaziakis et al., 1999). To determine if IDE deficiency alters lipoprotein clearance, VLDL and LDL from $LDLr^{-/-}$ mice could be labeled with ^{125}I and injected into male $LDLr^{-/-}$ that had been reconstituted with wild type or $IDE^{-/-}$ bone marrow. Plasma decay and liver trapping of the labeled lipoproteins could then be monitored. Likewise, clearance of VLDL and LDL isolated from $LDLr^{-/-}$ mice reconstituted with male wild type or $IDE^{-/-}$ bone marrow could be evaluated in $LDLr^{-/-}$ mice.

Elevated plasma cholesterol levels in the male $LDLr^{-/-}$ mice reconstituted with $IDE^{-/-}$ bone marrow may not just promote foam cell formation but also favour a pro-inflammatory state. FPLC analysis indicates that the spike in total serum cholesterol of recipient mice reconstituted with IDE-null BMDC is due to increased VLDL and IDL/LDL cholesterol fractions. Increased cholesterol levels are intricately linked to the inflammatory response as lipoproteins are able to accumulate in the artery wall, which leads to the activation of several inflammatory pathways. It has been reported that VLDL and other triglyceride-containing particles can activate the transcription factor nuclear factor kappa-light-chain-enhancer of activated B cells (NF-κB) (Dichtl *et al.*, 1999), which subsequently upregulates many proinflammatory genes. Interestingly, insulin resistant states, which may occur in IDE-null animals, are associated with chronic inflammation and hepatic overproduction of apoB100. Tsai et al. (2009) used an insulin resistant hamster model as well as primary hamster hepatocytes to show that hepatic insulin resistance is associated

with NF-κB activation which subsequently upregulates apoB100 production at the levels of translation and proteasomal degradation. Knowledge of mechanism(s) linking hepatic inflammation with apoB100-lipoprotein metabolism is lacking, however, the finding that insulin resistant states can influence apoB100 metabolism via NF-κB activation further supports the finding that IDE hypofunction increased VLDL and LDL cholesterol fractions. Secondly, inherently hypercholesterolemic apoE and LDLr-null mouse models show higher levels of T lymphocytes in atherosclerotic segments of artery walls (Roselaar *et al.*, 1996) as compared to controls; indicating that dyslipidemia and hypercholesterolemia can affect inflammation and immunity. Inflammation and cholesterol levels appear to feed off each other. In fact, IFN-γ produced by activated T lymphocytes can directly affect macrophage cholesterol metabolism by inducing CE synthesis via inhibition of adenosine triphosphate-binding cassette transporter-A1 (ABCA1), thus decreasing cholesterol efflux and increasing foam cell morphology (Panousis and Zuckerman, 2000). Combining this effect with other IFN-γ downstream effects leading to increased macrophage activity fully shows the strong interplay between total cholesterol levels and inflammatory mediators.

6.2 IDE and SR-A

As summarized in the rationale for this study, IDE is able to bind the cytoplasmic domain of SR-A, so it was hypothesized that this association may affect SR-A mediated uptake of modified LDL, or another facet of SR-A biology. As such, a goal of ours was to see if IDE deficiency in BMDM affected the binding ability of acLDL to the cell surface. Although this experiment was done only once in triplicate, we saw a 25% and 18% reduction in acLDL binding to bone marrow derived macrophages obtained from male and female IDE-null mice, respectively. While at this point, still preliminary, these results may implicate IDE in the recycling or degradation of the SR-A protein. Further analysis of SR-A surface expression on $IDE^{-/-}$ BMDC with methods such as biotinylation or flow cytometry would be useful to define the mechanisms responsible for decreased acLDL association.

We further looked at uptake of ac-LDL-associated ^{3}H-cholesterol by wild type and $IDE^{-/-}$macrophages. Uptake analysis of bone marrow-derived macrophages procured from

IDE-null mice treated with ^{3}H-cholesterol-acLDL revealed no differences in uptake at 2, 6, 12 and 24 hours of lipoprotein exposure, compared to wild type cells. These experiments were carried out under normoinsulinemic conditions but, as will be discussed later, IDE-null macrophages may not display a pro-atherogenic phenotype without excessive insulin levels being present. As the oil red O assay and Sudan IV-stained aortic root sections show marked foam cell formation, we went on to quantify the rate of incorporation of ^{3}H-oleate into cholesteryl ester in IDE$^{-/-}$ and wild type BMDM following exposure to acetylated LDL. This experiment was done only once in triplicate, however there was a marked increase in cholesteryl ester lipid fraction in IDE-null macrophages. This result, while taking into account the lack of change in uptake, suggests that IDE may play an important role in intracellular processing of cholesterol, possibly through cytoplasmic association with lipid enzymes and/or organelles.

6.3 Is the increased atherosclerosis in IDE-null mice SR-A-mediated?

The putative interaction of IDE with SR-A may or may not be responsible for observed change in lesion size. As mentioned above, more recent studies suggest that the effects of scavenger receptors on atherogenesis are very complex. Along with modified lipoprotein uptake, these proteins are now known to regulate apoptotic cell clearance, initiate signal transduction, and serve as pattern recognition receptors for pathogens. As such, the downstream activities of SRA may contribute both to proinflammatory and anti-inflammatory forces regulating atherogenesis, therefore differentially impacting early and more complex lesions.

Many studies indicate that deletion of the genes encoding for SRA-I and SRA-II or deletion of CD36 in hyperlipidemic mouse models substantially decreases aortic sinus atherosclerosis and arterial lipid accumulation (Sakaguchi, 1998; Babaev, 2000; Febbraio). These findings led to the paradigm that uptake of oxidized LDL via SR-A and CD36 constitutes the major pathways for foam cell formation *in vivo* and that lipid uptake by either receptor is a proatherosclerotic event. To further explore the involvement of these macrophage receptors in foam cell formation and atherosclerosis, a group generated mice

lacking both SR-A and CD36. Macrophages isolated from these mice showed a profound impairment in the uptake of either oxidized or acetylated LDL (Kunjathoor *et al.*, 2002). However, it is unknown as to the degree with which *in vitro* preparations of modified lipoproteins mimics *in vivo* lipoproteins, so it was necessary to demonstrate the impact of SR-A/CD36 deletion *in vivo*. Aortic root atherosclerosis in apoE$^{-/-}$CD36$^{-/-}$SR-A$^{-/-}$ mice, as assessed by morphometry, electron microscopy, and immunohistochemistry, showed no decrease in lesion area or *in vivo* foam cell formation when compared to apoE$^{-/-}$ mice. However, apoE$^{-/-}$CD36$^{-/-}$SR-A$^{-/-}$ lesions showed reduced expression of inflammatory genes as well as a near 30% decrease in macrophage apoptosis and 50% decrease in plaque necrosis in aortic root lesions of these mice (Manning-Tobin, 2009). These results indicate that SR-A/CD36 pathways may hold a more crucial role in lesion complexity and plaque stability, rather than progression of lesion size.

6.4 Male-specific effect of IDE knockout

It is of interest to note that the presence/absence of IDE in BMDC of male mice affects both atherosclerosis and serum cholesterol, but not that of female. Reduced IDE expression and/or activity have been implicated in the etiology and development of AD (Perez, 2000; Zhao, 2007). Estrogen therapy, when initiated at the onset of menopause, has been reported to reduce the risk or delay the onset of AD in women (Zhao and Brinton, 2007; Zhao, 2005). In agreement with clinical observations, basic science indicates that estrogen is neuroprotective and efficacious in preventing or slowing the development of AD pathology, most notably Aβ accumulation and plaque formation in diverse animal models of AD (Carroll, 2007; Petanceska, 2000; Zheng, 2002). In fact, past research indicates that estrogen regulates the expression and activity of IDE in female reproductive system, where IDE is involved in cellular growth and differentiation (Udrisar, 2005). Moreover, another study revealed an ovariectomized- induced decline in IDE expression occurred in the hippocampus and not in the cerebellum of adult female rats. These observations are of great interest because they may suggest that estrogen regulation of brain IDE expression is a regional rather than a global effect. This brain region-selective profile in response to ovariectomy is very consistent with clinical observations that also indicate a greater decline

in IDE expression and/or activity as a function of age or AD in the hippocampus as compared to other brain regions (Caccamo *et al.*, 2005; Zhao *et al.*, 2007). Traditionally, estrogens have conferred a survival phenotype at the cellular level. Estradiol, the dominant form of estrogen in pre-menopausal women has been shown to preserve pancreatic β-cell function. In fact, rodent models of β-cell failure, when treated with physiological concentrations of estradiol show protection of β-cells against lipotoxicity, oxidative stress and proinflammatory cytokine-induced apoptosis (Le May *et al.*, 2006; Contreras *et al.*, 2002). These survival effects of estradiol are consistent with the observation that the overall prevalence of diabetes is lower in premenopausal women, a trend that is reversed after menopause (Wild et al., 2004). There are certain phenotypical differences between males and females that can affect metabolism such as body composition, regional fat distribution and aerobic fitness. We are now discovering that many genes are expressed in a sexually dimorphic manner, and there is evidence for differences in post-translational changes in men and women, which will almost certainly result in different enzyme activities, abundance of cellular signal transduction elements and substrate kinetics (Mittendorfer, 2005). Although these results may not shed light on the mechanisms responsible for our observation that IDE deficiency in BMDC increases atherosclerosis in $LDLr^{-/-}$ male but not female recipients, they clearly illustrate the potential for sexual dimorphism in IDE gene expression and function.

6.5 Limitations of the current study

One setback to my *in vitro* studies is the use of acetylated LDL in order to specifically target SR-A biology. Within a lesion, there are many receptors other than SR-A as well as non-receptor mediated mechanisms that result in lipid uptake. Aside from oxidation or acetylation, modifications to lipoproteins may be induced by enzymes (e.g., phospholipase C, phospholipase A2), leading to increased retention within the matrix, as well as aggregation into larger complexes that may then be internalized by phagocytic or pinocytic mechanisms (Kruth, 2002; Kruth, 2005).

Studies from Suzuki's work suggest that SR-A pathways account for ~80% of macrophage uptake of acetylated LDL, but have a lower affinity for oxidized LDL (Suzuki *et al*, 1997; Kunjathoor *et al*., 2002). By treating BMDM with acLDL only, the majority of lipid uptake will be via an SR-A pathway, which may not facilitate sufficient binding and uptake to adequately demonstrate a difference in cholesterol binding and uptake as well as cholesteryl ester accumulation *in vitro*. This holds true especially when taking into consideration that oxLDL is a much more physiologically relevant modification *in vivo* than is acLDL.

Chapter 7: Conclusions

The goal of this study was to establish if IDE deficiency in bone marrow-derived cells had an affect on atherosclerotic lesion size and macrophage foam cell formation. Indeed, IDE hypofunction plays well established roles in both Alzheimer's disease and type 2 diabetes. The present study illustrates an important atheroprotective role for IDE in males (Figure. 20), in that male $LDLr^{-/-}$ mice reconstituted with IDE-expressing bone marrow-derived cells had significantly smaller lesions in 2 vascular beds as compared to $LDLr^{-/-}$ mice reconstituted with IDE-null macrophages. The reverse bone marrow transplant study recapitulated this IDE-mediated atheroprotection in males, as $IDE^{-/-}/LDLr^{-/-}$ male recipients had significantly smaller lesions in 2 vascular beds when reconstituted with wild type bone marrow, compared to IDE-null bone marrow. Moreover, male $LDLr^{-/-}$ recipients reconstituted with $IDE^{-/-}$ bone marrow had a significant increase in their total serum cholesterol levels and LDL-cholesterol fraction, which may provide a mechanism by which these chimeras generate more atherosclerosis. *In vitro* studies suggest that IDE-null macrophages exhibit foam cell formation, may have altered SR-A degradation and/or recycling and undergo increased cholesteryl ester accumulation compared to wild type macrophages. There is a wealth of biological and clinical links between IDE, Alzheimer's disease, type 2 diabetes as well as prospective studies associating said etiologies with atherosclerosis. As such, the results of this study provide an impetus for further mechanistic knowledge with regards to IDE and its roles in foam cell formation and atherosclerosis.

Figure 20. Summary of IDE hypofunction in Alzheimer's disease, type 2 diabetes and atherosclerosis

A summary of phenotypical changes in IDE-deficient models and their associated pathologies highlights the importance of this protein in proper physiology.

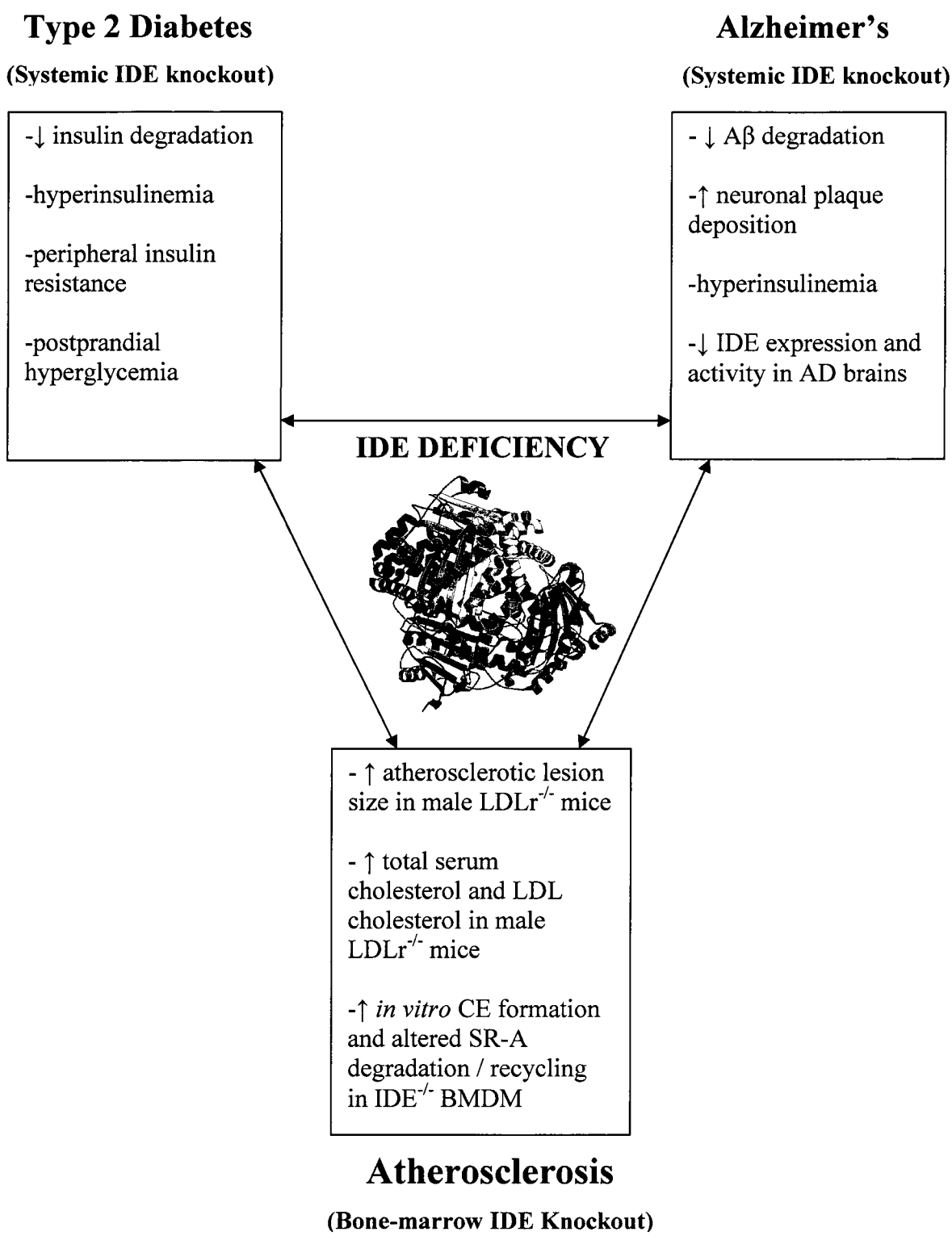
Type 2 Diabetes
(Systemic IDE knockout)
-↓ insulin degradation
-hyperinsulinemia
-peripheral insulin resistance
-postprandial hyperglycemia
Alzheimer's
(Systemic IDE knockout)
- ↓ Aβ degradation
-↑ neuronal plaque deposition
-hyperinsulinemia
-↓ IDE expression and activity in AD brains
IDE DEFICIENCY
- ↑ atherosclerotic lesion size in male LDLr-/- mice
- ↑ total serum cholesterol and LDL cholesterol in male LDLr-/- mice
-↑ in vitro CE formation and altered SR-A degradation / recycling in IDE-/- BMDM
Atherosclerosis
(Bone-marrow IDE Knockout)

Chapter 8: Future directions

This study was initiated following our demonstration of an association of IDE with the SR-A cytoplasmic tail. Therefore, we concentrated our efforts on elucidating potential roles of IDE in SR-A-mediated foam cell formation both in a mouse model of atherosclerosis and with *in vitro* experiments. However, as was described in the literature review, IDE is an important regulator of plasma insulin levels. While we did not measure plasma insulin levels in our mice, or determine insulin resistance, there is an abundance of literature in support of hyperinsulinemia and insulin resistance in $IDE^{-/-}$ mice. The increase in atherosclerosis seen in $LDLr^{-/-}$ mice reconstituted with $IDE^{-/-}$ BMDC could be due to multiple effects of hyperinsulinemia. Much of the literature has cited insulin-resistant macrophages and their proinflammatory properties. Considering that the BMDM cholesterol uptake assay showed no difference under normal conditions, I think it would be prudent to repeat the assay in the presence of hyperinsulinemic conditions. Macrophages do have insulin receptors (IR), which can be down regulated with insulin treatment (Liang, 2007), resulting in suppression of insulin signalling, thereby showing the hallmarks of insulin resistance.

There is a great deal of literature covering the pro-inflammatory effects of macrophage insulin resistance. Mita *et al.* (2010) demonstrated proatherosclerotic properties in obese KKAy mice with insulin resistance. Most notably, this group demonstrated enhanced monocyte/macrophage adhesion to the endothelium accompanied by increased inflammatory cytokines (IL-6 and MCP-1) and reduced insulin signalling in macrophages. Interestingly, this phenotype was completely independent of LDL cholesterol level. Although the lipid profile of KKAy mice was less atherogenic than that of KK mice fed a high cholesterol diet, KKAy mice showed expanded atherosclerotic lesions (Mita *et al.*, 2010). These results complement the results in my study as we report a significant change in lesion size with modest changes in lipid profile. The increased inflammatory cytokine release seen in this study also provides a rationale to do a cytokine array on the IDE-null BMDM as they should exhibit insulin resistance under high insulin conditions. Enhanced macrophages adhesion as reviewed in macrophage insulin resistance literature

provides an impetus to determine if perhaps there is more macrophage adhesion in my aortic root sections, via a specific macrophage stain.

Using different models of insulin resistance, Alan Tall and colleagues showed that primary macrophages from ob/ob and transgenically rescued IR-deficient mice exhibit enhanced binding and uptake of modified LDL and elevated CE formation (Liang *et al.*, 2004), which suggests that macrophage insulin resistance promotes uptake of atherogenic lipoproteins. Moreover, an insulin-sensitizing PPAR γ activator known as rosiglitazone was shown to improve insulin signalling and decrease modified LDL binding in macrophages from treated ob/ob / $LDLR^{-/-}$ mice (Liang *et al.*, 2004). Another study used bone marrow transplantation from $IR^{-/-}$ mice into $LDLr^{-/-}$mice fed a western diet containing 0.2% cholesterol, and showed no significant differences in plasma lipoprotein, insulin or glucose levels between transplant groups (Han *et al.*, 2006). $LDLr^{-/-}$ mice reconstituted with $IR^{-/-}$ bone marrow showed no difference in the area of early foam cell lesions, but did produce larger, more complex lesions at a later stage, along with increased apoptotic cells and necrotic core formation. If IDE deficiency is able to promote atherosclerosis by inducing insulin resistance, perhaps 12 weeks of HFD would be more prudent than the 8-week schedule used for this study. This also holds true for SR-A/CD36 mechanisms since the dysfunction of these receptors as well as insulin resistance have been implicated in late stage lesion complexity, apoptosis and necrotic core formation.

In fact, Tall's group continued to show that insulin resistant macrophages had increased CD36 protein. Treatment of WT macrophages with an inhibitor of insulin signalling via phosphatidylinositol 3-kinases (PI3K) results in an increase in CD36, and there is a post-transcriptional increase in CD36 protein shown in IR null macrophages. (Liang *et al.*, 2004). Finally, administration of thiazolidinediones to ob/ob mice and ob/ob / $LDLr^{-/-}$ mice results in decreased CD36 protein (Liang *et al.*, 2004). All models of insulin resistance, whether it be genetic deletion of the IR, preincubation with insulin, pharmacological inhibition of insulin signalling, or macrophages isolated from hyperinsulinumic mice, they all show increased expression of SR-A (Liang *et al.*, 2007; Liang *et al.*, 2004). Enhanced monocyte/macrophage adhesion, proinflammatory cytokine

expression, and SR-A/CD36 expression are phenotypes in many models of insulin resistance, and so any of these phenotypes may become evident in $IDE^{-/-}$ tissue and may provide mechanistic evidence of a role for IDE in atherosclerosis. This may provide a rationale to treat IDE-null BMDM with insulin pretreatment and determine SR-A and CD36 receptor expression using a method such as flow cytometry. It is crucial to elucidate the mechanism by which IDE knockout results in more atherosclerosis and I think various analyses of insulin treated $IDE^{-/-}$ BMDM should answer some important questions.

Along with increased expression of SR-A and CD36, the binding and uptake studies could be repeated with hyperinsulinemic conditions. Indeed, an insulin-resistant macrophage should have more atherogenic surface receptors, theoretically resulting in greater binding and uptake of modified LDL. Aside from increased binding and uptake, insulin-resistant states have shown an increased adhesion of monocytes/macrophages. Knowing this, it would be interesting to stain the aortic root for active macrophage markers, to perhaps signify a greater recruitment and adherence of these cells to the site of injury.

Evidence that the Alzheimer's peptide Aß can be found in coronary arteries, coupled with IDE's propensity to cleave amyloid forming peptides, serves as a strong rationale to stain for amlyoid in the aortic root sections of IDE-null mice to see if there is more amyloid deposition than that of wild type. Interestingly, Aβ can bind to the receptor for advanced glycation end products (RAGE) and activate pro-inflammatory intracellular signalling pathways (Schmidt *et al.*, 2009) and RAGE has a well established role in the development of atherosclerosis in both diabetic and non-diabetic mice (Yan *et al.*, 2010). Furthermore, microglia are able to secrete IDE into the cytoplasm for the extracellular degradation of Aβ (Qui *et al.*, 1998), and neurons exhibit extracellular, cell surface bound IDE mediated degradation of Aβ (Vekrellis *et al.*, 2000). These findings shed light on the possibility that IDE may be released extracellularly by bone marrow derived macrophages within a lesion.

Finally, the recruitment of monocytes, differentiation and activation of macrophages is dependant on many cytokines interactions within and around the site of the lesion. As such, it would be prudent to carry out a cytokine array on bone marrow derived

macrophages from both wild type and IDE-null mice to determine if IDE deficiency regulates any major players in atherosclerosis.

Reference List

Aliev G, Gasimov E, Obrenovich ME, Fischbach K, Shenk JC, Smith MA, Perry G. Atherosclerotic lesions and mitochondria DNA deletions in brain microvessels: implication in the pathogenesis of Alzheimer's disease. Vasc Health Risk Manag. 2008;4(3):721-30

Arad Y, Ramakrishnan R, Ginsberg HN: Lovastatin therapy reduces low density lipoprotein apoB levels in subjects with combined hyperlipidemia by reducing the production of apoB-containing lipoproteins: Implications for the pathophysiology of apoB production. J Lipid Res 31:567-582, 1990

Araki, N., et al. "Macrophage scavenger receptor mediates the endocytic uptake and degradation of advanced glycation end products of the Maillard reaction." Eur.J.Biochem. 230.2 (1995): 408-15.

Arvanitakis Z, Wilson RS, Bienias JL, Evans DA, Bennett DA. Diabetes mellitus and risk of Alzheimer disease and decline in cognitive function. Archiv Neurol 2004;61:661–6.

Austin MA, Hokanson JE: Epidemiology of triglycerides, small dense low-density lipoprotein, and lipoprotein (a) as risk factors for coronary heart disease. Med Clin North Am 78:99-115, 1994

Authier, F., B. I. Posner, and J. J. Bergeron. "Insulin-degrading enzyme." Clin.Invest Med. 19.3 (1996): 149-60.

Authier F, Cameron PH, Taupin V 1996 Association of insulin degrading enzyme with a 70 kDa cytosolic protein in hepatoma cells. Biochem J 319:149–158

Babaev, V.R., et al. Reduced atherosclerotic lesions in mice deficient for total or macrophagespecific expression of scavenger receptor-A. Arterioscler. Thromb. Vasc. Biol. (2000) 20:2593–2599.

Backer JM, Kahn CR, White MF 1990 The dissociation and degradation of internalized insulin occur in the endosomes of rat hepatoma cells. J Biol Chem 265:14828–14835

Baumeister H, Muller D, Rehbein M, Richter D. The rat insulindegradingenzyme. Molecular cloning and characterization of tissuespecific transcripts. FEBS Lett 1993;317:250–4.

Becker, M., et al. "Expression of the class A macrophage scavenger receptor on specific subpopulations of murine dendritic cells limits their endotoxin response." Eur.J.Immunol. 36.4 (2006): 950-60.

Becker AB, Roth RA. Insulysin and pitrilysin: insulin-degrading enzymes of mammals and bacteria. Meth Enzymol 1995;248:693–703.

Bennett RG, Duckworth WC, Hamel FG. Degradation of amylin by insulin-degrading enzyme. J Biol Chem 2000;275:36621–5.

Bertram, L., et al. "Evidence for genetic linkage of Alzheimer's disease to chromosome 10q." Science 290.5500 (2000): 2302-03.

Bickel, P. E. and M. W. Freeman. "Rabbit aortic smooth muscle cells express inducible macrophage scavenger receptor messenger RNA that is absent from endothelial cells." J.Clin.Invest 90.4 (1992): 1450-57.

Bowdish DM, Gordon S. Conserved domains of the class A scavenger receptors: evolution and function. Immunol Rev. 2009 Jan;227(1):19-31.

Breckenridge WC, Little JA, Steiner G, et al: Hypertriglyceridemia associated with deficiency of apolipoprotein C-II. N Engl J Med 298:1265-1273, 1978)

Brown MS, Goldstein JL: How LDL receptors influence cholesterol and atherosclerosis. Sci Am 251:58-66, 1984

Brown MS, Goldstein JL. Lipoprotein Receptors: therapeutic implications. J Hypertens Suppl 1990;8:S33-6

Brown MS, Goldstein JL: The SREBP pathway: Regulation of cholesterol metabolism by proteolysis of a membrane-bound transcription factor. Cell 89:331-340, 1997

Buja LM, Kita T, Goldstein JL, Watanabe Y, Brown MS. Cellular pathology of progressive atherosclerosis in the WHHL rabbit. An animal model of familial hypercholesterolemia. Arteriosclerosis. 1983 Jan-Feb;3(1):87-101

Bulloj A, Leal MC, Xu H, Castaño EM, Morelli L. Insulin-degrading enzyme sorting in exosomes: a secretory pathway for a key brain amyloid-beta degrading protease. J Alzheimers Dis. 2010 Jan;19(1):79-95.

Cao, X. and T. C. Sudhof. "A transcriptionally [correction of transcriptively] active complex of APP with Fe65 and histone acetyltransferase Tip60." Science 293.5527 (2001): 115-20.

Carantoni M, Zuliani G, Munari MR, D'Elia K, Palmieri E, Fellin R. Alzheimer disease and vascular dementia: relationships with fasting glucose and insulin levels. Dement Geriatr Cogn Disord 2000;11:176–80.

Cardoso S. M., Santos S., Swerdlow R. H. and Oliveira C. R. (2001) Functional mitochondria are required for amyloid beta-mediated neurotoxicity. FASEB J. 15, 1439–1441.

Cathcart MK, McNally AK, Morel DW, Chisolm GM III. Superoxide anion participation in human monocyte-mediated oxidation of low-density lipoprotein and conversion of low-density lipoprotein to a cytotoxin.J Immunol 1989;142:1963–1969.

Contreras JL, Smyth CA, Bilbao G, Young CJ, Thompson JA, Eckhoff DE.17beta-Estradiol protects isolated human pancreatic islets against proinflammatory cytokine-induced cell death: molecular mechanisms and islet functionality. Transplantation. 2002 Nov 15;74(9):1252-9.

Cook DG, et al. Reduced hippocampal insulin-degrading enzyme in late-onset Alzheimer's disease is associated with the apolipoprotein E-epsilon4 allele. Am J Pathol 2003;162:313–9.

Daugherty, A., et al. "Scavenger receptors are present on rabbit aortic endothelial cells in vivo." Arterioscler.Thromb.Vasc.Biol. 17.11 (1997): 2369-75.

de Tullio MB, Morelli L, Castaño EM.The irreversible binding of amyloid peptide substrates to insulin-degrading enzyme: a biological perspective. Prion. 2008 Apr;2(2):51-6. Epub 2008 May 1.

de Winther, MPJ., et al. "Overexpression of the human macrophage scavenger receptor reduces atherosclerosis in both low density lipoprotein receptor deficient mice and apoE3Leiden transgenic mice." Circulation (suppl)100 (1999) :I-751

Dichtl W, Nilsson L, Goncalves I, Ares MP, Banfi C, Calara F, Hamsten A, Eriksson P, Nilsson J. Very low-density lipoprotein activates nuclear factorkappaB in endothelial cells. Circ Res 1999;84:1085–1094.

Dixon JL, Ginsberg HN: Regulation of hepatic secretion of apolipoprotein B-containing lipoproteins: Information obtained from cultured liver cells. J Lipid Res 34:167-179, 1993

Doi, T., et al. "Charged collagen structure mediates the recognition of negatively charged macromolecules by macrophage scavenger receptors." J.Biol.Chem. 268.3 (1993): 2126-33.

Duckworth, W. C., R. G. Bennett, and F. G. Hamel. "Insulin degradation: progress and potential." Endocr.Rev. 19.5 (1998): 608-24.

Duckworth WC, Bennett RG, Hamel FG 1997 The significance of intracellular insulin to insulin action. J Invest Med 45:20–27

Edbauer, D., et al. "Insulin-degrading enzyme rapidly removes the beta-amyloid precursor protein intracellular domain (AICD)." J.Biol.Chem. 277.16 (2002): 13389-93.

el, Khoury J., et al. "Macrophages adhere to glucose-modified basement membrane collagen IV via their scavenger receptors." J.Biol.Chem. 269.14 (1994): 10197-200.

Emi, M., et al. "Structure, organization, and chromosomal mapping of the human macrophage scavenger receptor gene." J.Biol.Chem. 268.3 (1993): 2120-25.

Farris, W., et al. "Insulin-degrading enzyme regulates the levels of insulin, amyloid beta-protein, and the beta-amyloid precursor protein intracellular domain in vivo." Proc.Natl.Acad.Sci.U.S.A 100.7 (2003): 4162-67.

Farris W, Mansourian S, Leissring MA, Eckman EA, Bertram L, Eckman CB, Tanzi RE, Selkoe DJ. Partial loss-of-function mutations in insulin-degrading enzyme that induce diabetes also impair degradation of amyloid beta-protein. Am J Pathol 2004;164:1425–34.

Fazio S, Hasty AH, Carter KJ, Murray AB, Price JO, Linton MF. Leukocyte low density lipoprotein receptor (LDL-R) does not contribute to LDL clearance in vivo: bone marrow transplantation studies in the mouse. J Lipid Res. 1997 Feb;38(2):391-400.

Febbraio, M., et al. Targeted disruption of the class B scavenger receptor CD36 protects against atherosclerotic lesion development in mice. J. Clin. Invest. (2000) 105:1049–1056.

Freeman, M., et al. "Expression of type I and type II bovine scavenger receptors in Chinese hamster ovary cells: lipid droplet accumulation and nonreciprocal cross competition by acetylated and oxidized low density lipoprotein." Proc.Natl.Acad.Sci.U.S.A 88.11 (1991): 4931-35.

Fukuhara-Takaki K, Sakai M, Sakamoto Y, Takeya M, Horiuchi S. Expression of class A scavenger receptor is enhanced by high glucose in vitro and under diabetic conditions in vivo: one mechanism for an increased rate of atherosclerosis in diabetes. J Biol Chem. 2005 Feb 4;280(5):3355-64. Epub 2004 Nov 19.

Gehm BD, Kuo WL, Perlman RK, Rosner MR 1993 Mutations in a zinc-binding domain of human insulin-degrading enzyme eliminate catalytic activity but not insulin binding. J Biol Chem 268: 7943–7948

Ginseberg H. LIPOPROTEIN PHYSIOLOGY. Endocrinology and Metabolism Clinics - Volume 27, Issue 3 (September 1998)

Goldberg IJ: Lipoprotein lipase and lipolysis: Central roles in lipoprotein metabolism and atherosclerosis. J Lipid Res 37:693-707, 1996)

Goldstein, J. L., et al. "Binding site on macrophages that mediates uptake and degradation of acetylated low density lipoprotein, producing massive cholesterol deposition." Proc.Natl.Acad.Sci.U.S.A 76.1 (1979): 333-37.

Gotto AM Jr, Pownall HJ, Havel RJ: Introduction to the plasma lipoproteins. Methods Enzymol 128:3-41, 1986

Guest, C. B., et al. "Phagocytosis of cholesteryl ester is amplified in diabetic mouse macrophages and is largely mediated by CD36 and SR-A." PLoS.ONE. 2.6 (2007): e511.

Hamel FG, Mahoney MJ, Duckworth WC 1991 Degradation of intraendosomal insulin by insulin degrading enzyme without acidification. Diabetes 40:436–443
Hamel FG, Peavy DE, Ryan MP, Duckworth WC 1987 High performance liquid chromatographic analysis of insulin degradation products from isolated hepatocytes: effects of inhibitors suggest intracellular and extracellular pathways. Diabetes 36:702–708

Hamel FG, Posner BI, Bergeron JJM, Frank BH, Duckworth WC1988 Isolation of insulin degradation products from endosomesderived from intact rat liver. J Biol Chem 263:6703–6708

Hampton, R. Y., D. T. Golenbock, M. Penman, M. Krieger, and C. R. Raetz. 1991. Recognition and plasma clearance of endotoxin by
scavenger receptors. Nature. 352: 342–344.

Han S, Liang CP, DeVries-Seimon T, Ranalletta M, Welch CL, Collins- Fletcher K, Accili D, Tabas I, Tall AR. Macrophage insulin receptor deficiency increases ER stress-induced apoptosis and necrotic core formation in advanced atherosclerotic lesions. Cell Metab. 2006;3: 257–266.

Hansson GK. Inflammation, atherosclerosis, and coronary artery disease. N Engl J Med. 2005 Apr 21;352(16):1685-95.

Harada S, Smith RM, Smith JA, Jarett L 1993 Inhibition of insulin degrading enzyme increases translocation of insulin to the nucleus in H35 rat hepatoma cells: evidence of a cytosolic pathway. Endocrinology 132:2293–2298

Harada S, Smith RM, Smith JA, Shah N, Jarett L 1995 Demonstration of specific insulin binding to cytosolic proteins in H35 hepatoma cells, rat liver and skeletal muscle. Biochem J 306:21–28

Hari J, Shii K, Roth RA. In vivo association of [125I]-insulin with a cytosolic insulin-degrading enzyme: detection by covalent crosslinking and immunoprecipitation with a monoclonal antibody. Endocrinology 1987;120:829–31.

HAVEL RJ, EDER HA, BRAGDON JH. The distribution and chemical composition of ultracentrifugally separated lipoproteins in human serum. J Clin Invest. 1955 Sep;34(9):1345-53.

Haworth, R., N. Platt, S. Keshav, D. Hughes, E. Darley, H. Suzuki, Y. Kurihara, T. Kodama, and S. Gordon. 1997. The macrophage scavenger receptor type A is expressed by activated

macrophages and protects the host against lethal endotoxic shock. J. Exp. Med. 186: 1431–1439.

Hayden MR, Liu MS, Ma Y: Gene environment interaction and plasma triglyceride levels: The crucial role of lipoprotein lipase. Clin Genet 46:15-18, 1994

Hirsch-Reinshagen V, Maia LF, Burgess BL, et al. The absence of ABCA1 decreases soluble ApoE levels but does not diminish amyloid deposition in two murine models of Alzheimer disease. J Biol Chem 2005; 280:43243– 43256.

Horiuchi, S., Sakamoto, Y., and Sakai, M. (2003) Scavenger receptors for oxidized and glycated proteins. Amino Acids 25, 283–292.

Howard BV: Lipoprotein metabolism in diabetes mellitus. J Lipid Res 28:613-628, 1987.

Hui D, Innerarity T, Mahley R. 1981.Lipoprotein binding to canine hepatic membranes--metabolically distinct apo-E and apooB,E receptors. J. Biol.Chem. 256:5646-55

Husemann, J., Loike, J. D., Anankov, R., Febbraio, M., and Silverstein, S. C. (2002) Scavenger receptors in neurobiology and neuropathology: Their role on microglia and other cells of the nervous system. Glia 40, 195–205.

Im, H., et al. "Structure of substrate-free human insulin-degrading enzyme (IDE) and biophysical analysis of ATP-induced conformational switch of IDE." J.Biol.Chem. 282.35 (2007): 25453-63.

Ishibashi Shun, Michael S. Brown, Joseph L. Goldstein, Robert D. Gerard, Robert E. Hammer, and Joachim Herz. J.Clin. Invest. Volume 92, August 1993, 883-89

Ishibashi S, Goldstein JL, Brown MS, Herz J, Burns DK. Massive xanthomatosis and atherosclerosis in cholesterol-fed low density lipoprotein receptor-negative mice. J Clin Invest. 1994 May;93(5):1885-93

Janson J, Laedtke T, Parisi JE, O'Brien P, Petersen RC, Butler PC.Increased risk of type 2 diabetes in Alzheimer disease. Diabetes. 2004 Feb;53(2):474-81.

Kane J. P., Hardman D. A., Paulus H. E.. Heterogeneity of apolipoprotein Bisolation of a new species from human chylomicrons. Proc. Natl. Acad. Sci. U.S.A. 1980;77:2465-2469.

Kaprio J, Ferrell RE, Kottke BA, Kamboh MI, Sing CF. Effects of polymorphisms in apolipoproteins E, A-IV, and H on quantitative traits related to risk for cardiovascular disease. Arterioscler Thromb. 1991;11:1330-1348

Kimberly, W. T., et al. "The intracellular domain of the beta-amyloid precursor protein is stabilized by Fe65 and translocates to the nucleus in a notch-like manner." J.Biol.Chem. 276.43 (2001): 40288-92.

Kishor M. Wasan, Dion R. Brocks, Stephen D. Lee, Kristina Sachs-Barrable & Sheila J. Thornton. Impact of lipoproteins on the biological activity and disposition of hydrophobic drugs: implications for drug discovery. Nature Reviews Drug Discovery 7, 84-99 January 2008

Kissebah AH, Alfarsi A, Adams PW: Integrated regulation for very low density lipoprotein triglyceride and apolipoprotein-B kinetics in man: Normolipidemic subjects, familial hypertriglyceridemia and familial combined hyperlipidemia. Metabolism 20:856-868, 1981

Kodama, T., et al. "Type I macrophage scavenger receptor contains alpha-helical and collagen-like coiled coils." Nature 343.6258 (1990): 531-35.

Koldamova R, Staufenbiel M, Lefterov I. Lack of ABCA1 considerably decreases brain ApoE level and increases amyloid deposition in APP23 mice. J Biol Chem 2005; 280:43224–43235.

Kosswig, N., et al. "Class A scavenger receptor-mediated adhesion and internalization require distinct cytoplasmic domains." J.Biol.Chem. 278.36 (2003): 34219-25.

Krieger, M. "The other side of scavenger receptors: pattern recognition for host defense." Curr.Opin.Lipidol. 8.5 (1997): 275-80.

Kruth HS, Huang W, Ishii I, Zhang WY. Macrophage foam cell formation with native low density lipoprotein. J Biol Chem. 2002;277:34573–34580.

Kruth HS, Jones NL, Huang W, Zhao B, Ishii I, Chang J, Combs CA, Malide D, Zhang WY. Macropinocytosis is the endocytic pathway that mediates macrophage foam cell formation with native LDL. J Biol Chem. 2005;280:2352–2360.

Kunitomo, M. "[Oxidative stress and atherosclerosis]." Yakugaku Zasshi 127.12 (2007): 1997-2014.

Kunjathoor VV, Febbraio M, Podrez EA, Moore KJ, Andersson L, Koehn S, Rhee JS, Silverstein R, Hoff HF, Freeman MW. Scavenger receptors class A-I/II and CD36 are the principal receptors responsible for the uptake of modified low density lipoprotein leading to lipid loading in macrophages. J Biol Chem. 2002; 277:49982– 49988.

Kuo, W. L., A. G. Montag, and M. R. Rosner. "Insulin-degrading enzyme is differentially expressed and developmentally regulated in various rat tissues." Endocrinology 132.2 (1993): 604-11.

Kuo WL, Gehm BD, Rosner MR, Li W, Keller G. Inducible expression and cellular localization of insulin-degrading enzyme in a stably transfected cell line. J Biol Chem 1994;269:22599–606.

Kupfer S, Marschke K, Wilson E, French F 1993 Receptor accessory factor enhances specific DNA binding of androgen and glucocorticoid receptors. J Biol Chem 268:17519–17527

Leibson CL, Rocca WA, Hanson VA, Cha R, Kokmen E, O'Brien PC, Palumbo PJ. The risk of dementia among persons with diabetes mellitus: a population-based cohort study. Ann NY Acad Sci 1997;826:422–7.

Leissring MA, Farris W, Chang AY, Walsh DM, Wu X, Sun X, Frosch MP, Selkoe DJ. Enhanced proteolysis of beta-amyloid in APP transgenic mice prevents plaque formation, secondary pathology, and premature death. Neuron 2003;40:1087–93.

Leissring MA, Selkoe DJ. Structural biology: enzyme target to latch on to. Nature. 2006 Oct 19;443(7113):761-2.

Le May C, Chu K, Hu M, Ortega CS, Simpson ER, Korach KS, Tsai MJ, Mauvais-Jarvis F.Estrogens protect pancreatic beta-cells from apoptosis and prevent insulin-deficient diabetes mellitus in mice. Proc Natl Acad Sci U S A. 2006 Jun 13;103(24):9232-7. Epub 2006 Jun 5.

Levy J, Olefsky JM 1987 The effect of insulin concentration on retroendocytosis in isolated rat adipocytes. Endocrinology 120: 450–456

Li, P., et al. "The C-terminal domain of human insulin degrading enzyme is required for dimerization and substrate recognition." Biochem.Biophys.Res.Commun. 343.4 (2006): 1032-37.

Liang CP, Han S, Okamoto H, Carnemolla R, Tabas I, Accili D, Tall AR. Increased CD36 protein as a response to defective insulin signalling in macrophages. J Clin Invest. 2004;113:764 –773

Liang CP, Han S, Senokuchi T, Tall AR. The macrophage at the crossroads of insulin resistance and atherosclerosis. Circ Res. 2007;100:1546–1555.

Liu SL, Li YH, Shi GY, Tang SH, Jiang SJ, Huang CW, Liu PY, Hong JS, Wu HL. Dextromethorphan reduces oxidative stress and inhibits atherosclerosis and neointima formation in mice. Cardiovasc Res. 2009 Apr 1;82(1):161-9. Epub 2009 Feb 3

Lougheed M, Steinbrecher UP. Mechanism of uptake of copper-oxidized low density lipoprotein in macrophages is dependent on its extent of oxidation. J Biol Chem. 1996;271:11798 –11805.

Luoma, J., et al. "Expression of alpha 2-macroglobulin receptor/low density lipoprotein receptor-related protein and scavenger receptor in human atherosclerotic lesions." J.Clin.Invest 93.5 (1994): 2014-21.

Lustbader J. W., Cirilli M., Lin C. et al. (2004) ABAD directly links Abeta to mitochondrial toxicity in. Alzheimer's disease. Science 304, 448–452.

Mahley RW: Apolipoprotein E: Cholesterol transport protein with expanding role in cell biology. Science 240:622-630, 1988

Malcolm, A., et al. "Structural Biology: Enzyme target to latch on to."Nature 443 (2006): 761-762

Manning-Tobin JJ, Moore KJ, Seimon TA, Bell SA, Sharuk M, Alvarez-Leite JI, de Winther MP, Tabas I, Freeman MW. Loss of SR-A and CD36 activity reduces atherosclerotic lesion complexity without abrogating foam cell formation in hyperlipidemic mice. Arterioscler Thromb Vasc Biol. 2009 Jan;29(1):19-26. Epub 2008 Oct 23.

Matsumoto, A., et al. "Human macrophage scavenger receptors: primary structure, expression, and localization in atherosclerotic lesions." Proc.Natl.Acad.Sci.U.S.A 87.23 (1990): 9133-37.

Mattson M. P. (2004) Pathways towards and away from Alzheimer's disease. Nature 430, 631–639.

McDermott JR, Gibson AM. Degradation of Alzheimer's betaamyloid protein by human and rat brain peptidases: involvement of insulin-degrading enzyme. Neurochem Res 1997;22:49– 56.

Mietus-Snyder, M., et al. "Regulation of scavenger receptor expression in smooth muscle cells by protein kinase C: a role for oxidative stress." Arterioscler.Thromb.Vasc.Biol. 17.5 (1997): 969-78.

Mita T, Goto H, Azuma K, Jin WL, Nomiyama T, Fujitani Y, Hirose T, Kawamori R, Watada H. Impact of insulin resistance on enhanced monocyte adhesion to endothelial cells and atherosclerogenesis independent of LDL cholesterol level. Biochem Biophys Res Commun. 2010 Apr 9.

Mittendorfer B. J Nutr. 2005 Apr;135(4):681-6. Sexual dimorphism in human lipid metabolism. J Nutr. 2005 Apr;135(4):681-6.

Moulton, K. S., et al. "Cell-specific expression of the macrophage scavenger receptor gene is dependent on PU.1 and a composite AP-1/ets motif." Mol.Cell Biol. 14.7 (1994): 4408-18.

Murphy JE, Tedbury PR, Homer-Vanniasinkam S, Walker JH, Ponnambalam S. Biochemistry and cell biology of mammalian scavenger receptors. Atherosclerosis. 2005;182:1–15.

Nacci C, Tarquinio M, Montagnani M. Molecular and clinical aspects of endothelial dysfunction in diabetes. Intern Emerg Med. 2009 Apr;4(2):107-16. Epub 2009 Mar 10.

Nakashima Y, Plump AS, Raines EW, Breslow JL, Ross R. 1994. Apo E-deficient mice develop lesions of all phases of atherosclerosis throughout the arterial tree, Arlcrioscler. Thromb, 14:13.3-40

Mukherjee, A., et al. "Insulysin hydrolyzes amyloid beta peptides to products that are neither neurotoxic nor deposit on amyloid plaques." J.Neurosci. 20.23 (2000): 8745-49.

Ohara Y, Peterson TE, Harrison DG. Hypercholesterolemia increases endothelial superoxide anion production. J Clin Invest 1993;91:2546–2551.

Palinski, W., V. Ord, A. S. Plump, J. L. Breslow, D. Steinberg, and J. L. Witztum. 1994. ApoE-deficient mice are a model of lipoprotein oxidation in atherogenesis: demonstration of oxidation-specific epitopes in lesionsand high titers of autoantibodies to malondialdehyde-lysine in serum. Arterioscler. Thromb. 14: 605-616.

Palkama, T. "Induction of interleukin-1 production by ligands binding to the scavenger receptor in human monocytes and the THP-1 cell line." Immunology 74.3 (1991): 432-38.

Panousis CG, Zuckerman SH. Interferon-g induces downregulation of Tangier disease gene (ATP-binding-cassette transporter-1) in macrophage-derived foam cells. Arterioscler Thromb Vasc Biol 2000;20:1565–1571.

Pell ME, Duckworth WC, Peavy DE 1986 Localization of insulin degradation products to an intracellular site in isolated rat hepatocytes. Biochem Biophys Res Commun 137:1034–1040

Perez A, Morelli L, Cresto JC, Castano EM. Degradation of soluble amyloid beta-peptides 1-40, 1-42, and the Dutch variant 1-40Q by insulin degrading enzyme from Alzheimer disease and control brains. Neurochem Res 2000;25:247–55.

Piedrahita JA, Zhang SH, Hagaman JR, Oliver PM, Maeda N. Spontaneous hypercholesterolemia and arterial lesions in mice lacking apolipoprotein E. Proc Natl Acad Sci U S A. 1992;89:4471–4475.

Pluddemann, A., S. Mukhopadhyay, and S. Gordon. "The interaction of macrophage receptors with bacterial ligands." Expert.Rev.Mol.Med. 8.28 (2006): 1-25.

Pluddemann, A., C. Neyen, and S. Gordon. "Macrophage scavenger receptors and host-derived ligands." Methods 43.3 (2007): 207-17.

Plump, Andrew S. and Breslow, Jan L. Apolipoprotein E and the Apolipoprotein E Deficient Mouse. Ann,, Rev. Nutr. 1995. 1.5:495-518

Plump AS, Forte TM, Eisenberg S,Breslow JL. 1993. Atherogenic ~-VLDL in the apoE-deficient mouse: composition, origin, and fate. Circulation 88(4):1-2

Plump AS, Smith JD, Hayek T, Aalto-Setiilii K, Walsh A, et ai. 1992. Severe hypercholesterolcmia and athcrosclcresisin apolipoprotein E-deficient mice created by homologous recombination in ES cells. Cell 71:343-53

Potenza MA, Gagliardi S, Nacci C, Carratu' MR, Montagnani M. Endothelial dysfunction in diabetes: from mechanisms to therapeutic targets. Curr Med Chem. 2009;16(1):94-112.

Qiu WQ, Walsh DM, Ye Z, Vekrellis K, Zhang J, Podlisny M, Rosner MR, Safavi A, Hersh LB, Selkoe DJ (1998) Insulin-degrading enzyme regulates extracellular levels of amyloid 3-protein by degradation. J Biol Chem 273:32730-32738

Reaven GM: Role of insulin resistance in human disease. Diabetes 37:1595-1607, 1988

Roselaar SE, Kakkanathu PX, Daugherty A. Lymphocyte populations in atherosclerotic lesions of apoE 2/2 and LDL receptor 2/2 mice. Decreasing density with disease progression. Arterioscler Thromb Vasc Biol 1996;16:1013– 1018.

Runyan K, Duckworth WC, Kitabchi AE, Huff G. The effect of age on insulin-degrading activity in rat tissue. Diabetes 1979;28:324–5.

Ryan MP, Gifford JD, Solomon SS, Duckworth WC 1985 The calcium dependence of insulin degradation by rat skeletal muscle. Endocrinology 117:1693–1698

Sakaguchi, H., et al. "Role of macrophage scavenger receptors in diet-induced atherosclerosis in mice." Lab Invest 78.4 (1998): 423-34.

Saric T, Muller D, Seitz HJ, Pavelic K. Non-covalent interaction of ubiquitin with insulin-degrading enzyme. Mol Cell Endocrinol 2003;204:11–20.

Schmidt AM, Sahagan B, Nelson RB, Selmer J, Rothlein R, Bell JM (2009) The role of RAGE in amyloid-beta peptide-mediated pathology in Alzheimer's disease. Curr Opin Investig Drugs10, 672-80

Selkoe D. J. (2001) Alzheimer's disease: genes, proteins, and therapy.
Physiol. Rev. 81, 741–766.

Seta KA, Roth RA 1997 Overexpression of insulin degrading enzyme: cellular localization and effects on insulin signalling. Biochem Biophys Res Commun 231:167–171

Shachter NS, Ebara T, Ramakrishnan R, et al: Combined hyperlipidemia in transgenic mice overexpressing human apolipoprotein CI. J Clin Invest 98:846-855, 1996

Shen, Y., et al. "Structures of human insulin-degrading enzyme reveal a new substrate recognition mechanism." Nature 443.7113 (2006): 870-74.

Shii K, Roth RA. Inhibition of insulin degradation by hepatoma cells after microinjection of monoclonal antibodies to a specific cytosolic protease. Proc Natl Acad Sci USA 1986;83:4147–51.

Smith RM, Harada S, Jarett L 1997 Insulin internalization andother signalling pathways in the pleiotropic effects of insulin. Int Rev Cytol 173:243–280

Song, E. S., et al. "Mutation of active site residues of insulin-degrading enzyme alters allosteric interactions." J.Biol.Chem. 280.18 (2005): 17701-06.

Song, E. S., et al. "Substrate activation of insulin-degrading enzyme (insulysin). A potential target for drug development." J.Biol.Chem. 278.50 (2003): 49789-94.

Surmacz CA, Wert JJ, Ward WF, Mortimore GE 1988 Uptake and intracellular fate of [14C] sucrose-insulin in perfused rat livers.AmJ Physiol 255:C70–C75

Suzuki, H., et al. "A role for macrophage scavenger receptors in atherosclerosis and susceptibility to infection." Nature 386.6622 (1997): 292-96.

Tangirala RK, Rubin EM, Palinski W. Quantitation of atherosclerosis in murine models: correlation between lesions in the aortic origin and in the entire aorta, and differences in the extent of lesions between sexes in LDL receptor-deficient and apolipoprotein E-deficient mice. J Lipid Res. 1995 Nov;36(11):2320-8

Tanzi R. E. and Bertram L. (2005) Twenty years of the Alzheimer's disease amyloid hypothesis: a genetic perspective. Cell 120, 545–555.

Tall AR: Plasma high density lipoproteins: Metabolism and relationship to atherogenesis. J Clin Invest 86:379-384, 1990

Tsai J, Zhang R, Qiu W, Su Q, Naples M, Adeli K.Inflammatory NF-kappaB activation promotes hepatic apolipoprotein B100 secretion: evidence for a link between hepatic inflammation and lipoprotein production. Am J Physiol Gastrointest Liver Physiol. 2009 Jun;296(6):G1287-98. Epub 2009 Apr 2.

Van, Eck M., et al. "Effect of human scavenger receptor class A overexpression in bone marrow-derived cells on cholesterol levels and atherosclerosis in ApoE-deficient mice." Arterioscler.Thromb.Vasc.Biol. 20.12 (2000): 2600-06.

Vekrellis K, Ye Z, Qiu WQ, Walsh D, Hartley D, Chesneau V, Rosner MR, Selkoe DJ. Neurons regulate extracellular levels of amyloid beta-protein via proteolysis by insulin-degrading enzyme. J Neurosci. 2000 Mar 1;20(5):1657-65.

Voyiaziakis, E., Ko,C., O'Rourke, S.M., Huang, L.S. (1999) Genetic control of hepatic apoB-100 secretion in human apoB transgenic mouse strains. J. Lipid Res. 40, 2004-2012

Wang, H., Chen, X., Fisher, E. A. 1993. N-3 fatty acids stimulate intracellular degradation of apoprotein-B in rat hepatocytes. J. Clin. Invest. 91:1380-1389

Wang X, Zheng Y, Xu Y, Ben J, Gao S, Zhu X, Zhuang Y, Yue S, Bai H, Chen Y, Jiang L, Ji Y, Xu Y, Fan L, Sha J, He Z, Chen Q. A novel peptide binding to the cytoplasmic domain of class A scavenger receptor reduces lipid uptake in THP-1 macrophages. Biochim Biophys Acta. 2009 Jan;1791(1):76-83. Epub 2008 Nov 12.

Weinstock PH, Bisgaier CL, Aalto-Setala K, et al: Severe hypertriglyceridemia, reduced high density lipoprotein, and neonatal death in lipoprotein lipase knockout mice: Mild hypertriglyceridemia with impaired very low density lipoprotein clearance in heterozygotes. J Clin Invest 96:2555-2568, 1995

Whitman, Stewart. Practical Approach to Using Mice in Atherosclerosis Research. Clin Biochem Rev Vol 25 February 2004.

Wild S, Roglic G, Green A, Sicree R, King H. Global prevalence of diabetes: estimates for the year 2000 and projections for 2030. Diabetes Care. 2004 May;27(5):1047-53

Winder E, Chao Y, Havel R. 1980. Regulation of the hepatic uptake of triglyceride-rich lipoproteins in the rat: opposing effects of homdogous apolipoproteins E and individual C apoproteins. J. Biol. Chem. 257:14642-47

Weirich G et al. Immunohistochemical evidence of ubiquitous distribution of the metalloendoprotease insulin-degrading enzyme (IDE; insulysin) in human non-malignant tissues and tumor cell lines." Biol Chem. 2008 Nov;389(11):1441-5

Weisgraber KH, Innerarity TL, Mahley RW. Abnormal lipoprotein receptor-binding activity of the human E apoprotein due to cysteine-arginine interchange at a single site. J Biol Chem. 1982;257:2518-2521.

Xhignesse M, Lussier-Cacan S, Sing CF, Kessling AM, Davignon J. Influences of common variants of apoliproprotein E on measures of lipid metabolism in a sample selected for health. Arterioscler Thromb. 1991;11:1100-1110.

Yki-Jarvinen H, Taskinen M: Interrelationship among insulin's antilipolytic and glucoregulatory effects and plasma triglycerides in nondiabetic and diabetic patients with endogenous hypertriglyceridemia. Diabetes 37:1271-1278, 1988

Yonezawa K, Yokono K, Shii K, Hari J, Yaso S, Amano K, Sakamoto T, Kawase Y, Akiyama H, Nagata M, Baba S 1988 Insulindegrading enzyme is capable of degrading receptor-bound Insulin. Biochem Biophys Res Commun 150:605–614

Yan, S.F., Ramsamy, R. Schmidt, A.M. (2010) The RAGE axis: a fundamental signalling danger to the vulnerable vasculature. Circ. Res. 106, 842-853.

Yao Z, McLeod RS. Synthesis and secretion of hepatic apolipoprotein B-containing lipoproteins. Biochim Biophys Acta. 1994 May 13;1212(2):152-66.

Zhang Q, Powers ET, Nieva J, et al. Metabolite-initiated protein misfolding may trigger Alzheimer's disease. Proc Natl Acad Sci U S A 2004; 101:4752– 4757.

Zhang H, Yang Y, Steinbrecher UP. Structural requirements for the binding of modified proteins to the scavenger receptor of macrophages. J Biol Chem. 1993;268:5535–5542.

Zhao, L., Brinton, R.D., 2007b. WHI and WHIMS follow-up and human studies of soy isoflavones on cognition. Exp. Rev. Neurother. 7,1549–1564.

Zhao, L., O'Neill, K., Brinton, R.D., 2005. Selective estrogen receptor modulators (SERMs) for the brain: current status and remaining challenges for developing NeuroSERMs. Brain Res. Brain Res. Rev. 49, 472–493.

Zhao, Z., Xiang, Z., Haroutunian, V., Buxbaum, J.D., Stetka, B., Pasinetti, G.M., 2007. Insulin degrading enzyme activity selectively decreases in the hippocampal formation of cases at high risk to develop Alzheimer's disease. Neurobiol. Aging 28, 824–830.